



2023

## Investigating the Impact of Nonenzymatic Lysine Acetylation on the Function of the Bacterial Ribosome

Sarah Caldwell Feid

Follow this and additional works at: [https://ecommons.luc.edu/luc\\_diss](https://ecommons.luc.edu/luc_diss)

 Part of the [Microbiology Commons](#)

---

### Recommended Citation

Feid, Sarah Caldwell, "Investigating the Impact of Nonenzymatic Lysine Acetylation on the Function of the Bacterial Ribosome" (2023). *Dissertations*. 4017.

[https://ecommons.luc.edu/luc\\_diss/4017](https://ecommons.luc.edu/luc_diss/4017)

This Dissertation is brought to you for free and open access by the Theses and Dissertations at Loyola eCommons. It has been accepted for inclusion in Dissertations by an authorized administrator of Loyola eCommons. For more information, please contact [ecommons@luc.edu](mailto:ecommons@luc.edu).



This work is licensed under a [Creative Commons Attribution-NonCommercial-No Derivative Works 3.0 License](#).

Copyright © 2023 Sarah Caldwell Feid

LOYOLA UNIVERSITY CHICAGO

INVESTIGATING THE IMPACT OF NONENZYMATIC LYSINE ACETYLATION ON THE  
FUNCTION OF THE BACTERIAL RIBOSOME

A DISSERTATION SUBMITTED TO  
THE FACULTY OF THE GRADUATE SCHOOL  
IN CANDIDACY FOR THE DEGREE OF  
DOCTOR OF PHILOSOPHY

PROGRAM IN MICROBIOLOGY AND IMMUNOLOGY

BY

SARAH CALDWELL FEID

CHICAGO, IL

DECEMBER 2023

Copyright by Sarah Caldwell Feid, 2023  
All rights reserved.

## ACKNOWLEDGMENTS

First and foremost, I would like to thank my parents, Rick and Kathy, for fostering a love of questions within me. Their support, encouragement, and love is invaluable. I would also like to thank my family and friends, too numerous to name, who have made my life full of joy.

I would like to thank my mentor, Dr. Alan Wolfe, for being willing to take a chance on this project. Alan's dedication to his students is unmatched. His advice and mentorship have shaped the scientist I want to be as I move forward. I would like to thank the members of the Wolfe Lab, past and present, who have given me advice and friendship. I would particularly like to thank Dr. David Christensen for teaching me the fundamentals of lysine acetylation and Thomas Bank for also being more interested in lysine acetylation than the microbiome. I would like to thank the members of the Microbiology and Immunology Department for providing an environment that encourages collaboration within our community of labs. I would like to thank the members of my committee for their guidance and support. Their interest in this project and perspectives have always been appreciated.

Finally, I would like to thank the collaborators who have helped make this work possible. Thank you to Dr. Christopher Rao for being a part of this project from the start. He has been a secondary mentor to me, and I value his input highly. Thank you to Dr. Hanna Walukiewicz for pioneering the use of polysome profiling, especially during the pandemic. I particularly appreciate the time she took to teach me the proper technique when I was finally able to visit. Thank you to Dr. Ernesto Nakayasu for providing his expertise in mass spectrometry.

Anything found to be true of *E. coli* must also be true of elephants.

— Dr. Jacques Monod

## TABLE OF CONTENTS

ACKNOWLEDGMENTS	iii
LIST OF TABLES	viii
LIST OF FIGURES	ix
LIST OF ABBREVIATIONS	x
ABSTRACT	xiii
CHAPTER ONE: LITERATURE REVIEW	1
Introduction	1
Translation in Bacteria	2
Initiation	2
Elongation	4
Termination	6
Recycling	7
The Ribosome Under Stress	7
Ribosome Hibernation and the 100S Ribosome	7
(p)ppGpp, the Stringent Response, and the Ribosome	9
Ribosomes Respond Differently to Different Nutritional Stresses	11
Central Carbon Metabolism	12
Glycolysis, AcCoA Metabolism, and Acetate Metabolism	13
Acetylation as a Post-Translational Modification	16
Enzymatic Acetylation by Lysine Acetyltransferases	17
Nonenzymatic or Chemical Acetylation	19
Deacetylation	22
The Breadth of Lysine Acetylation	23
Acetylomes	23
Functionally Relevant Lysine Acetylations	30
Summary	34
CHAPTER TWO: MATERIALS AND METHODS	37
Bacterial Strains, Plasmids, and Primers	37
Media and Growth Conditions	37
Generalized P1 Transduction	40
Elimination of Kanamycin Cassettes Flanked by FRT Sites	40
Transformation	41

TBF	41
Electroporation	42
CRIM (Conditional-replication, integration, and modular) Plasmid System	42
Polysome Profiling	43
Cell Lysate Preparation	43
Sucrose Gradient Preparation	44
Gradient Centrifugation and Fractionation	44
RNA Purification and Electrophoresis	45
Western Blots	45
$\beta$ -Galactosidase Induction Assay for Translational Reporters	46
Cell-Free Transcription/Translation Assay	48
Purification of CobB	48
Deacetylation Reactions	49
Quantitative PCR	49
Mass Spectrometry	50
Preparation of Ribosomes for Mass Spectrometry	50
Mass Spectrometry	50
CHAPTER THREE: EXPERIMENTAL RESULTS	52
Acetyl Phosphate Levels Alter Translation <i>in vitro</i> and <i>in vivo</i>	52
Introduction	52
The Addition of Acetyl Donors Impair Translation in an <i>in vitro</i> Transcription-Translation System	53
High Acetylation Mutants Have an Altered Ribosome Population in Rich Media	55
Proteins from the 30S and 50S Ribosomal Subunit Fractions are More Acetylated Than Proteins from the 70S Ribosome Complex Fractions	56
Summary	58
Acetyl Phosphate-Dependent Acetylation Does Not Impact Translation Elongation Rate in Stationary Phase	59
Introduction	59
There is No Difference in Elongation Rate Between <i>E. coli</i> Cultured in Low or High Acetylation Media	60
Summary	60
Subunit Skew Is Dependent on Central Metabolic Flux and Growth Phase of Culture	62
Introduction	62
Media Conditions that Favor Nonenzymatic Acetylation Alter Polysome Profiles	62
The Emergence of Increased Ribosome Dissociation Occurs as Cultures Exit Exponential Growth	63
Summary	66
CobB-Sensitive Acetylated Lysine Residues Contribute to Some, But Not All, Observed Acetylation-Dependent Changes in Translation	67
Introduction	67
Purified CobB Does Not Restore Translation Function to Acetylated <i>in vitro</i> Transcription-Translation Reactions	68

CobB-Sensitive Lysine Residues Contribute to the Acetylation-Dependent Changes Observed in Polysome Profiles	71
There is Variability in the Length of Exponential Phase in TB7 Prepared with Different Lots of Tryptone	73
Summary	76
Preliminary Mass Spectrometry Data Identify Several Conserved Acetylation Sites Specific to Wild-Type Subunit Fractions	76
Introduction	76
Mass Spectrometry Identifies Several Acetylations Unique to the Subunit Fractions in Wild- Type <i>E. coli</i>	77
Summary	78
CHAPTER FOUR: DISCUSSION	80
Overall Summary	80
Which Step of Translation is Affected by Nonenzymatic Lysine Acetylation?	81
The Reversibility of Ribosomal Lysine Acetylation	83
Lysine Acetylations Link Ribosome Function to Central Carbon Metabolism	87
Future Directions	89
Concluding Remarks	91
REFERENCE LIST	93
VITA	124

## LIST OF TABLES

Table 1. List of Archaeal, Bacterial, and Some Simple Eukaryotic Acetylomes	24
Table 2. Strain and Plasmid List	38
Table 3. Primer List	39
Table 4. Portion of Ribosomes in 30S, 50S, and 70S Fractions Over Time	66
Table 5. Acetylated Residues Unique to Wild-Type <i>E. coli</i> Subunit Fractions	78

## LIST OF FIGURES

1. The Bacterial Ribosome With and Without mRNA and tRNAs.	4
2. Central Carbon Metabolism	15
3. Genetic and Metabolic Manipulations of Nonenzymatic Acetylation in <i>E. coli</i>	21
4. Stress-Induced and Glucose-Induced <i>cpxP</i> Transcription	32
5. Addition of Acetyl Donors Inhibits Translation but Not Transcription	54
6. High Acetylation Conditions Favor Dissociated Subunits	57
7. RNA and Protein Analysis of Polysomal Gradient Profiling Fractions	58
8. Elongation Rate is Not Affected by Conditions Promoting Acetylation	61
9. Growth on Acetate Favors Dissociated Ribosomes	64
10. The Acetylation-Associated Increase in Dissociated Subunits is Specific to Post-Exponential Growth	65
11. Purification of Active CobB	69
12. Addition of Active CobB Does Not Restore Translation Function to Acetylated <i>in vitro</i> TXTL Reactions	70
13. The Loss of <i>cobB</i> Alters the Ribosome Population from Wild-Type but Not to the Extent of the $\Delta$ <i>ackA</i> Mutant	72
14. The Loss of <i>cobB</i> Shifts the Ribosome Population in a Pattern the Resembles the Loss of <i>ackA</i> Over Time	74
15. Exponential Phase is Shorter in TB7 + 0.4% Glucose Prepared with Different Lots of Tryptone	75

## LIST OF ABBREVIATIONS

30S IC	30S initiation complex
30S PIC	30S pre-initiation complex
70S IC	70S initiation complex
$\alpha$ CTD	$\alpha$ -C-terminal domain
AcCoA	acetyl-coenzyme A
AcK	acetyl-lysine
AcP	acetyl phosphate
BCA	bicinchoninic acid
cAMP	cyclic AMP
CRIM	Conditional-replication, integration, and modular
ED	Entner-Doudoroff
EF-G	elongation factor G
EF-P	elongation factor P
EF-Tu	elongation factor Tu
EMP	Embden-Meyerhof-Parnas
GNAT	GCN5-related N-acetyltransferase
HPF	hibernation promoting factor
IF1	initiation factor 1
IF2	initiation factor 2

IF3	initiation factor 3
IPTG	Isopropyl $\beta$ -D-1-thiogalactopyranoside
KAT	lysine acetyltransferase
KDAC	lysine deacetylase
IHPF	long hibernation promoting factor
LSU	large subunit
MUG	4-methylumbelliferyl-D-galactopyranoside
OD600	optical density at 600 nm
PP	pentose phosphate
ppGpp	guanosine tetraphosphate
pppGpp	guanosine pentaphosphate
(p)ppGpp	guanosine tetraphosphate and guanosine pentaphosphate
PTM	post-translational modification
RF1	release factor 1
RF2	release factor 2
RF3	release factor 3
RFU	relative fluorescence units
RMF	ribosome modulation factor
RNAP	RNA polymerase
R/P	RNA to protein
RRF	ribosome recycling factor
SDS-PAGE	sodium dodecyl sulfate-polyacrylamide gel electrophoresis
SSU	small subunit

TB7	tryptone broth buffered to pH 7
TCA	tricarboxylic acid
TXTL	transcription-translation
WT	wild-type

## ABSTRACT

Lysine acetylation, either by lysine acetyltransferase (KAT) enzymes or nonenzymatic (chemical) acetyl donors such as acetyl phosphate (AcP), is a common post-translational modification across all domains of life. Though it has only recently been recognized as a relevant modification in bacteria, there is a rapidly growing body of work investigating the impact of lysine acetylation, particularly on bacterial metabolism.

An under-investigated target of lysine acetylation is the bacterial ribosome. Although lysine acetylations on the bacterial ribosome are common and conserved in diverse bacterial species, little work has been done to understand how lysine acetylation might affect the bacterial ribosome. The goal of this work is to determine if lysine acetylation has functional impact on the bacterial ribosome.

To that end, I have identified *in vitro* and *in vivo* effects of nonenzymatic, AcP-dependent lysine acetylation on translation and the ribosome. *In vitro* acetylation of transcription-translation reactions causes a translation-specific defect that is unaffected by the addition of the CobB deacetylase. This suggests certain AcP-sensitive residues that are part of the translation machinery can inhibit translation, and these acetylations are not reversible.

*In vivo*, I have demonstrated that high acetylation bacterial cultures have a ribosome population that favors the presence of dissociated 30S and 50S subunits over intact 70S ribosomes in stationary phase. This is true for cultures that are acetylation high due to genetic

manipulation and cultures that are acetylation high due to media manipulation. This suggests that the impact of nonenzymatic lysine acetylation on the ribosome is linked to central carbon metabolism, due to the relationship between AcP levels and carbon flux. I have also demonstrated that there is some contribution by the CobB deacetylase to the subunit skew pattern. However, complications caused by the sensitivity of the pattern to growth conditions have stymied efforts to determine if the shift is caused primarily by CobB-sensitive acetylated lysines or a mixture of CobB-sensitive and -insensitive acetylated lysines.

Although I have been unable to determine which step of translation is targeted by lysine acetylation, I have shown that when nonenzymatic lysine acetylation is increased by supplementing cultures with acetate, the elongation rate of translation is unaltered. This suggests that the impact of lysine acetylation, at least under these growth conditions, is not at the level of elongation, and may act at other steps such as initiation or recycling.

Finally, preliminary mass spectrometry data of 30S, 50S, and 70S fractions from wild-type *E. coli* grown in a rich medium until stationary phase have allowed me to identify 18 acetylated lysine that are only observed in the subunit fractions. Of these acetylations, acetylated lysines on uS7 and bL12 have functional roles that make them promising targets for future studies into the mechanistic effects of lysine acetylation on the ribosome.

CHAPTER ONE  
LITERATURE REVIEW

**Introduction**

Post-translational modifications (PTMs) are a major form of regulation in bacteria. From the common phosphorylation of a signal transduction cascade to the various forms of acylation, PTMs allow bacteria to alter their proteome more rapidly than transcriptional or translational responses.

The bacterial ribosome is a hotspot of PTMs, with protein acetylations and phosphorylations, as well as methylations of protein and rRNA. While ribosomal phosphorylation and ubiquitination are increasingly accepted as relevant modifications of the eukaryotic ribosome, the impact of PTMs on the bacterial ribosome have not been deeply explored (1).

Lysine acetylations on the bacterial ribosome are highly conserved across diverse bacterial species (2). The conservation of lysine acetylations is particularly interesting as lysine acetylation in several species is predominated by nonenzymatic acetylations(3-5). This mechanism of acetylation links the modification directly to central carbon metabolism (6). Therefore, it is likely that lysine acetylations on the bacterial ribosome respond to shifts in carbon flux. To study what an accumulation of these modifications means for the bacterial ribosome, it is helpful to use a model organism where central carbon metabolism is well-studied, and the acetylome is well-characterized. *Escherichia coli* fulfills these criteria, long serving as a model for studying central metabolism. There are several published *E. coli* acetylomes, across

several conditions, and several allowing for the distinction between nonenzymatic and enzymatic modifications. In this chapter, I will provide an overview of the bacterial ribosome and translation as well as discuss how bacterial ribosomes respond to certain stresses. Next, I will review metabolism in *E. coli*, with a focus on the generation of the acetyl donor acetyl phosphate (AcP), and how AcP levels shift based on metabolic factors. Finally, I will provide an overview of what is known about protein acetylation, the mechanisms of lysine acetylation, and examples of known effects of lysine acetylation on protein function.

### **Translation in Bacteria**

The *E. coli* ribosome is comprised of two subunits: a 30S small subunit (SSU) containing the 16S rRNA and 21 proteins and a 50S large subunit (LSU) containing the 23S rRNA, the 5S rRNA, and 36 proteins (7). At each step in the translation process, numerous translation factors are involved at each step. A typical round of protein translation consists of initiation, elongation, termination, and recycling. While it is beyond the scope of this work to elaborate on eukaryotic translation, I will note where translation is understood to be similar between bacteria and eukaryotes and where it diverges. It should also be noted that throughout the work, I will be using a universal system for the naming of ribosomal proteins: “b” denotes proteins unique to bacteria, “e” denotes proteins unique to eukaryotes and archaea, and “u” denotes proteins shared between the three domains (8). This system is intended to eliminate any confusion between similarly named proteins that differ between bacteria, eukaryotes, and archaea.

#### **Initiation**

Initiation is understood to be divergent between bacteria and eukaryotes. For the purposes of this review, I will focus on initiation in the context of Shine-Dalgarno-containing mRNAs, as this process is the best understood. While mRNAs lacking a Shine-Dalgarno sequence and

leaderless mRNA without a 5' untranslated region are found in bacteria, the process of initiation for these mRNAs is not well understood (9-11). An exploration of the questions regarding these types of mRNA is beyond the focus of this dissertation.

For Shine-Dalgarno-containing mRNAs, initiation begins with the 30S small subunit (SSU), initiation factor 1 (IF1), initiation factor 2 (IF2), initiation factor 3 (IF3), and fMet-tRNA<sup>fMet</sup> forming the 30S pre-initiation complex (30S PIC) (12-14). This association is unstable, and the factors can bind the SSU independently. However, the binding order of IF3 and IF1, then IF2, and finally fMet-tRNA<sup>fMet</sup> recruitment to the A site (**Fig. 1A**) of the complex by IF2 is most kinetically favored (15).

The complex is stabilized to the 30S initiation complex (30S IC) by the recognition of the start codon of an mRNA. The mRNA binds the complex independent of the initiation factors, and the rate of mRNA association is understood to be most influenced by properties of the mRNA, such as secondary structures, as well as the concentration of mRNA (15, 16). Upon start codon recognition, the binding of fMet-tRNA<sup>fMet</sup> is stabilized while the binding of IF3 is destabilized (15, 17-19).

Next, the large subunit (LSU) docks with the 30S IC. The rate of docking is influenced by the presence of IF1, IF3, IF2•GTP, and fMet-tRNA<sup>fMet</sup>, as well as the sequence of the mRNA (20-22). Charged interactions between LSU protein bL12 and IF2 are critical for rapid subunit association *in vitro* (23).

GTP hydrolysis by IF2 shifts fMet-tRNA<sup>fMet</sup> to the P site (**Fig. 1A**), and displacement of IF3 and dissociation of IF1 and IF2 allows for the formation of intersubunit bridges, resulting in the mature 70S IC (21, 22, 24-29).

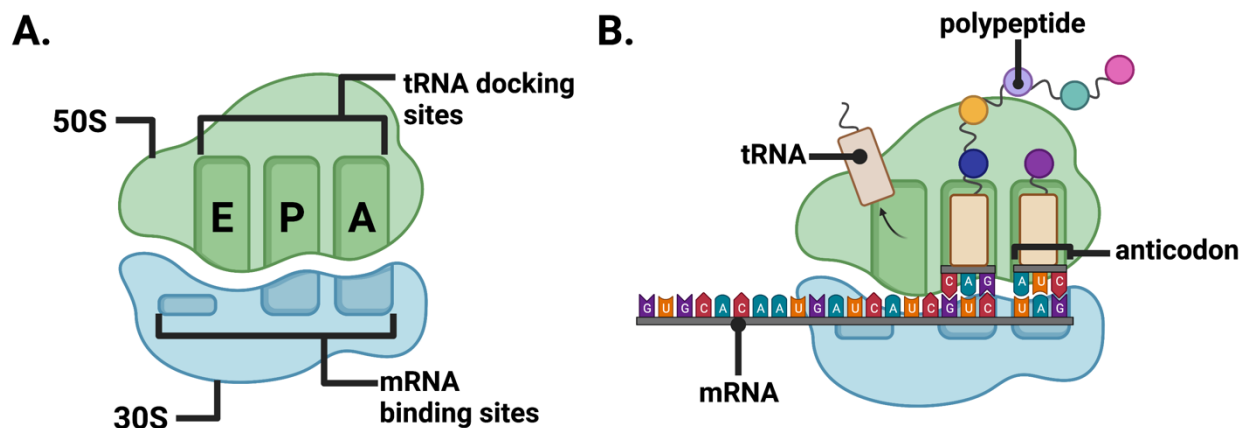


**Figure 1. The Bacterial Ribosome With and Without mRNA and tRNAs.** **A.** A simplified schematic of the 50S and 30S subunits for conceptualizing the E, P, and A sites. **B.** A basic model of the progression of tRNAs through the 70S ribosome. The tRNA enters and forms a codon/anti-codon pair with the mRNA at the A site. The polypeptide bond between the amino acid carried by the tRNA and the polypeptide chain is catalyzed at the P site. The codon/anti-codon pairing is disrupted and the tRNA exits the ribosome at the E site. Figure created with Biorender.com.

## Elongation

Once the 70S IC is formed, the ribosome proceeds rapidly into elongation. Elongation is a cycle of decoding, peptide bond formation, and translocation, ending when the ribosome reaches the stop codon. Unlike initiation, the mechanism of elongation is similar between bacteria and eukaryotes, and the elongation factors are largely homologous (30, 31).

Decoding is the process of matching the codons of the mRNA to the amino acid sequence being built. A codon is exposed in the ribosome A site and is recognized by aa-tRNAs (**Fig. 1B**). The aa-tRNAs arrive at the ribosome in a complex with EF-Tu and GTP and are recruited at the bL12 stalk. Codon-anticodon pairing of the aa-tRNA with the A site codon triggers hydrolysis of GTP by EF-Tu. As EF-Tu shifts to its GDP-bound form, it releases the aa-tRNA, which moves fully into the A site as EF-Tu•GDP dissociates.

The peptidyl transferase center of the ribosome catalyzes the formation of a peptide bond between the peptidyl-tRNA in the P site and the aa-tRNA in the A site. This is an rRNA active

site. The peptide bond is formed through nucleophilic attack from the amino group of the aa-tRNA on the carbonyl carbon of the ester bond in the peptidyl-tRNA. Water molecules within the reaction center and the 2'OH group of A76 of the P-site t-RNA and the 2'OH of A2451 of the 23S rRNA assist in proton transfer and stabilize the charges of the reaction (32-34). Most amino acid combinations can form peptide bonds within the peptidyl transferase center without any additional factors. However, poly-Pro stretches with three or more prolines or certain XPPX sequences can induce ribosome stalling due to the low rate of peptide bond formation (35-38). The specialized translation factor EF-P (or its eukaryotic counterpart eIF5A) rescues proline-induced stalling (38-40). This appears to be the specific function of EF-P, while eIF5A has multiple roles in elongation and termination (31, 41, 42).

Once the peptide bond is formed, the ribosomal subunits move to shift the tRNAs in the P and A sites to the E and P sites respectively (**Fig. 1B**). Prior to translocation, the subunits are in a nonrotated (N) state, with the tRNAs bound to the P and A sites on the SSU and the LSU. During translocation, the subunits move to the rotated (R) state, which binds the tRNAs in hybrid P/E and A/P states. Simultaneously, the uL1 stalk domain changes from an open to a closed conformation relative to the P-site tRNA. Modern models divide translocation into as many as eight discrete structural states, which I will briefly summarize.

The process of translocation is powered by EF-G GTP hydrolysis (43). EF-G binding promotes rotation of the SSU head and body domains counterclockwise (CCW) relative to the LSU, corresponding with the direction of translocation (44-46). After EF-G hydrolyzes GTP, it does not immediately release the  $P_i$  (47, 48). First, the SSU body rotates in the clockwise (CW) direction, while the SSU head domain maintains its rotated conformation (44-46). This is speculated to open the decoding region and disrupt the tRNA interactions with the ribosome that

hold the mRNA and the tRNA anticodons in the A and P site (30). The SSU head domain then starts to rotate back to its original conformation, the tRNAs shift into their post-translocation positions in the P and E sites, and EF-G releases Pi (44-47). The E-site tRNA shifts away from the P-site tRNA and loses its codon-anticodon pairing as the SSU head continues to shift backward (49, 50). Dissociation of the E-site tRNA and EF-G completes the return to the unrotated N state (45).

### **Termination**

When the ribosome reaches a stop codon in the mRNA, termination occurs. In bacteria, stop codons are recognized by the release factors RF1, which reads UAG/UAA, and RF2, which reads UGA/UAA (51, 52). This is distinct from eukaryotes, which use eRF1 to recognize all stop codons (53). Once RF1 or RF2 recognize a stop codon, a conserved GGQ motif in the release factors assists in peptidyl-tRNA hydrolysis by the peptidyl transferase center of the ribosome (54-57).

RF3 is required for release of RF1/RF2 from the ribosome, but the mechanism of RF3 function is still debated. One model suggests RF3•GDP binds with RF1/RF2 after peptide release, and GDP dissociation stabilizes the RF3-ribosome complex. Then GTP binding to RF3 promotes RF1/RF2 dissociation. Finally, RF3 hydrolyzes GTP and dissociates (58, 59).

Although RF3•GDP binding is plausible, most recent models favor the initial binding of RF3•GTP, as cellular concentrations of GTP favor the GTP-bound form of RF3 (60, 61). In one RF3•GTP model, peptide release stabilizes the RF3•GTP-ribosome complex, promoting RF1/RF2 dissociation, and concluding with GTP hydrolysis and dissociation of RF3•GDP. Yet another model suggests RF3 hydrolyzes GTP and dissociates prior to RF1/2 dissociation, promoting RF1/RF2 dissociation by inducing SSU rotation (62). Some recent insights suggest

the relevance of RF3 differs between RF1 and RF2 (63, 64). Regardless of the precise mechanism of termination, the result is peptide release and dissociation of the release factors.

### **Recycling**

The mRNA and tRNA remain in the ribosome post-termination and must be released for subsequent rounds of initiation. This process is referred to as recycling and requires ribosome recycling factor (RRF) and EF-G. Like termination, eukaryotic ribosome recycling requires proteins not found in bacteria, although it is unclear if this has functional significance (53). Although the precise order of recycling steps is debated, EF-G hydrolyzes GTP, which pushes RRF against a key intersubunit bridge and promotes subunit splitting (65-67).

Bacterial ribosome recycling is catalyzed by ribosome recycling factor (RRF) and EF-G. RRF binds at the ribosome A site, stabilizing the complex in a fully rotated state (65, 68). Although RRF and EF-G can bind the ribosome independently, effective ribosome recycling requires RRF to bind before EF-G•GTP (69-71). Two pathways have been suggested for ribosome recycling. In the first, GTP hydrolysis by EF-G and P<sub>i</sub> release leads to subunit splitting, with the mRNA and tRNA remaining on the SSU. The mRNA is exchanged spontaneously, while dissociation of the tRNA is facilitated by IF3 (69-73). In the second pathway, GTP hydrolysis promotes mRNA release, followed by tRNA dissociation, and ending with subunit splitting (74, 75). It has been speculated that various dissociation pathways might be possible, perhaps depending on the mRNA present (30, 74).

## **The Ribosome Under Stress**

### **Ribosome Hibernation and the 100S Ribosome**

When bacteria experience nutrient limitation and enter stationary phase, one of the changes they undergo is a global reduction in protein synthesis. However, any reduction in

protein synthesis needs to be rapidly undone to resume growth when conditions become favorable. One way bacteria mediate the stationary phase reduction in translation is through ribosome-associated factors that form inactive 70S monomers or 100S dimers of the ribosome, in a process known as ribosome hibernation (76). This process is ubiquitous in bacteria (although specific factors involved can vary) and similar mechanisms are thought to occur in eukaryotic cells (77-81).

100S ribosomes are formed by the dimerization of 70S ribosomes. Although initially observed around 60 years ago, it is only more recently that 100S ribosomes have been investigated as a form of ribosome with a function (82-84). The 100S complex is arranged in a 50S-30S-30S-50S structure without mRNA (85-89). The presence of 100S dimers is tied to growth phase; they are not seen or uncommon in exponentially growing cells but appear or increase during stationary phase (90-92). Importantly, 100S dimers disappear rapidly from the ribosome pool when cells exit stationary phase (90, 93).

The factors required to form 100S dimers vary between bacteria. In the gammaproteobacteria, which includes *E. coli*, 100S dimerization uses ribosome modulation factor (RMF) and hibernation promoting factor (HPF). RMF-HPF-formed 100S dimers are only observed in stationary phase (90, 91). RMF is necessary and sufficient for 100S formation; loss of *rnf* abolishes 100S formation. RMF can dimerize 70S ribosomes *in vitro* to a 90S dimer without HPF (87, 91, 94-96). HPF stabilizes the 90S dimer into the mature, stable 100S dimer, and *in vitro* cannot dimerize 70S ribosomes without RMF (95, 97). Despite being dispensable *in vitro*, HPF is required *in vivo*, as *E. coli hpf* mutants do not form ribosome dimers *in vivo* (96). This is thought to be caused by the activity of a third hibernation factor, RaiA, which creates stable, inactive 70S monomers (98, 99). HPF and RaiA share the same binding site, so it is likely

that in the absence of HPF, the activity of RaiA skews the inactive ribosome population towards monomers (99-101).

Bacteria outside of the gammaproteobacteria contain an HPF homolog that is necessary and sufficient for the formation of 100S ribosomes, referred to as long HPF (IHPF) (78, 102-104). Interaction between two IHPF molecules mediates 100S dimerization. Unlike RMF-HPF-100S dimers, IHPF-100S are observed at low levels in exponentially growing cells (78, 102-105). The presence of IHPF in the 70S fraction of the ribosome pool, as well as in the 100S fraction suggests that IHPF also can form an inactive 70S monomer, like RaiA (78, 103, 105, 106).

Because hibernation factors are found across the entire spectrum of the bacterial domain, their regulation is varied, although it is usually tied to stress or stationary phase signals. For example, *rmf* transcription can be induced by amino acid starvation (the stringent response), heat and cold shocks, pH shifts, osmotic stress, and envelope stress (107-111). Less is known about *hpf* and *raiA*, but, like *rmf*, they can be induced by (p)ppGpp, the major stringent response signal (112, 113). Consistent with the presence of IHPF during exponential growth, *lhpf* is usually expressed at a basal level that increases in response to different signals (78, 105). Like *rmf*, *hpf*, and *raiA*, *lhpf* is induced by the stringent response (102, 114, 115).

### **(p)ppGpp, the Stringent Response, and the Ribosome**

In response to a variety of nutrient stresses, the molecules guanosine pentaphosphate (pppGpp) and guanosine tetraphosphate (ppGpp), collectively abbreviated as (p)ppGpp, accumulate in most bacteria. First identified as a response to amino acid starvation, the stringent response is now understood to be induced by a variety of nutrient stresses (116, 117). Because

(p)ppGpp mediates many responses, it is impractical to include an in-depth review. Therefore, I will focus on the impact of the stringent response on the ribosome and translation.

As part of the wide variety of transcriptional changes induced by (p)ppGpp, rRNA synthesis is repressed. In addition to reducing the transcription of rRNA genes, the stringent response inhibits ribosome maturation by inhibiting small GTPases needed for the maturation of the 50S and 30S subunits (118, 119). These changes prevent the ribosome pool from growing in adverse conditions.

The stringent response also alters the function of mature ribosomes in many ways. The initiation factor IF2 is inhibited by ppGpp, which may block the formation of the 30S IC (120). However, the affinity of 30S-bound IF2 for ppGpp varies based on the mRNA bound to the 30S pre-IC. For example, the 30S pre-ICs containing *tufA* (elongation factor EF-Tu) or *rnr* (RNase R) mRNA have reduced affinity for ppGpp (121). For pppGpp-bound IF2 specifically, 30S IC formation requires higher concentrations of IF2 (121). In this way, (p)ppGpp can reduce overall translation while allowing for the continued production of a subset of necessary proteins.

Elongation, termination, and ribosome recycling also can be impaired by (p)ppGpp. EF-Tu and EF-G are inhibited by (p)ppGpp, stalling elongation (122). RF3, necessary for releasing RF1/RF2 from the ribosome, is inhibited by ppGpp, and EF-G inhibition by (p)ppGpp is likely to affect its role in recycling, as well as elongation (123).

Finally, (p)ppGpp promotes the formation of hibernating ribosome species. A strain of *B. subtilis* that overproduces (p)ppGpp favors the formation of 100S ribosomes, consistent with (p)ppGpp-induced transcription of hibernation factor genes (115).

The stringent response is a clear example of the many ways translation can be altered in response to nutrient stress, but it is clear the stringent response is only one of the many layers of regulation that modulate the translational response to nutrient stress.

### **Ribosomes Respond Differently to Different Nutritional Stresses**

Because (p)ppGpp synthesis is induced in response to many nutrient stresses, if it was the only way that translation responded to nutritional stress, most nutrient stress responses would be the same. This not what is experimentally observed.

During rapid or moderate growth, there is a linear relationship between ribosome content, elongation rate, and growth rate (124). However, some translational capacity is maintained during stationary phase. In fact, the linear relationship amongst ribosome content, elongation rate, and growth rate breaks down during stationary phase, as the bacteria maintain a minimum elongation rate of around 8 amino acids/second (125). Overall, translational capacity is diminished by reducing the pool of available active ribosomes (125). This is true as a broad model for nutrient limitation, but, in fact, work in *E. coli* suggests specific strategies for the loss of specific nutrients.

*E. coli* cells limited for phosphorus have a lower RNA to protein (R/P) ratio than cells limited for nitrogen or carbon at similar growth rates, suggesting they can make the same amount of protein with fewer ribosomes (126). In contrast, nitrogen-limited *E. coli* has a lower elongation rate compared to phosphorus- or carbon-limited *E. coli* cells, while carbon-limited *E. coli* cells have a larger proportion of inactive 70S compared to the other conditions (126). Carbon-limited *E. coli* cells have many ribosomes, but few of them are actively translating (126). Nitrogen-limited *E. coli* cells have a mid-range of ribosomes and a mid-range of working

ribosomes, but they translate more slowly. Phosphorus-limited *E. coli* cells have fewer ribosomes overall, but most of them translate rapidly.

It is also clear that ribosome function responds differently to stresses other than nutrient stress. For example, in response to hyperosmotic stress (an excess concentration of salts or sugars), *E. coli* reduces its elongation rate more than is observed during nutrient limitation but maintains a higher overall ribosome content than nutrient-limited cells (127).

All of this indicates that there are many layers of regulation in place to alter translation in response to a wide variety of situations. The bacterial ribosome must sense several factors. Considering the variety of ways the ribosome can respond to different nutrient stressors, it is reasonable to hypothesize that the ribosome must monitor cellular metabolism in some other ways.

### **Central Carbon Metabolism**

The molecules necessary for lysine acetylation are closely associated with central carbon metabolism. Acetyl phosphate (AcP) for nonenzymatic acetylations and acetyl-coenzyme A (AcCoA) for enzymatic acetylations are both produced by central carbon metabolism. NAD<sup>+</sup>, which is necessary for the function of sirtuin deacetylases, is a necessary cofactor for glycolysis and the TCA cycle. This connection suggests acetylation could be a means of sensing the metabolic state of the cell.

For the purposes of this overview, I will focus on the metabolism of glucose and acetate by *E. coli*. The glucose and acetate metabolism pathways of *E. coli* make it a useful model organism for studying nonenzymatic acetylation by acetyl phosphate for several reasons. First, the central metabolic pathways of *E. coli* are well-characterized, which means the methods for manipulating the system genetically or through medium choices are established. Second, and

importantly for the consideration of nonenzymatic acetylation, while *E. coli* often generates AcP as a metabolic by-product, it is not an essential part of *E. coli* metabolism under most conditions. For certain bacteria (e.g., the *Bifidobacterium* genus), AcP is an unavoidable by-product of their metabolic pathways (128). Because the levels of AcP production in *E. coli* can be tuned, either through choice of carbon source or genetic manipulation, it is a model system where nonenzymatic acetylation can be low or high.

To understand how AcP levels can be altered in *E. coli*, a basic understanding of central metabolism is necessary. In this section, I will outline how glucose is processed to AcCoA and how the AcCoA proceeds to the TCA cycle or is fermented to acetate, generating AcP. I will also describe the basics of acetate metabolism.

### **Glycolysis, AcCoA Metabolism, and Acetate Metabolism**

Glucose is imported as glucose-6-phosphate, which can be metabolized by three different paths: the Embden-Meyerhof-Parnas (EMP) pathway, the Entner-Doudoroff (ED) pathway, or the pentose phosphate (PP) pathway. These pathways all generate energy and AcCoA, but the EMP has a high carbon flux relative to the ED and PP pathways. As it is highly relevant to AcP production, I will focus on the EMP.

In actively growing cells, glucose flux through the EMP generates 2 NADH, nets 2 ATP, and results in 2 pyruvate. The pyruvate is converted to AcCoA which can enter the TCA cycle to generate amino acid precursors and ATP (**Fig. 2**). However, particularly when glucose is in excess, the flux from the EMP to the AcCoA node can exceed the flux of AcCoA into the TCA cycle. This creates a shortage of free CoA. To prevent a bottleneck, CoA is regenerated by fermenting acetate.

The ability of *E. coli* to ferment acetic acid (acetate) aerobically in the presence of excess glucose is called aerobic fermentation or the Crabtree Effect (129, 130). First described in cancer cells and observed in yeast, all three forms result in cells excreting excess carbon as partially oxidized metabolites (for *E. coli*, acetate) instead of putting the carbon towards biomass. In *E. coli*, this is tied to overflow metabolism or acetate overflow, based on the constraints of NADH turnover rate and the velocity of key TCA cycle enzymes (131). This also is proposed to assist in maintaining the NAD/NADH redox balance, as rapid flux through the TCA cycle generates a lot of NAD(P)H and FADH<sub>2</sub>, but fermentation of acetate produces no NADH (**Fig. 2**).

To ferment acetate, *E. coli* uses the phosphotransacetylase (Pta) acetate kinase (AckA) pathway, which is common in bacteria (132). Pta converts AcCoA and inorganic phosphate to AcP and free CoA. Then AckA converts acetyl phosphate into acetate by transferring its phosphoryl group to ADP, generating one molecule of ATP and acetate, which is excreted (**Fig. 2**).

In addition to excreting acetate, *E. coli* can consume acetate as a carbon source (**Fig. 2**). *E. coli* contains a high affinity acetate assimilation pathway that is efficient at scavenging small amounts of acetate as well as a low affinity pathway effective at consuming high concentrations of acetate. The high affinity pathway relies on acetyl-CoA synthetase (Acs). Acs has a high affinity for acetate and is efficient at assimilating acetate at concentrations below 7 mM (133). The low affinity pathway uses the Pta-AckA pathway for acetate uptake at high concentrations of acetate. While both pathways are needed for complete consumption of acetate, the Pta-AckA pathway is the route for most acetate consumption, while the Acs pathway is important for acetate scavenging (133, 134).

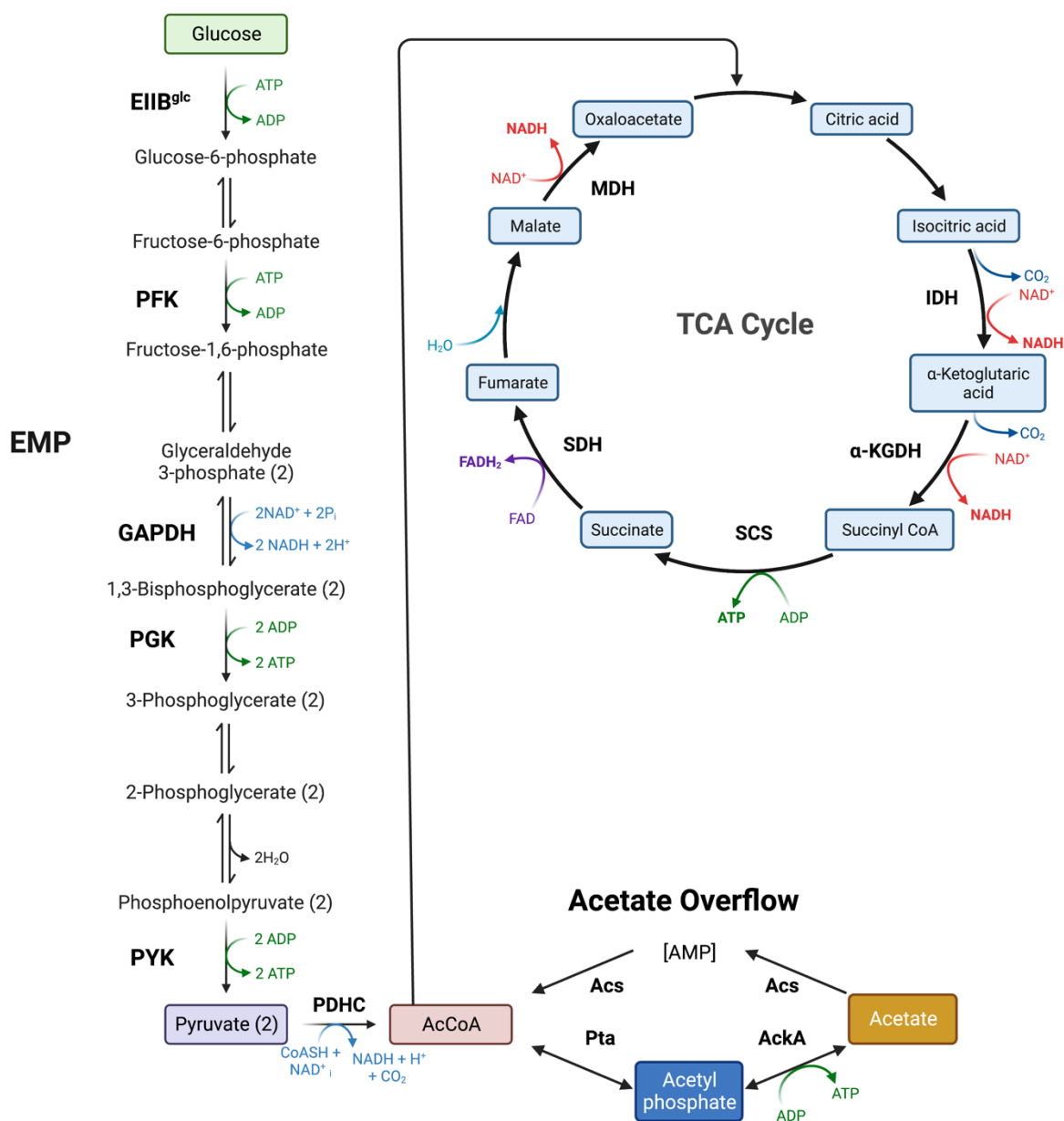


**Figure 2. Central Carbon Metabolism.** A basic schematic of central carbon metabolism, including the Embden-Meyerhof-Parnas pathway (EMP), the tricarboxylic acid cycle (TCA), and the acetate overflow pathway. All enzymes of the acetate overflow pathway and enzymes responsible for producing ATP or redox products have been highlighted. **EIIB<sup>glc</sup>** glucose-specific enzyme II (*ptsG*) **PFK** phosphofructokinase **GAPDH** glyceraldehyde-3-phosphate dehydrogenase **PGK** phosphoglycerate kinase **PYK** pyruvate kinase **PDHC** pyruvate dehydrogenase complex **IDH** isocitrate dehydrogenase  **$\alpha$ -KGDH**  $\alpha$ -ketoglutarate dehydrogenase **SCS** succinyl-CoA synthetase **SDH** succinate dehydrogenase **MDH** malate dehydrogenase **Pta** phosphate acetyl transferase **AckA** acetate kinase **Acs** acetyl-CoA synthetase. Figure created with Biorender.com.

The specifics of manipulating *E. coli* carbon metabolism to favor nonenzymatic acetylation are explored further in the following section.

### **Acetylation as a Post-Translational Modification**

Acetylation is a common post-translational modification long studied in eukaryotic cells and more recently also recognized as having important physiological roles in bacteria and archaea (2, 135-144). The basic mechanism of protein acetylation requires a nucleophilic acyl substitution reaction between a nucleophile and an activated acetyl group ( $\text{CH}_3\text{CO-X}$ ), usually AcCoA or AcP (140). Acetylation can occur nonenzymatically between an acetyl donor and protein or enzymatically between a protein acetyltransferase, an acetyl donor, and a specific amino acid on a protein substrate. Reactive amino acids for acetylation (cysteines, serines, threonines, and lysines) contain a primary amino group, hydroxyl group, or sulfhydryl group (145).

N-acetylation of primary amino groups can occur either on the alpha amino group ( $\text{N-}\alpha$ ) of N-terminal amino acids or on the epsilon amino group ( $\text{N-}\epsilon$ ) of lysines within a protein.  $\text{N-}\alpha$  acetylation is common in eukaryotes, where it is typically cotranslational (146). Roughly 50% of soluble proteins in *Saccharomyces cerevisiae* have been identified as  $\text{N-}\alpha$  acetylated, and the number is estimated to be around 80% in mammalian cells (147-149). In bacteria this form of acetylation is rare and posttranslational; approximately 1% of the expressed proteome in *E. coli* is estimated to be  $\text{N-}\alpha$  acetylated (150, 151). However, the dearth of bacterial species analyzed for  $\text{N-}\alpha$  acetylation means the current available proteomic data may be insufficient to conclude if reduced prevalence is broadly the case for bacteria (135).

For the remainder of this section, I will focus on  $\text{N-}\epsilon$  acetylation (referred to as lysine acetylation) in bacteria. I will outline the mechanisms of enzymatic and nonenzymatic

acetylation, discuss lysine deacetylation in bacteria, and provide an overview of the prevalence and relevance of lysine acetylations.

### **Enzymatic Acetylation by Lysine Acetyltransferases**

Lysine acetyltransferases or KATs catalyze a targeted transfer of an acetyl group from AcCoA to an epsilon amino group of lysine. In bacteria, two superfamilies of KATs have been identified: GNATs and YopJ effector proteins (140, 152-155). The basic acid/base catalytic mechanism is the same for all KATs, but the specifics vary between families.

GNATs generally contain a glutamate in the active site as the deprotonating base for the amino group of the targeted protein and a tyrosine as the reprotonating acid (156, 157). In certain exceptions, a water molecule can replace the glutamate as the deprotonating base via a proton wire (157, 158). The kinetics of this mechanism are a sequential/direct transfer mechanism that proceeds through a ternary complex (156).

The YopJ effector family uses histidine to deprotonate a proximal cysteine, which then forms an acyl-enzyme intermediate with AcCoA, then transfers the acetyl group to the protein substrate (154). Rather than the sequential mechanism seen in the GNATs, the YopJ proteins use a ping-pong/double-displacement mechanism.

Multiple forms of bacterial GNATs have been observed. To classify these GNATs, I will use the classification scheme proposed in Christensen et al., which synthesizes systems proposed by Hentchel and Escalante-Semerena and Lu et al. into a single scheme (135, 140, 159). This divides the GNATs into three classes (class I, II, or III) based on sequence length and the number of GNAT domains present and five types (types I to V) based on domain identities and arrangements. Class I KATs are large multidomain enzymes with a single GNAT domain, class II are smaller but still with only a single GNAT domain, and class III contain multiple GNAT

domains. Class I KATs can be divided in class I $\alpha$ , which contain an NDP-forming acyl-CoA synthetase domain and a GNAT catalytic domain, and class I $\beta$ , which contain an effector/regulator domain and a GNAT catalytic domain. Then, each class of KAT is categorized into types. Type I and II KATs are both within class I $\alpha$ ; type I KATs have a C-terminal GNAT domain, while type II KATs have an N-terminal GNAT domain. Type III KATs belong to class I $\beta$  and contain an N-terminal regulatory domain and a C-terminal GNAT domain. Type IV KATs belong to class II and type V KATs belong to class III.

Type I and type II GNATs are the best-studied class of bacterial KATs, exemplified by YfiQ and its homologs (also known as Pat, PatZ, and Pka). YfiQ is a conserved acetyltransferase with homologs found across various bacterial species (140, 160-166). *S. enterica* Pat (SePat) and *E. coli* YfiQ (EcYfiQ) have been observed to form oligomers in the presence of AcCoA, suggesting positive cooperativity in these enzymes (158, 167). The best-studied role for YfiQ is the acetylation of acetyl-CoA synthetase (Acs), which is discussed in-depth later. However, it is also implicated in protections against acid stress, high temperature, and reactive oxygen species, and the identification of various substrates for EcYfiQ suggests several potential regulatory roles (168-170).

Type III or class I $\beta$  GNATs are mainly KATs with allosteric regulator domains. Identified regulatory domains fused to the GNAT catalytic domain include an amino acid binding domain (ACT), a cAMP binding domain, and an NADP<sup>+</sup> binding domain (159, 171-173). These regulatory domains likely serve to tie the regulation of these KATs to metabolic pathways.

Type IV (class II) GNATs are small proteins (150 to 200 amino acids) with a single catalytic GNAT domain, while type V (class III) GNATs are medium proteins (~400 amino

acids) made of multiple GNAT domains. While many type IV KATs have been identified, their role in protein acetylation is less characterized than the class I GNATs (164, 170, 174-180). The only known type V KAT is enhanced intracellular survival (Eis) protein from *M. tuberculosis* (181-183). However, both type IV and type V KATs are often capable of additional activities. For example, Eis from *M. tuberculosis* was initially discovered as an aminoglycoside acetyltransferase and is capable of acetylating host proteins as well as its own proteins (183-185). Also, type IV GNAT RimI was known as an N- $\alpha$ -acetyltransferase before also being characterized as a KAT (170, 186-189).

### **Nonenzymatic or Chemical Acetylation**

In bacteria, AcP, a high-energy small metabolite, can nonenzymatically acetylate proteins. For a lysine residue to be sensitive to nonenzymatic acetylation, the reactive lysine must be deprotonated, either by a negatively charged amino acid in close proximity (i.e., Asp or Glu) or by a water molecule. Then, the protein must be able to coordinate AcP for nucleophilic attack by the activated lysine. This can be achieved through interactions of the phosphoryl group of AcP with positively charged amino acids (Lys or Arg), hydrogen bonds from hydroxyls (Ser, Thr, or Tyr), or side chain amide groups (Gln or Asn). While a specific linear sequence is not required for nonenzymatic acetylation, it is common to observe glutamate or aspartate near the +1 or -1 position relative to the acetylated lysine, as this lowers the pK<sub>a</sub> of the lysine (4, 190-193).

AcP-dependent acetylation is the predominant type of acetylation in *E. coli* and several other bacteria (3, 4, 190). However, it should be noted that most acetylome studies have not distinguished between enzymatic and nonenzymatic acetylation; thus, for most bacteria, we do not know which mechanism is predominant. In species where AcP-dependent acetylation

predominates, AcP is generated through the Pta-AckA pathway, as previously described. *E. coli* does have alternative routes to generate AcP, but their activity is either more situational than the activity of Pta-AckA or not well-studied for their contribution to AcP synthesis (194-197).

In other bacteria, there are alternative routes of AcP production. *Lactobacillus* and *Streptococcus* species synthesize AcP with pyruvate oxidase (SpxB). This is distinct from *E. coli* pyruvate oxidase (PoxB), which is acetate-forming (133). While the Pta-AckA pathway is nonessential, in certain Gram-positive species AcP synthesis is a key component of their metabolism. For example, *Lactobacillus* and *Bifidobacterium* species cannot metabolize glucose without generating AcP (198).

In *E. coli*, AcP levels can be manipulated genetically or metabolically. A  $\Delta ackA$  mutant accumulates high levels of AcP and consequently shows increased levels of acetylation, while a  $\Delta ackA\Delta pta$  mutant is defective in AcP synthesis and has a weak acetylation pattern (**Fig. 3A**) (3, 4). Under most conditions, a  $\Delta pta$  mutant phenocopies the double mutant (**Fig. 3A**) but supplementing a  $\Delta pta$  mutant with acetate allows for acetyl phosphate synthesis by AckA, increasing global acetylation, although a band of acetylation (most likely Acs) at approximately 75 kDa is lost (**Fig. 3B**) (4). Acetate supplementation also is sufficient to increase global acetylation in wild-type *E. coli* as well (**Fig 3B**). Depending on carbon source and strain background, *E. coli* intracellular concentration of AcP can reach high-micromolar to low-millimolar ranges (3, 199, 200).

Build-up of AcP and nonenzymatic acetylations depends on two factors: rapid carbon flux and a carbon-nutrient imbalance that restricts growth (6, 144, 201). As discussed above, the Pta-AckA pathway is active during overflow metabolism, leading to increased protein

acetylation when cells have access to high carbon levels. However, when the cells are actively growing, dividing, and synthesizing nascent protein, the overall level acetylation remains low.

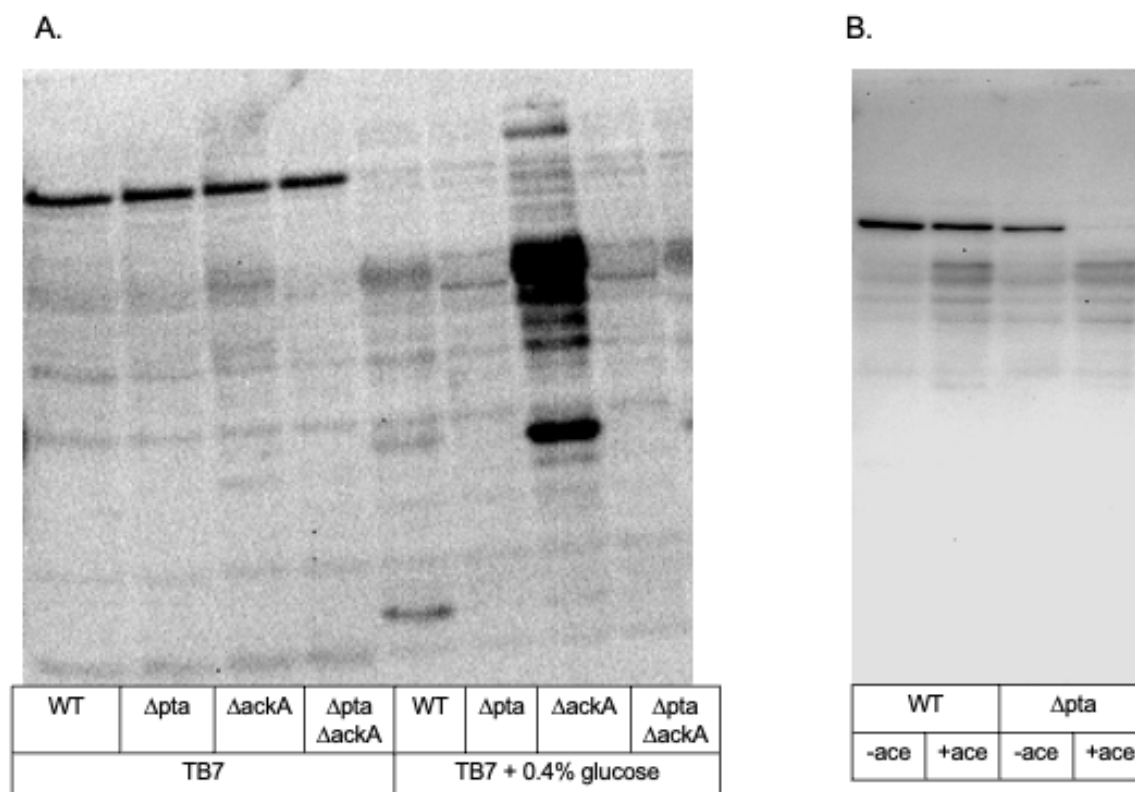


**Figure 3. Genetic and Metabolic Manipulations of Nonenzymatic Acetylation in *E. coli*.** **A.** *E. coli* BL21 (DE3) WT,  $\Delta$ pta,  $\Delta$ ackA, and  $\Delta$ ackApta were grown for 8 hours in buffered tryptone broth or buffered tryptone broth supplemented with 0.4% glucose then harvested for Western blots using anti-acetyllysine antibody. Samples were normalized by protein content for loading. The blot is representative of 3 biological replicates. **B.** *E. coli* MG1655 WT and  $\Delta$ pta was grown in MOPS + 0.2% glucose for 8 hours then harvested for Western blots using anti-acetyllysine antibody. When noted, cultures were supplemented with 0.27% acetate at 6 hours of growth. Samples were normalized by protein content for loading. The blot is representative of 3 biological replicates.

When a culture enters stationary phase due to the lack of a noncarbon nutrient (for example: nitrogen or magnesium), flux continues through the Pta-AckA pathway (3, 202). However, the

stationary phase reduction in nascent protein synthesis and division leads to an accumulation of AcP and thus acetylations within the cell.

### **Deacetylation**

The removal of an acetyl group requires a lysine deacetylase (KDAC). There are two known families of KDACs: the zinc-dependent Rpd3/Hda1 and the NAD<sup>+</sup>-dependent sirtuin family (203, 204). Both families can be found across bacteria, but this review will focus on sirtuins, as the only known KDAC in *E. coli* and *S. enterica* is the sirtuin CobB (205). This has made it the best studied bacterial KDAC. YcgC has been proposed as a second KDAC in *E. coli* but was later found to be misidentified (206, 207). In fact, a  $\Delta cobB$  *E. coli* mutant had almost no deacetylase activity when tested against an acetylated peptide library, suggesting it is the sole deacetylase for this species (205).

The number of acetylated targets deacetylated by CobB is much lower than the number of targets acetylated by YfiQ or AcP. Although it can vary based on the conditions, between 5% and 14% of acetylated targets in *E. coli* are deacetylated by CobB *in vivo* (3, 4, 193). However, CobB deacetylation targets acetylations generated via enzymatic and nonenzymatic mechanisms without preference (160, 208-211). In fact, CobB appears to have promiscuous deacylase activity, being able to remove succinyl, propionyl, lipoyl, and homocysteine groups as well as acetyl groups (212-216).

Perhaps not surprisingly, considering its promiscuous function, the determinants for acetyllysine sensitivity to CobB are not clear. CobB substrates tend to be surface exposed on  $\alpha$ -helices and loops. Buried acetylations are inaccessible to CobB. It has been proposed that there is a population level “deacetylation” of irreversible acetylations through protein turnover and dilution through nascent protein synthesis (135).

I would argue that sensitivity to deacetylation is not the key determining factor in the physiological relevance of a lysine acetylation. However, it is still important to consider the sensitivity of an acetylation to deacetylation, as this can provide insight into the purpose of the acetylation.

### **The Breadth of Lysine Acetylation**

Lysine acetylation is a prevalent post-translational modification, but in bacteria, the purpose of much of the observed acetylation is unknown. In this section, I will discuss the variety of available acetylomes and elaborate on several specific examples of lysine acetylation's functional relevance. Due to the large pool of available studies, this section cannot possibly hope to be exhaustive but aims to provide useful examples and context.

#### **Acetylomes**

As mass spectrometry techniques have become more advanced, a variety of strategies have been developed to identify specific lysine acetylations and even quantitatively characterize the acetylome (217). This includes isotope or chemical labeling strategies as well as label-free quantification methods (4, 136, 170, 218-220).

While many acetylomes focus on identifying specific acetylations in a given bacterium under one condition, the early and extensive exploration of the *E. coli* acetylome can serve as an example of what is possible (221, 222). Using mutants lacking YfiQ or CobB, mass spectrometry was used to identify enzyme-regulated acetylation sites (4, 158, 193, 205, 212, 223). More recently, overexpression of several novel *E. coli* KATs was used to characterize their putative targets (170). To identify AcP-regulated acetylation sites, studies have utilized  $\Delta$ *ackA* and  $\Delta$ *pta* $\Delta$ *ackA* mutants, compared WT *E. coli* growing in high or low glucose, and compared WT *E. coli* growing on glucose or xylose (3, 4, 6, 201).

**Table 1. List of Archaeal, Bacterial, and Some Simple Eukaryotic Acetylomes**

Study	Organism	Mutant(s) assessed	Conditions assessed		No. of lysines	No. of proteins
			Time/Growth phase	Medium		
(2)	48 bacteria from <i>Proteobacteria</i> , <i>Firmicutes</i> , <i>Bacteroidetes</i> , <i>Actinobacteria</i> , <i>Cyanobacteria</i> , and <i>Fibrobacteres</i>	None	See Table S1 in (2)	See Table S1 in (2)	24,397	9,107
(224)	<i>Acinetobacter baumannii</i> ATCC 17978	None	SP	MHB	551	441
(225)	<i>Aeromonas hydrophila</i> ATCC 7966	None	1.0 OD	LB	3,189	1,013
(226)	<i>Aspergillus flavus</i> CA43 (fungus)	None	48 h	PDA-cellophane	1,383	652
(227)	<i>Bacillus amyloliquefaciens</i> DSM7	None	EP	LB	3,268	1,254
(228)	<i>Bacillus nematocidal</i> B16	None	12 h	Solid LB with or without nematode incubation	529	349
(229)	<i>Bacillus subtilis</i> 168	None	0.5 OD (EP)	Minimal medium with glucose	1,355	629
(230)	<i>Bacillus subtilis</i> 168	None	Multiple conditions from previous mass spectrometry runs	Multiple conditions from previous mass spectrometry runs	4,893	1,277

(231)	<i>Bacillus subtilis</i> 3610	<i>pta, acuA</i>	SP	LB with 1% (vol/vol) glycerol and 100 µM manganese	1,172	826
(232)	<i>Bacillus subtilis</i>	None	EP and SP	Minimal glucose medium	2,372	841
(233)	<i>Borrelia burgdorferi</i> B31-A3	<i>pta, ackA</i>	EP and SP	BSK-II medium	199	68
(234)	<i>Brenneria nigrifluens</i> LMG 2,694	None	24 h	TSB	1,866	737
(235)	<i>Clostridium acetobutylicum</i>	None	EP, transition, and SP	Defined medium	458	254
(236)	<i>Corynebacterium glutamicum</i> ATCC 13869	None	9 h	Glutamate-producing medium +/- Tween 40	1,328	288
(237)	<i>Cyanobacterium Synechococcus</i> sp. PCC 7002	None	EP (under various stresses)	A+ medium	1,653	802
(238)	<i>Edwardsiella tarda</i> EIB202	None	1.0 OD	LB	1,511	589
(239)	<i>Erwinia amylovora</i> Ea1189, Ea273	None	SP	MBMA minimal medium	141	96
(223)	<i>Escherichia coli</i> BL21	<i>cobB</i>	SP	2XYT	2,206	899
(201)	<i>Escherichia coli</i> BW25113, BL21, MG1655	<i>yfiQ, cobB, ackA, pta</i>	EP and SP; growth arrested	M9/glucose, nitrogen-limited M9/glucose	8,284	1,000
(240)	<i>Escherichia coli</i> DH10	None	EP	LB	1,070	349
(212)	<i>Escherichia coli</i> DH10B	None	EP	M9/glucose/lysine/arginine	2,803	782
(221)	<i>Escherichia coli</i> DH5a	None	EP	LB	138	91
(4)	<i>Escherichia coli</i> MG1655	<i>ackA, pta, ackA, cobB, yfiQ</i>	1 OD (EP-SP transition)	TB7 and TB7/glucose	2,730	806

(241)	<i>Escherichia coli</i> MG1655 and BW25113	MG1655: <i>cobB</i> ; BW25113: <i>ackA</i> , <i>pta</i>	EP and SP; EP	M9/glucose/lysine/arginine	3,669	Not stated
(222)	<i>Escherichia coli</i> W3110	None	EP and SP	LB	125	85
(193)	<i>Escherichia coli</i> BW25113	<i>yfiQ</i> , <i>cobB</i>	EP and SP; EP; steady state	Minimal glucose batch; minimal acetate batch; glucose chemostat	2502	809
(242)	<i>Francisella tularensis</i> spp. <i>novidica</i> U112	None	20-22 h	TSB + 0.1% cysteine/sodium acetate; TSB + 0.1% cysteine/glucose; BHI broth pH = 6.8	1,178	280
(243)	<i>Fusarium</i> <i>graminearum</i> PH-1 (grain fungal pathogen)	<i>Fggcn5</i>	4 days (mycelia)	Potato dextrose agar	2,626	1,875
(244)	<i>Geobacillus</i> <i>kaustophilus</i> 7263	None	SP	Difco nutrient broth	253	114
(141)	<i>Haloferax</i> <i>mediterranei</i>	None	EP	MG medium	1,017	643
(245)	<i>Mycobacterium</i> <i>abscessus</i> GZ002	None	EP	Middlebrook 7H9 medium	459	289
(246)	<i>Mycobacterium</i> <i>smegmatis</i> MC2155	None	EP, early SP, and middle SP	Middlebrook 7H9 liquid with 10 mM glucose	146	121
(247)	<i>Mycobacterium</i> <i>tuberculosis</i> H37Ra	None	EP and SP	Middlebrook 7H9 liquid culture medium	226	137
(248)	<i>Mycobacterium</i> <i>tuberculosis</i> H37Ra	None	EP; 3 wk	Middlebrook 7H9 aerobically; Middlebrook 7H9 anaerobically	441; 111	286; 83
(249)	<i>Mycobacterium</i> <i>tuberculosis</i> H37Rv	None	EP	Middlebrook 7H9 medium	1,128	658

(250)	<i>Mycobacterium tuberculosis</i> H37Rv	None	12 days (EP)	7H9 broth aerobically and anaerobically	1,215	679
(251)	<i>Mycobacterium tuberculosis</i> L7-35, L7-28, and H37Rv	None	32 days	Middlebrook 7H10 plates	141	109
(252)	<i>Mycoplasma pneumoniae</i> M129	<i>pnkB</i> , <i>hprK</i> (kinases); <i>prpC</i> (phosphatase); Mpn027, Mnp114 (putative acetyltransferases)	EP	Hayflick medium	719	221
(5)	<i>Neisseria gonorrhoeae</i> 1291	<i>ackA</i>	Overnight	IsoVitaleX-supplemented GC broth	2,686	656
(253)	<i>Porphyromonas gingivalis</i> W50	None	SP	BHI	130	92
(254)	<i>Pseudomonas aeruginosa</i> PA14	None	24 h	Minimal glucose medium	430	320
(255)	<i>Pseudomonas aeruginosa</i> PA14	None	SP (24 h)	Minimal medium with citrate, glucose, glutamate, or succinate	1,102	522
(164)	<i>Rhodopseudomonas palustris</i> CGA009	<i>ldaA srtN</i> , <i>ldaA srtN pat</i> , <i>ldaA srtN pat katA</i>	0.5 OD	Photosynthetic medium with benzoate	32	24
(256)	<i>Saccharomyces cerevisiae</i> BY4742	<i>rpd3</i>	EP	Synthetic complete medium	2,878	1,059
(257)	<i>Saccharopolyspora erythraea</i> NRRL233338	None	EP	TSBY	664	363
(258)	<i>Salmonella enterica</i> serovar Typhimurium ATCC 13311	Ciprofloxacin resistant vs WT	EP	LB	1,259	631

(259)	<i>Salmonella enterica</i> serovar Typhimurium LT2 (G2466)	<i>pat, cobB</i>	EP	M9/glucose and M9/citrate	235	191
(260)	<i>Shewanella baltica</i>	None	0.7 OD	LB	2,929	1,103
(261)	<i>Spiroplasma eriocheiris</i> TDA-040725-5T	None	EP	R2 medium	2,567	555
(262)	<i>Staphylococcus aureus</i> 209P	None	24 h	Cell medium	1,361	412
(263)	<i>Staphylococcus aureus</i>	None	EP	TSB	1,778	794
(264)	<i>Streptococcus pneumoniae</i> D39	None	EP	THY medium	653	392
(265)	<i>Streptomyces coelicolor</i> M145	$\Delta SccobB1$ ; $\Delta SccobB2$	EP	TSB/glucose	1,298	601
(166)	<i>Streptomyces griseus</i> IFO13350	None	SP; sporulation	Liquid TMPD medium, solid YMPD medium	162	134
(266)	<i>Streptomyces roseosporus</i> NRRL15998	None	EP (3 days)	F10A medium	1,143	667
(267)	<i>Sulfolobus islandicus</i> E233S	$\Delta SisPat$ ; $\Delta SisArd1$	EP	Zillig's medium with uracil (20 $\mu$ g/ml)	1,708	158
(268)	<i>Sulfurospirillum halorespirans</i> DSM 13726	None	Early and late EP	Defined mineral medium	Not stated	640
(269)	<i>Synechocystis</i> sp. PCC 6803	None	EP	BG11 medium	776	513
(192)	<i>Thermus thermophilus</i> HB8	None	SP	TT broth	197	128
(270)	<i>Thermococcus gammatolerans</i> EJ3	None	16 h (EP-SP transition)	VSM supplemented with S <sup>o</sup> (2 g/l) anaerobically	338	181

	(extremophile archaeon)					
(271)	<i>Toxoplasma gondii</i> RH strain	None	64-128 parasites/vacuole	Infected hTERT+HFF cells in DMEM	411	274
(272)	<i>Toxoplasma gondii</i> RH strain	None	95% host lysis	Infected hTERT+HFF cells in DMEM	571	386
(273)	<i>Trichophyton rubrum</i> (fungal pathogen)	None	Conidia; mycelia	PDA; Sabouraud liquid medium	386; 5,414	285; 2,335
(274)	<i>Vibrio alginolyticus</i> HY9901	None	EP	LB	2,537	1,178
(275)	<i>Vibrio cholerae</i> V52	None	EP and SP	LB	3,402	1,240
(276)	<i>Vibrio mimicus</i>	None	1.0 OD	DMEM	1,097	582
(277)	<i>Vibrio</i> <i>parahaemolyticus</i> O3:K6	None	8 h	High-salt LB	1,414	656
(278)	<i>Vibrio vulnificus</i> Vv180806	None	0.6 OD	LB; 3% alkaline peptone water medium; artificial seawater	6,626	1,924

As shown in **Table 1**, mass spectrometry strategies have been used to explore acetylomes in a wide variety of bacteria, archaea, and simple eukaryotic organisms. While this list is meant to provide insight into the wide-ranging prevalence of lysine acetylation, it is worth highlighting a few unique examples.

First, it is worth discussing Nakayasu et al. 2017. While other commonly used mass spectrometry workflows for generating acetylomes include a step that enriches acetylated peptides after cell lysis, Nakayasu and colleagues analyzed acetylation sites directly from bacterial protein lysates (2). They used this approach to investigate the acetylomes of 48 phylogenetic distant bacteria, revealing that acetylation is a highly conserved and ancient post-translational modification. Relevant for this dissertation, they also identified the ribosome as one of the pathways most enriched for acetylations across these bacterial species.

Also of interest are two studies that could not be easily fit into the organization of **Table 1**. These studies characterize the acetylome of the human gut microbiome (279, 280). These acetylomes are unique for looking not at a specific species, but rather at the acetylome of the microbiome as a whole. For example, one analysis revealed differences in the community acetylomes from samples taken from patients with Crohn's disease and those without (280). The acetylation state of the microbiome may impact how it interacts with the host. Considering the high concentration of acetate in the large intestine (~70 mM), it is plausible much of the acetylation in the gut microbiome comes from AcP-dependent acetylation.

### **Functionally Relevant Lysine Acetylations**

While the purpose of many lysine acetylations are unknown, several lysine acetylations have evidence suggesting a physiological role for the modification. In this section, I will discuss

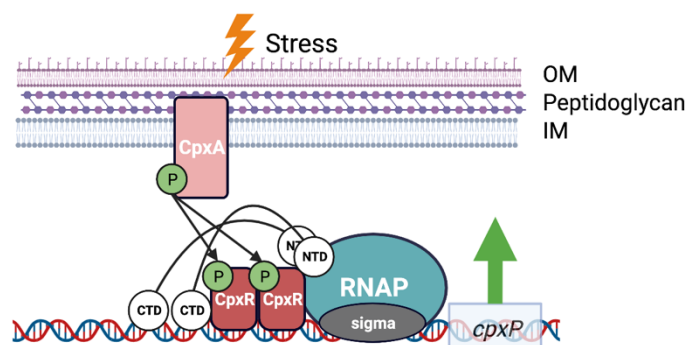
a few specific examples to provide an overview of the current state of the field, but this is not an exhaustive review.

The earliest example of functionally relevant lysine acetylation is the acetylation of the *E. coli* chemotaxis protein CheY (281). However, CheY acetylation differs from most other lysine acetylations, as the acetylations of CheY are catalyzed by acetyl-CoA synthetase (Acs) or occur nonenzymatically using AcCoA as an acetyl donor (282, 283). The use of AcCoA as an acetyl donor is interesting, as most nonenzymatic acetylation in *E. coli* uses AcP as the acetyl donor (3, 4). Therefore, while it has historic importance for the field, when considering the relevance of global lysine acetylation, it might be considered an outlier, as Acs and AcCoA are not common mechanism of acetylation.

The regulation of acetyl-CoA synthetase (Acs) by the lysine acetyltransferase YfiQ (also known as Pat in *Salmonella* or PatZ in *E. coli*) and deacetylase CobB is the most classical example of regulation through acetylation. First identified in *Salmonella enterica*, Acs acetylated at K609 is inactive, and thus unable to assimilate acetate (162, 284). Removal of the acetylation by the sirtuin CobB restores functionality (284). Regulation of Acs in this manner is also observed in *E. coli*, and although the specific enzymes involved are different, *Bacillus subtilis* Acs is also regulated by lysine acetyltransferases and deacetylases (160, 176, 285, 286).

However, the role of lysine acetylations can often be more complicated than the example of Acs. One example is the regulation of the *cpxP* promoter in *E. coli*, which responds to extracytoplasmic stress. Transcription of the *cpxP* promoter is controlled by the two-component system CpxAR. The histidine kinase CpxA autophosphorylates in response to extracytoplasmic signals, phospho-CpxA functions as the phosphoryl donor for the aspartate kinase CpxR, and phospho-CpxR activates *cpxP* transcription (**Fig. 4**).

### Stress-Induced *cpxP* Transcription



### CpxA-Independent, Glucose-Induced *cpxP* Transcription

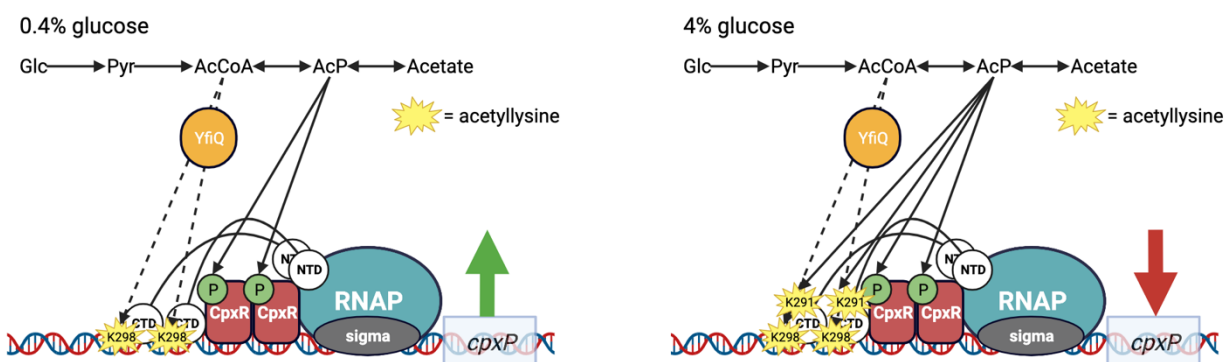


**Figure 4. Stress-Induced and Glucose-Induced *cpxP* Transcription.** Stress-induced *cpxP* transcription occurs when stresses to the outer membrane (OM) are sensed by CpxA. This leads to CpxA autophosphorylation and subsequent transfer of the phosphoryl group to CpxR. Phospho-CpxR activates *cpxP* transcription. CpxA-independent *cpxP* transcription responds to glucose levels. At 0.4% glucose, the acetyltransferase YfiQ acetylates K298 in the C-terminal domain (CTD) of the RNA polymerase (RNAP). Acetyl phosphate (AcP) phosphorylates CpxR and together the acetylation of RNAP and the phosphorylation of CpxR activate *cpxP* transcription. At 4% glucose, increased levels of AcP allow for AcP-dependent acetylation of K291 in the CTD of RNAP. This acetylation dampens the effect of phosphor-CpxR and the acetylation of K298 in the CTD.

In the absence of stress signals, CpxA acts as a net phosphatase towards CpxR, removing phosphoryl groups. However, CpxA-independent activation of *cpxP* transcription occurs when glucose is added to cultures in tryptone broth.

Glucose-induced *cpxP* transcription is regulated by the interplay between phosphorylation, enzymatic acetylation, and nonenzymatic acetylation. This response requires the enzymatic acetylation of K298 on the  $\alpha$ CTD of RNA polymerase (RNAP), the AcP-dependent phosphorylation of D51 on CpxR, and can be tuned by the AcP-dependent acetylation of K291 on the  $\alpha$ CTD of RNAP. The addition of 0.4% glucose induces YfiQ acetylation of K298 on RNAP and AcP-dependent phosphorylation of CpxR, activating *cpxP* transcription (**Fig. 4**) (287, 288). The addition of 4% glucose does not induce *cpxP* as strongly as 0.4% glucose, but induction can be restored by replacing K291 of RNAP with an alanine. Strains lacking *ackA* do not induce *cpxP* transcription in response to glucose at either concentration, and acetylation of K291 has been identified as AcP-dependent (4, 287). The interplay of multiple post-translational modifications allows glucose-induced *cpxP* transcription to respond differently to different concentrations of glucose, with lower concentrations of glucose favoring YfiQ-dependent acetylation at K298 and high concentrations allowing for AcP-dependent acetylation at K291 (**Fig. 4**).

There has been much discussion in the field arguing that one area likely to be regulated by lysine acetylation is central carbon metabolism. Several enzymes that contribute to glycolysis and the TCA cycle, including malate dehydrogenase, isocitrate dehydrogenase, citrate synthase, and enolase, have been shown to be inhibited by acetylation *in vitro* (2, 209, 289, 290). However, questions remain about the function of these acetylations *in vivo*. Most acetylation studies do not

analyze the stoichiometry of the modification, which may be important for physiological relevance.

Recent work has attempted to address this question in an interesting way. After purifying 19 *E. coli* central metabolic enzymes with identified *in vivo* as acetylated in an AcP-dependent manner, Schastnaya, et al. incubated the purified proteins with 1 mM AcP for 1 hour and then analyzed them with intact protein mass spectrometry (291). This allowed them to identify the stoichiometry of acetylated proteins in a way that mass spectrometry techniques that require proteins digestion prior to analysis cannot. Of the proteins investigated, only GapA and GpmA were found to have significant levels of acetylation, with approximately 80% of the GapA and 50% of the GpmA acetylated. *In vitro* comparisons of enzymatic activity between WT and AcP-treated GapA and GpmA demonstrated reduced activity for the AcP-treated proteins. With the caveat that there are *in vivo* influences that *in vitro* experiments cannot capture, this work demonstrates that certain nonenzymatic acetylations can occur at specific sites with a high degree of stoichiometry and that these acetylations can alter protein function.

It is also worth noting that the GapA and GpmA residues investigated by Schastnaya et al. are not verified targets of the CobB deacetylase. This suggests that the reduction in activity must be relieved by protein turnover. As discussed earlier, most lysine acetylations in *E. coli* are not observed to be sensitive to CobB deacetylation. While reversible modifications are easy to classify as a regulatory loop, it likely that a number of lysine acetylations have physiological impacts that can only be alleviated by introducing new, unacetylated protein.

### Summary

The ribosome is a complex and critical piece of molecular machinery. In bacteria, the function of the ribosome responds to a variety of signals to properly tune translation. Because the

ribosome responds differently to different stresses, many signals must exist to regulate translation. Additionally, the ribosome has different functions during different growth phases.

One potential form of regulation is the acetylation state of the ribosome. The bacterial ribosome is a consistent site of enriched lysine acetylation in a wide variety of bacterial acetylomes and a number of these acetylated residues are widely conserved in bacteria (2, 292). It is therefore reasonable to wonder if the modification has some functional relevance. While the source of a given acetylation in many bacteria is unknown, the number of acetylomes available for *E. coli* allows for discrimination between enzymatic acetylations by KATs and nonenzymatic acetylations by AcP. In *E. coli*, roughly half of the acetylations observed on the ribosome occur nonenzymatically, including several at conserved residues.

If AcP-dependent acetylation alters the behavior of the bacterial ribosome, it could serve as a link between the ribosome and central carbon metabolism. The levels of AcP in *E. coli* shift based on the amount of carbon flux through the Pta-AckA pathway. Growth on excess glucose and growth on acetate promote carbon flux through the Pta-AckA pathway, and mutations in the genes for AckA and Pta alter global acetylation levels in specific ways depending on carbon source.

There are many examples of acetylations that can alter the function of a protein, both enzymatic and nonenzymatic acetylations. Some acetylations that impact protein function can be removed by a deacetylase, but some cannot.

Based on this background, the goal of this work is to investigate AcP-dependent acetylation as a potential modifier of bacterial ribosome function. In Chapter 3 of this dissertation, I will demonstrate that AcP levels affect aspects of ribosome function both *in vitro* and *in vivo*. While I am unable to conclusively demonstrate which step of translation is impacted,

using LacZ as a translational reporter, I show that elongation rate is unaltered under high acetylation conditions, despite other changes to the ribosome population. Using a variety of genetic mutants and media conditions, I will show that these effects are due to flux through the Pta-AckA pathway, not a quirk of one specific mutant or *in vitro* system. Next, I will investigate the impact of the CobB deacetylase on AcP-dependent acetylation effects on the ribosome *in vitro* and *in vivo*. CobB-sensitive lysine residues appear to contribute to some changes in ribosome function observed, but it seems likely a mix of sensitive and non-sensitive residues are involved. Finally, I will attempt to identify potentially relevant lysine residues. While qualitative differences are apparent between individual 50S and 30S subunits and intact 70S ribosomes in both WT and  $\Delta ackA$  (acetylation high) strains, the initial mass spectrometry experiment was insufficient to resolve differential acetylations between the subunits and the 70S in  $\Delta ackA$ . Residues only acetylated on the subunits could be identified in WT, but comparisons between the extent acetylations in WT and  $\Delta ackA$  could not be drawn.

## CHAPTER TWO

### MATERIALS AND METHODS

#### **Bacterial Strains, Plasmids, and Primers**

All strains used in this study are derivatives of *Escherichia coli* K-12 strains BW25113 or MG1655 or of the *E. coli* B strain BL21 and are described in **Table 2**. Plasmids used in this study are described in **Table 2**. Primers used in this study are described in **Table 3**. Mutants were constructed using generalized transduction with P1kc (see “Generalized P1 Transduction” for details) or the Conditional-replication, integration, and modular (CRIM) plasmid system (see “CRIM Plasmid System” for details). Transformants were generated by two methods described in “Transformations.”

#### **Media and Growth Conditions**

Cells were cultured for strain construction in Lysogeny Broth (LB, Lennox) containing 10 g/liter tryptone, 5 g/liter yeast extract, and 5 g/liter sodium chloride. LB plates contained 15 g/liter agar. As specified in the given experiments, cells were cultured in either a TB7 (buffered tryptone broth), M9 minimal medium, or MOPS minimal medium as described by McCleary and Stock (293). TB7 contains 10 g/liter tryptone and is buffered to pH 7.0 with 100 mM potassium phosphate (61.5 mM potassium phosphate dibasic and 38.5 mM potassium phosphate monobasic). Where specified the TB7 was supplemented with 0.4% or 0.2% [w/v] glucose. MOPS minimal medium contains 40 mM MOPS salts, 4 mM tricine, 50 mM sodium chloride, 9.52 mM NH<sub>4</sub>Cl, 0.52 mM MgCl<sub>2</sub>, 0.275 mM K<sub>2</sub>SO<sub>4</sub>, 0.01 mM FeSO<sub>4</sub> – 7H<sub>2</sub>O, 0.5 μM CaCl<sub>2</sub>, 0.2 mM KH<sub>2</sub>PO<sub>4</sub>, and 2.0 mM KH<sub>2</sub>PO<sub>4</sub>, and pH to 7.2 with hydrochloric acid.

**Table 2. Strain and Plasmid List**

<b>Strain</b>	<b>Description</b>	<b>Reference</b>
BW25113	F <sup>-</sup> λ <sup>-</sup> Δ( <i>araD-araB</i> ) <sub>567</sub> Δ( <i>rhaD-rhaB</i> ) <sub>568</sub> Δ <i>lacZ</i> <sub>4787</sub> <i>rrnB3 rph-1 hsdR514</i>	(294)
MG1655	λ- <i>rph-1</i>	A. Ninfa (University of Michigan)
AJW6217	BW25113 Δ <i>ackA::frt kn</i>	(292)
AJW6267	BW25113 Δ <i>ackA::frt</i>	(292)
AJW6215	BW25113 Δ <i>pta::frt kn</i>	(292)
AJW6266	BW25113 Δ <i>pta::frt</i>	(292)
HW3125	BW25113 Δ <i>ackA::frt λatt::ackA</i>	(292)
HW3126	BW25113 Δ <i>pta::frt λatt::pta</i>	(292)
AJW6341	MG1655 Δ <i>pta::frt kn</i>	(292)
AJW6372	MG1655 Δ <i>pta::frt</i>	(292)
AJW6377	MG1655 Δ <i>pta::frt λatt::pta</i>	(292)
JW2293	Δ <i>ackA::frt kn</i>	(295)
JW2294	Δ <i>pta::frt kn</i>	(295)
JW1106	Δ <i>cobB::frt kn</i>	(295)
AJW5884	BW25113 Δ <i>cobB::frt kn</i>	This study
AJW6386	BW25113 Δ <i>ackA::frt ΔcobB::frt kn</i>	This study
AJW6385	BW25113 Δ <i>ackA::frt pCA24n-cobB</i>	This study
AJW6413	BL21 (DE3) pCA24n- <i>cobB</i>	This study
<b>Plasmids</b>		
pINT-ts	Int <sub>λ</sub> helper plasmid	(296)
pAH125-ackA	CRIM integration plasmid	This study
pAH125-pta	CRIM integration plasmid	This study
pCA24n- <i>cobB</i>	ASKA collection, contains 6xHis-CobB	(297)
pTXTL-P70a(2)-deGFP	Plasmid for cell-free transcription-translation of GFP	(298)

**Table 3. Primer List**

<b>Primer</b>	<b>Sequence</b>
Kan RV	Check Dave's dissertation, because the sequence isn't in his primer list
ackA FW	5'-GCGCTACGCTCTATGGCT-3'
ackA RV	5'-CGTTCCATTGCACGGATCAC-3'
pta FW	5'-GCGGTGGTTATCCCAACC-3'
pta RV	5'-GCAAAGTGGGATGGCGC-3'
cobB FW	5'-AGCTCGTGTTCGCGC-3'
cobB RV	5'-CCACAAAACCCGCAAATTCA-3'
P1 CRIM	5'-GGCATCACGGCAATATAC-3'
P2 CRIM	5'-ACTTAACGGCTGACATGG-3'
P3 CRIM	5'-ACGAGTATCGAGATGGCA-3'
P4 CRIM	5'-TCTGGTCTGGTAGCAATG-3'
16S FW	5'-CGGTGGAGCATGTGGTTTA-3'
16S RV	5'-GAAAACCTCCGTGGATGTCAAGA-3'
deGFP FW	5'-GCACAAGCTGGAGTACAATA-3'
deGFP RV	5'-TGTTGTGGCGGATCTTGAA-3'

MOPS media was supplemented with 0.2% [w/v] glucose or 0.2% [w/v] glucose and 0.27% [w/v] sodium acetate. All cultures were grown at 37 °C and aerated at 225 rpm with a flask-to-medium ratio of 5:1.

Antibiotics were prepared as stock solutions 1000 times the working concentration. Working concentrations were as follows: ampicillin, 100 µg/mL; kanamycin, 40 µg/mL; and chloramphenicol, 25 µg/mL, 34 µg/mL, or 100 µg/mL as specified by experiment. Stock solutions of ampicillin and kanamycin were dissolved in water and filter sterilized. Stock solutions of chloramphenicol were dissolved in 100% ethanol and filter sterilized. All antibiotic stocks were stored at -20 °C. To induce expression from the pCA24n plasmid, IPTG (Isopropyl β-D-1-thiogalactopyranoside) was added to a final concentration of 100 µM.

### **Generalized P1 Transduction**

To generate phage lysates, the donor strain (typically from the KEIO collection) was aerated until 0.3 OD 600 in TBT (TB with 0.2% [w/v] glucose, 10 mM CaCl<sub>2</sub>, 10 mM MgSO<sub>4</sub>, 0.004 ferric chloride) with antibiotic, if appropriate. When appropriate density was reached, 100 μL of a P1kc phage lysate was added and aeration was resumed for three to five hours until complete lysis. The lysate was treated with 100 μL of chloroform, vortexed, and centrifuged at 4000 x g for 15 minutes. The supernatant was transferred to a new tube, treated with 100 μL chloroform and stored at 4°C in the dark.

To transduce a recipient strain, the recipient strain was grown overnight in LB and diluted into 5 mL TBT to an OD600 of 0.02-0.04. The recipient was aerated until 1.0 OD600 and 1 mL of culture was transferred into 1.5 mL tubes. 100 μL of donor phage lysate was added to the recipient culture, and the tube was incubated statically for 30 minutes at 37°C. Further infection was stopped with 200 μL of 1 M sodium citrate, pH 5.5. The infected cells were pelleted and suspended in 500 μL LB, then another 200 μL 1 M sodium citrate, pH 5.5 was added. The cells were incubated statically at 37°C for 70 minutes then pelleted and suspended in 100 μL sodium citrate, pH 5.5. The entire 100 μL of transduced cells was plated onto LB plates containing the appropriate antibiotic and incubated at 37°C for 24 hours or until colonies appeared. Insertion of kanamycin cassette at the desired location was confirmed by PCR.

### **Elimination of Kanamycin Cassettes Flanked by FRT Sites**

The KEIO collection replaces each non-essential gene of *E. coli* with a kanamycin cassette flanked by FRT sites. These sites allow for the elimination of the cassette when Flp recombinase is expressed. To eliminate the cassette, a mutant containing an FRT-kanamycin-

FRT cassette was transformed using the TBF protocol (see “Transformation”) with the pCP20 plasmid carrying the *flp* gene. Cells were plated on LB/ampicillin, and recovery of the strain was performed at 30°C or below due to the temperature-sensitive origin of replication of pCP20. To ensure loss of the kanamycin cassette, individual colonies that arose were struck on LB and LB/kanamycin and grown at 30°C. pCP20 is temperature sensitive for replication; thus, to eliminate pCP20, kanamycin-sensitive colonies were struck on LB and grown at 42°C. Loss of pCP20 was confirmed by replica streaking on LB and LB/ampicillin. Resultant kanamycin-sensitive, ampicillin-sensitive strains were checked for kanamycin cassette elimination by PCR.

### **Transformation**

The transformation methods transformation buffers (TBF) and electroporation were used in this study.

#### **TBF**

To produce chemically competent cells, overnight cultures grown in LB (with antibiotic as appropriate) were subcultured into 100 mL LB (with antibiotic as appropriate) and aerated at 225 rpm at 37°C until the OD<sub>600</sub> reached 0.4-0.6. The culture was cooled on ice for 5 minutes and pelleted. The supernatant was removed, and the pellet was suspended with 7.5 mL cold TBF1 (30 mM potassium acetate, 100 mM potassium chloride, 10 mM calcium chloride, 50 mM manganese chloride, 15% glycerol, pH to 5.8 with acetic acid) and incubated for one hour on ice. The suspension was pelleted, supernatant removed, then the pellet was suspended with 2 mL cold TBF2 (10 mM MOPS, 75 mM calcium chloride, 10 mM potassium chloride, 15% glycerol, pH to 6.5 with potassium hydroxide). Cells were transformed immediately.

1  $\mu$ L plasmid DNA was added to 50  $\mu$ L chemically competent cells and chilled on ice for 30 minutes. The cell-DNA mixture was heat shocked in a water bath for 45 seconds at 42°C,

then chilled on ice for 2 minutes. 1 mL LB was added to the transformed cells, and the cells were shaken at 225 rpm at 37°C for one hour. 100 µL of the transformed cells were plated onto LB plates containing the appropriate antibiotic and incubated at 37°C overnight or until colonies appeared.

### **Electroporation**

Overnight cultures grown in LB (with antibiotic as appropriate) were subcultured into 50 mL LB (with antibiotic as appropriate) and aerated at 225 rpm at 37°C until the OD<sub>600</sub> reached 0.4-0.6. The culture was transferred into a 50 mL conical tube and incubated on ice for 30 minutes. The tube was centrifuged at 4000 x g for 7 minutes at 4°C. The supernatant was removed, and each pellet was suspended in cold water. The volume of each suspension was brought to 50 mL with 49 mL of cold water. This wash process was repeated three more times. After the last wash, the pellet was suspended in the liquid remaining after decanting. 1 µL plasmid DNA was added to 50 µL electrocompetent cells, which were then transferred to a chilled electroporation cuvette with a 0.2 cm gap and electroporated at 25 µF, 200 Ω, and 2.5 kV. 1 mL LB was added to the transformed cells, and the cells were aerated at 225 rpm at 37°C for one hour. 150 µL of the transformed cells were plated onto LB plates containing the appropriate antibiotics and incubated at 37°C overnight or until colonies appeared.

### **CRIM (Conditional-replication, integration, and modular) Plasmid System**

Complements for  $\Delta ackA$  and  $\Delta pta$  were constructed by using the CRIM plasmid system to integrate each gene into the  $\lambda$  attachment site (296). The Int-expressing helper plasmid (pINT-ts) was introduced to AJW6267 ( $\Delta ackA$ ) and AJW6266 ( $\Delta pta$ ) using electroporation and

recovered at 30°C to maintain the temperature sensitive plasmid before plating on LB plates containing ampicillin.

The Gibson assembly method was used to ligate the *ackA* gene (MG1655 genomic region 2411492-2412445) and the *pta* gene (MG1655 genomic region 2412769-2414943) with their respective promoter regions into the CRIM integration vector pAH125. The resulting plasmids (pAH125-*ackA* and pAH125-*pta*) were transformed by electroporation into AJW6267 and AJW6268, respectively. After recovery, an additional 30-minute incubation at 42°C was added to promote *int* expression and loss of the helper plasmid. Cells were plated on LB plates containing the appropriate antibiotic and incubated overnight at 37°C or until colonies appear. Individual colonies were struck for isolation on LB plates containing the appropriate antibiotic and incubated at 42°C overnight to ensure loss of the helper plasmid. Integration was confirmed by PCR using the primers P1, P2, P3, and P4 as described in Haldimann and Warner (296).

## **Polysome Profiling**

### **Cell Lysate Preparation**

Strains were grown overnight in LB (with antibiotic as appropriate) and subcultured to an OD<sub>600</sub> of 0.02 in 50 mL media as specified by experiment. Antibiotics were included as necessary. Cultures were aerated at 225 rpm at 37°C for 8 hours to 16 hours as specified by the experiment. When noted, the cultures were supplemented with 0.27% sodium acetate at 6 hours.

Five minutes prior to harvesting the cultures, chloramphenicol at the working concentration of 100 µL/mL was added to each culture. At harvest time, each culture was poured into a chilled 50 mL conical tube lightly packed with ice and put immediately on ice. Cells were pelleted at 4°C at 4000 x g for 15 minutes. The supernatant was decanted, and the pellets were put on ice. The pellets were suspended in 1 mL chilled lysis buffer (10 mM Tris-HCl pH 8.0, 10

mM magnesium chloride, 1 mg/mL lysozyme, and 80 units Ribolock) and transferred to RNase-free 1.5 mL tubes. The suspension was flash frozen in a dry ice-ethanol bath and thawed at room temperature. The freeze thaw cycle was performed three times. After the final freeze-thaw, 30  $\mu$ L of 10% sodium deoxycholate was added and the tube inverted several times to complete lysis. Cellular debris was pelleted by centrifugation at 9400 x g for 10 minutes at 4°C. The clarified portion of the lysate was collected into fresh RNase-free tubes and stored at -20°C prior to profiling.

### **Sucrose Gradient Preparation**

10%-40% sucrose gradients were prepared using the Biocomp Gradient Master 108. Solutions of 10% and 40% sucrose were prepared in Sucrose Buffer (20 mM Tris-HCl pH 7.8, 10 mM magnesium chloride, 100 mM ammonium chloride, 2 mM DTT, DEPC treated water). The sucrose solutions were layered into 13.2 mL thin wall polypropylene tubes and spun using the gradient maker program for 10%-40% sucrose gradients for the SW-41 Ti rotor with short caps. Gradients were balanced for weight and sample was loaded onto the gradients and centrifuged immediately after preparation.

### **Gradient Centrifugation and Fractionation**

Each gradient was loaded with 300  $\mu$ L of *E. coli* lysate and spun using an SW-41 rotor in an ultracentrifuge at 175,117 x g for 3 hours and 45 minutes at 4°C. After centrifugation, gradients were fractionated using the ISCO/Brandel fractionation system by injecting a 50% sucrose solution below the gradient at 1.5 mL/min. Ribosomes were detected by the system's UV spectrophotometer at 254 nm. Fractions were stored at -20°C for future analysis by Western blotting, RNA isolation, or mass spectrometry.

## **RNA Purification and Electrophoresis**

Ribosome peak fractions were pooled. To the individual pooled ribosomal fractions 1.5 x volume of TRIzol™ Reagent (Invitrogen) was added. Sample tubes were shaken for 15 s and incubated at room temperature for 10 minutes. Samples were layered onto a Direct-zol RNA MiniPrep (Zymo Research) spin column and purified following kit instructions. Samples were centrifuged for 1 minute at 9,400 x g. Columns were transferred to a new collection tube, and 400 µL RNA Wash Buffer was added before columns were centrifuged. In a separate RNase-free tube, 5 µL DNase I (6 U/µL) and 75 µL DNA Digestion Buffer were combined. This mix was added direct to the column matrix and incubated at room temperature for 15 minutes. 400 µL Direct-zol RNA PreWash was added to the column and centrifuged. The flow through was discarded and this step repeated. 700 µL RNA Wash Buffer was added to the column and centrifuged. Column was transferred to an RN-ase-free tube. RNA was eluted by adding 50 µL of DNase/RNase-Free water directly to the column matrix and centrifuging for 1 minute at 9,400 x g.

To visualize RNA, 0.5 ug of the purified RNA was mixed with 1.5x volume of deionized formaldehyde, and RNA loading buffer (0.25% bromophenol blue, 0.25% xylene cyanol, 30% glycerol) and the mixture was loaded onto a 1.2% agarose gel made in TBE (45 mM Tris-borate, 1 mM EDTA pH 8.0) using diethyl pyrocarbonate (DEPC) treated water. The gel was run for 45 minutes at 100 Volts and RNA bands were visualized using SYBR Green II RNA Gel Stain (ThermoFisher Scientific).

## **Western Blots**

Protein content from cell lysates or fractionated samples were normalized by total protein content using the bicinchoninic acid (BCA) assay (Thermo Scientific Pierce, Waltham, MA).

Protein was prepared for loading by combining protein sample with 10%  $\beta$ -mercaptoethanol and 1x NuPAGE LDS Sample Buffer (Invitrogen). 15  $\mu$ g of protein was loaded and separated by 12% sodium dodecyl sulfate-polyacrylamide gel electrophoresis (SDS-PAGE). After electrophoresis, gels were rinsed in transfer buffer (25 mM Tris, 192 mM glycine, 10% methanol). The proteins were transferred to a nitrocellulose membrane in transfer buffer for 1.5 hours at 100 V at 4°C. After transfer, membranes were blocked with 5% milk in PBST (137 mM NaCl, 2.7 mM KCl, 10 mM Na<sub>2</sub>HPO<sub>4</sub>, 1.8 KH<sub>2</sub>PO<sub>4</sub>, 0.1% Tween) for 1 hour at room temperature then washed with PBST four times for 5 minutes each. Primary rabbit anti-acetyllysine antibody (Cell Signaling, Danvers, MA) was diluted 1000-fold in 5% BSA. Membranes were incubated in the diluted antibody overnight at 4°C with shaking. Membranes were washed four times with PBST for 5 minutes each, then incubated shaking for 1 hour at room temperature with anti-rabbit IgG HRP-linked secondary antibody (Cell Signaling, Danvers, MA) diluted 2000-fold in 5% milk. The membrane was washed four times with PBST for 5 minutes each. Membranes were developed by incubating in ECL blotting substrate (Abcam) or Lumiglo substrate (Cell Signaling, Danvers, MA) and imaged in the Protein Simple machine (Bio-Techne).

### **$\beta$ -Galactosidase Induction Assay for Translational Reporters**

Strains of interest in the MG1655 (*lacZ*<sup>+</sup>) background were struck out on LB plates with antibiotic as appropriate. Strains were cultured overnight at 37°C in MOPS + 0.2% glucose with antibiotic, if necessary, then subcultured into 25 mL of MOPS + 0.2% glucose to an OD<sub>600</sub> of 0.1. Where noted, cultures were supplemented with 340  $\mu$ L of a 20% sodium acetate solution for a final acetate concentration of 0.27%.

At 8 hours, the OD600 was measured, cultures were removed from the shaker, given a magnetic stir bar, and placed on a stir plate. Immediately before isopropyl  $\beta$ -D-thiogalactopyranoside (IPTG) addition, a 200  $\mu$ L T<sub>0</sub> sample was collected into a pre-chilled 1.5 mL Eppendorf tube containing 5  $\mu$ L 34 mg/mL chloramphenicol. The *lac* operon was induced with 125  $\mu$ L of 1 M IPTG for a final concentration of 5 mM. Upon induction, 200  $\mu$ L samples were collected every 30 seconds for 5 minutes into pre-chilled 1.5 mL Eppendorf tubes containing 5  $\mu$ L 34 mg/mL chloramphenicol. Samples were frozen in a dry ice/ethanol bath for storage at -80°C.

$\beta$ -galactosidase activity was measured using a version of Miller's colorimetric method, substituting 4-methylumbelliferyl-D-galactopyranoside (MUG) for O-nitrophenyl- $\beta$ -galactopyranoside (ONPG) (125, 299). Samples were thawed then incubated with 400  $\mu$ L Z-Buffer (60 mM Na<sub>2</sub>HPO<sub>4</sub>, 40 mM NaH<sub>2</sub>PO<sub>4</sub>H<sub>2</sub>O, 10 mM KCl, 2 mM MgSO<sub>4</sub>, 35 mM  $\beta$ -mercaptoethanol, pH 7.0) for 10 minutes at 37°C. Each sample received 50  $\mu$ L MUG (2 mg/mL stock) and a timer was started. The reactions were incubated for 30 minutes at 37°C for 30 minutes. Reactions were stopped with 250  $\mu$ L 1 M sodium carbonate and the timer was stopped. 200  $\mu$ L of each sample was added in triplicate to a clear-bottom, black-sided 96 well plate. Fluorescence was measured with an excitation wavelength 360 nm and emission wavelength 460 nm. LacZ activity was calculated using the equation Activity = Fluorescence/Time\*OD600. Induction curves were made by plotting LacZ activity on the y-axis and the time post-induction on the x-axis. Induction was transformed using a square root plot to obtain the lag time for first LacZ molecule synthesis (T<sub>first</sub>). LacZ is 1024 amino acids in length, and the translation elongation rate is calculated as 1024/T<sub>first</sub>.

### Cell-free Transcription/Translation Assay

All experiments were performed using the myTXTL Sigma 70 Master Mix Kit and P70a(2)-deGFP positive control plasmid (Arbor Biosciences). For experiments without CobB, 15  $\mu$ L reactions were prepared by combining 12  $\mu$ L of master mix and plasmid (final concentration of 5 nM) and 3  $\mu$ L AcP or AcCoA at desired concentration. Distilled H<sub>2</sub>O was used for volume in no DNA and No AcP controls. For experiments including CobB, 20  $\mu$ L reactions were prepared by combining 12  $\mu$ L of master mix and plasmid (final concentration of 5 nM), 3  $\mu$ L of 33.33 mM AcP, 2  $\mu$ L 1 M NAD<sup>+</sup>, 2  $\mu$ L CobB, and distilled H<sub>2</sub>O. Reactions were incubated for 2 hours at 37 °C in heat block or overnight at 28 °C. Reactions were stopped on ice then diluted with 108 or 100  $\mu$ L PBS. For each reaction, 5  $\mu$ L was loaded in duplicate into 96-well clear-bottomed black-sided plates. GFP fluorescence was measured using the excitation wavelength of 488 nm and emission wavelength of 535 nm with a Synergy H1 microplate reader (BioTek). When noted, a standard GFP curve was used to calculate the amount of GFP synthesized. Alternatively, results were reported in relative fluorescent units (RFU).

### Purification of CobB

BL21 (DE3) containing pCA24n-*cobB* was incubated overnight at 37°C in 5 mL LB with 5  $\mu$ L chloramphenicol (25  $\mu$ g/mL). The bacteria were subcultured to an OD<sub>600</sub> of 0.1 in 500 mL LB containing 25  $\mu$ g/mL chloramphenicol. Cultures were incubated at 37°C, aerated at 225 rpm until they reached a density between OD<sub>600</sub> 0.4-0.6. Expression of His-tagged CobB was induced with 100  $\mu$ M IPTG, and cultures were incubated for an additional 4 hours. Cells were harvested by centrifugation at 14,000 x g for 10 minutes at 4°C. Cell pellets were stored up to 1 week at -20°C prior to purification.

Cell pellets were thawed on ice and resuspended in 10 mL resuspension buffer (50 mM sodium dibasic heptahydrate, 1.4 M NaCl, 50 mM imidazole, 0.1% Tween, 5% ethanol, 10% beta-mercaptoethanol) with 5  $\mu$ l lysozyme (50 mg/mL) added. Lysis reactions were incubated for 30 minutes at room temperature and lysed cells were pelleted by centrifugation at 14,000 x g for 30 minutes at 4°C. 10  $\mu$ L of supernatant was set aside for SDS-PAGE analysis. Remaining supernatant was run over 1 mL Ni-NTA beads in CellThru 10 mL columns. 10  $\mu$ L of the flow through was saved for SDS-PAGE analysis. The column was washed twice with 10 mL of resuspension buffer. 10  $\mu$ L from each wash was saved for SDS-PAGE analysis. CobB was eluted from the column with 1 mL of resuspension buffer with 200 mM, 225 mM, 250 mM, and 275 mM imidazole. The success of the purification was analyzed by SDS-PAGE and staining with Coomassie reagent. The presence of CobB in the final elutions was confirmed by SDS-PAGE and Western blot analysis with an HRP-conjugated anti-6xHis antibody (Cell Signaling).

### **Deacetylation Reactions**

*In vitro* deacetylations were prepared using purified CobB and RcsB AcK154 in deacetylation buffer (50 mM Tris-HCl pH 8.0, 135 mM NaCl, 2.5 mM KCl, 1 mM MgCl<sub>2</sub>). All reactions received 1 mM NAD<sup>+</sup> and protein concentrations are noted in relevant figures. The final reaction volume was 27  $\mu$ L. Reactions were incubated overnight at 28°C. Deacetylase activity was assessed qualitatively by anti-acetyllysine Western blot.

### **Quantitative PCR**

RNA was isolated from cell-free reactions using the MasterPure Complete DNA and RNA Isolation kit (Epicenter). After RNA isolation, cDNA was prepared using the iScript cDNA Synthesis kit (BioRad). A standard curve for qRT-PCR was prepared using *E. coli* B gDNA, iTaq Universal 2x SYBR green (BioRad) and 16S primers. Samples, no template controls, and

no iScript controls were combined with iTaq Universal 2x SYBR green (BioRad)) and primers for *deGFP*. Reactions were carried out using the CFX Opus 96 Real-Time PCR System (BioRad). Expression of *deGFP* was calculated relative to the no AcP control.

## Mass Spectrometry

### Preparation of Ribosomes for Mass Spectrometry

Initial collection of ribosome fractions was from sucrose gradient fractionation as previously described. Following fractionation, 30S, 50S, 70S, and polysome fractions were pooled for concentration and clean-up. Initial concentration of the pooled samples was estimated by A260 and confirmed by BCA assay and SDS-PAGE. 10 kDa Centricon centrifuge filters were washed twice with a buffer consisting of 10 mM Tris-acetate pH 8.0, 14 mM Mg-acetate, 60 mM K-acetate, and 10 mM NaCl. Pooled fractions were then applied to the filter. Samples were concentrated to a minimum concentration of 5  $\mu\text{g}/\mu\text{L}$ . Final concentrations were determined by A260 and confirmed by BCA assay and SDS-PAGE.

### Mass Spectrometry

Pooled 30S, 50S, 70S, and polysome fractions were denatured and reduced by incubating with 8 M urea and 5 mM dithiothreitol (prepared in 100 mM  $\text{NH}_4\text{HCO}_3$ ) at 60°C for 30 minutes, shaking at 850 rpm. Reactions were diluted 10-fold in 100 mM  $\text{NH}_4\text{HCO}_3$ , and 1 M  $\text{CaCl}_2$  was added to final concentration of 1 mM. Trypsin digestion was carried out for 3 h at 37°C with a 1/50 trypsin-protein ratio. After digestion, peptides were submitted to solid-phase extraction in 50 mg C18 cartridges to remove buffer salts and analyzed by liquid chromatography-tandem mass spectrometry (LC-MS/MS).

For LC-MS/MS data acquisition, peptides were resuspended in water, quantified by BCA assay, and loaded in a trap column (5 cm by 360  $\mu\text{m}$ -outer-diameter by 150- $\mu\text{m}$ -inner-diameter

fused silica capillary tubing) packed with 3.6- $\mu\text{m}$  Aeries C18 particles. Separation was performed in a capillary column (70 cm by 360- $\mu\text{m}$  OD by 75- $\mu\text{m}$  ID) packed with 3- $\mu\text{m}$  Jupiter C18 stationary phase with a 100 min-gradient of acetonitrile (solvent B) in water (solvent A), both containing 0.1% formic acid. Eluted peptides were analyzed online in a quadrupole-Orbitrap mass spectrometer (Q-Exactive, Thermo Fisher Scientific). Peptides were identified by searching spectra against *E. coli* K-12 sequences from Uniprot Knowledgebase using MaxQuant.

CHAPTER THREE  
EXPERIMENTAL RESULTS

**Acetyl Phosphate Levels Alter Translation *in vitro* and *in vivo***

**Introduction**

Although lysine acetylations are common and conserved on the bacterial ribosome, very little is known about how this modification affects the ribosome (2, 135). Therefore, I set out to establish a connection between increased lysine acetylation and a change in ribosome function.

I decided to focus my experiments on the role of nonenzymatic acetylations. My rationale is as follows. First, in our model system *E. coli* most lysine acetylations occur nonenzymatically (3, 4). This includes many acetylations on the ribosome. Second, the level of nonenzymatic acetylation observed is closely tied to central metabolic function. Nonenzymatic acetylations accumulate during stationary phase, particularly in the presence of excess carbon (6, 135, 201). The ribosome undergoes a variety of changes during stationary phase to decrease global protein synthesis (76, 125). There is evidence that some of these changes differ depending on which nutrient has become limiting, suggesting metabolism contributes to the regulation of these changes (126). Finally, AcP is a ready *in vitro* acetyl donor, and strategies for manipulating AcP levels in *E. coli* cultures are well established. While some information is known regarding the expression YfiQ and RimI, less is known about when the other *E. coli* KATs are active, particularly YjaB and YiaC (170). Focusing on nonenzymatic acetylation eliminates questions surrounding KAT expression.

These initial experiments were intended to ask broad questions. While I thought it likely nonenzymatic acetylations affected translation in some way, I was not entirely sure what I might see in these experiments. First, I investigated the effect of *in vitro* acetylation on the function of an *in vitro* transcription-translation system. Then I sought to establish an observable effect in culture by looking at polysome profiles of WT,  $\Delta ackA$ , and  $\Delta pta$  *E. coli* in stationary phase.

### **The Addition of Acetyl Donors Impair Translation in an *in vitro* Transcription-Translation System**

Using a cell-free transcription-translation system derived from *E. coli* lysates (myTXTL, Arbor Biosciences), I measured the production of green fluorescent protein (deGFP, a GFP optimized for cell-free synthesis) from a  $\sigma^{70}$ -dependent promoter on a plasmid in the presence and absence of the acetyl donors, AcCoA or AcP (**Fig. 5A**) (298, 300). Excess AcCoA or AcP strongly inhibited the synthesis of GFP based on fluorescence. As the *in vivo* contribution of AcCoA to nonenzymatic acetylation is difficult to determine but assumed to be low due to high demand in most bacteria, additional *in vitro* experiments only used AcP (135).

The concentration of AcP in *E. coli* fluctuates depending on medium and growth phase but can reach as high as 5 mM (199). Using 5 mM as the upper limit, I found that a spread of physiologically relevant concentrations of AcP inhibited GFP production in a dose-dependent fashion (**Fig. 5B**).

As the RNA polymerase is known to have acetylated lysine residues that can alter transcription, I wanted to determine whether the decrease in GFP production I observed was translation-specific. Using quantitative reverse-transcription PCR, I measured the relative *gfp* mRNA levels (**Fig. 5C**). Consistent with an AcP-dependent inhibition of translation, mRNA levels did not decrease with increasing AcP levels.

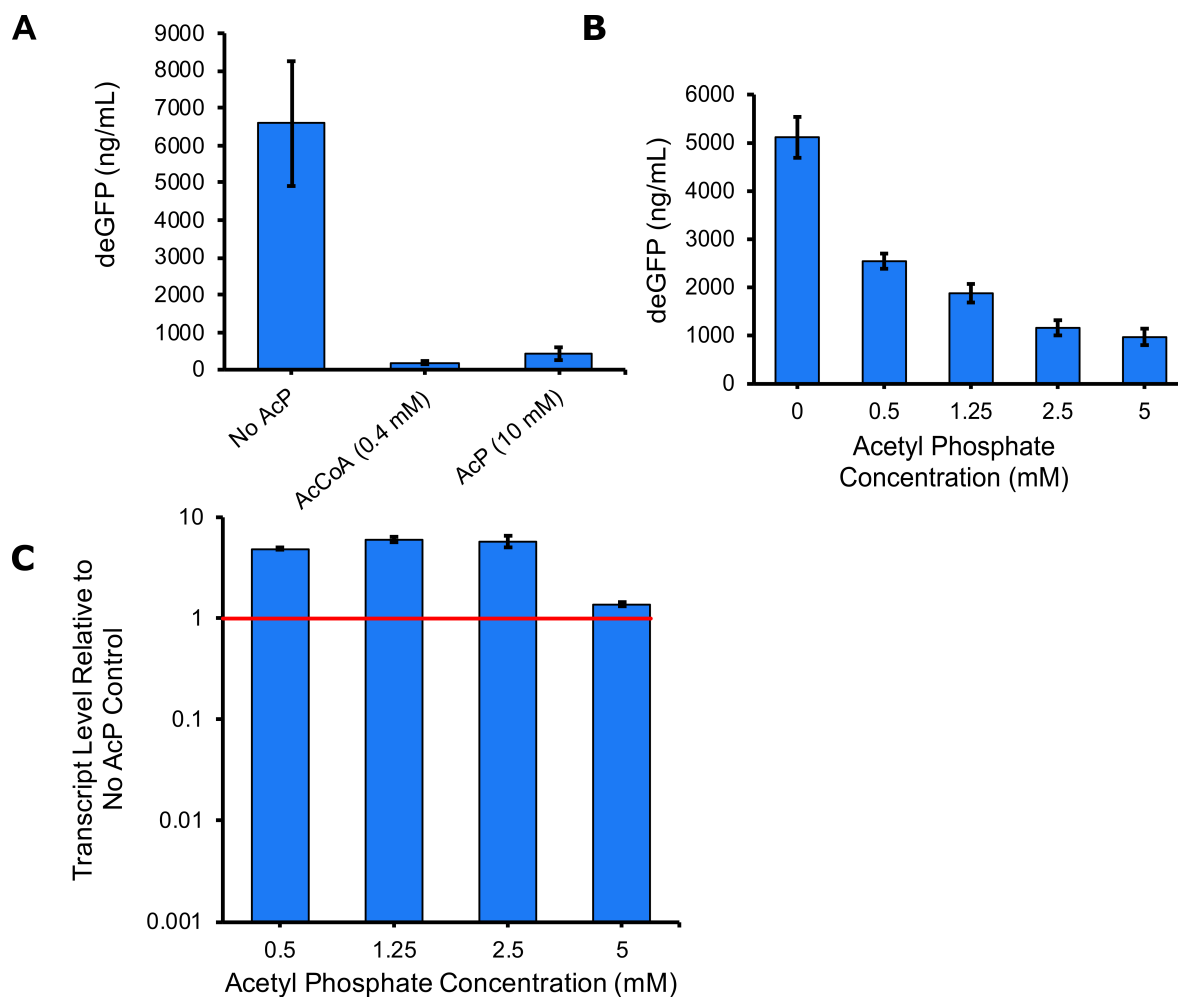


**Figure 5. Addition of Acetyl Donors Inhibits Translation but Not Transcription.** GFP synthesis (deGFP, which is optimized for cell-free synthesis) by a cell-free transcription-translation system was measured in the presence of (A) AcCoA or AcP and (B) various concentrations of AcP. All reactions were incubated for 2 hours at 37 °C. (C) RNA was isolated from reactions for qRT-PCR. Expression of GFP transcript was determined relative to the no AcP control. Error bars represent the standard deviation from two replicates.

At concentrations below 5 mM AcP, there was an increase in *gfp* mRNA. This may be related to opposing effects of acetylations on RNA polymerase. As my project is focused on translation, this observation was not explored.

Attempts were made to qualitatively demonstrate nonenzymatic acetylation of the cell-free system through anti-acetyllysine Western blots. However, I was unable to resolve acetylation differences between reactions with and without AcP. I suspect this is due to a combination of basal acetylation in the transcription-translation lysate and the small volume required for optimal function of the transcription-translation reaction. Available literature estimates the protein concentration in a typical transcription-translation reaction for this system to be 9-10  $\mu\text{g}/\mu\text{L}$ , and the necessary increase in reaction volume for *in vitro* acetylation lowers my overall concentration (298, 300).

Overall, these experiments demonstrate that the addition of known acetyl donors inhibits translation but not transcription *in vitro*. This inhibition is dose-dependent at physiologically relevant concentrations of AcP. The most likely cause of the translation inhibition is acetylation of the ribosome or associated translation machinery.

### **High Acetylation Mutants Have an Altered Ribosome Population in Rich Media**

To assess the effect of acetyl phosphate on the ribosome in bacterial cultures, I compared the polysome profiles for the wild-type strain (BW25113) and its  $\Delta\text{ackA}$  mutant (high acetylation in a rich medium), and  $\Delta\text{pta}$  mutant (low acetylation in a rich medium) following 10 h of growth in TB7 + 0.4% glucose (**Fig. 6**). These conditions were chosen for the initial experiments because this timing and medium favor the accumulation of AcP. Polysome profiling allows me to determine the state of the ribosome pool within the bacteria by separating the ribosomes into their different populations: polysomes (multiple 70S ribosomes on an mRNA), 70S (empty or on a single mRNA), 50S, and 30S, within a sucrose gradient. Shifts in the polysome profile correlate to shifts in ribosome function; for example, large and numerous polysome peaks are indicative of high translational activity.

The wild-type profile exhibited a large peak associated with the 70S ribosome and smaller peaks associated with the 30S and 50S subunits (**Fig. 6**). These peaks were verified using RNA gel electrophoresis (**Fig. 7A**). In contrast, the peak associated with the 70S ribosome was smaller in the  $\Delta ackA$  mutant (acetylation high), similar to the peaks associated with the 30S and 50S subunits in size (**Fig. 6**). While profiles for the  $\Delta pta$  mutant (acetylation low) had larger 30S and 50S peaks and more polysomes relative to the wild-type, it was more similar to the wild-type profile than the  $\Delta ackA$  profile. As a control, complemented  $\Delta ackA$  and  $\Delta pta$  mutants ( $\Delta ackA \lambda att::ackA$  and  $\Delta pta \lambda att::pta$ ) were profiled (**Fig. 6**). Their polysome profiles resembled the wild-type strain. These polysome profiles suggest that high acetylation conditions favor dissociated subunits and that there is a more subtle effect associated with low acetylation.

### **Proteins from the 30S and 50S Ribosomal Subunit Fractions are More Acetylated Than Proteins from the 70S Ribosome Complex Fractions**

The above polysome profiles demonstrate that mutants with a highly acetylated proteome favor dissociated subunits. Therefore, I hypothesized that the proteins within the dissociated subunit fractions would be more acetylated than the proteins within the 70S ribosome fractions. To test this idea, the 30S and 50S, 70S, and polysome fractions from the wild-type strain and its  $\Delta ackA$  mutant were pooled for Western blots using anti-acetyllysine antibodies (**Fig. 7B**). For both strains, the pooled 30S and 50S fractions were more acetylated than the 70S or polysome fractions. As expected, the difference was more pronounced in the  $\Delta ackA$  mutant.

Also, I observed a distinct band of acetylation in the polysome fractions of the  $\Delta ackA$  mutant that was not present in the polysome fractions of the wild-type strain. These results demonstrate that the dissociated 30S and 50S fractions contain more acetylated proteins than the 70S fractions, even in a strain not manipulated for high acetylation.

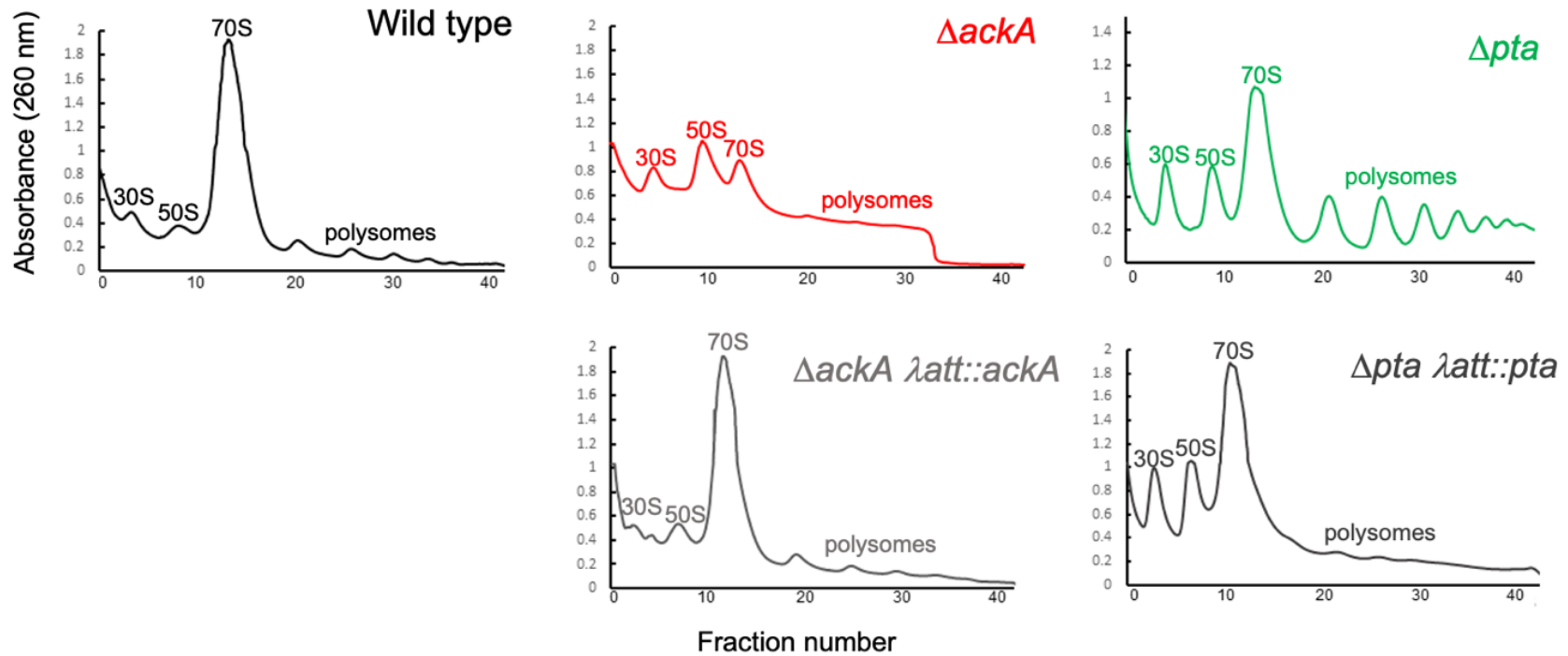


**Figure 6. High Acetylation Conditions Favor Dissociated Subunits.** Polysome profiles of wild type BW25113 and a series of isogenic mutants grown for 10 hours in TB7 + 0.4% glucose. 30S and 50S subunit peaks, 70S monosome peak, and polysome peaks are marked. Identity of each peak was confirmed by RNA gel (Figure 7A and data not shown).

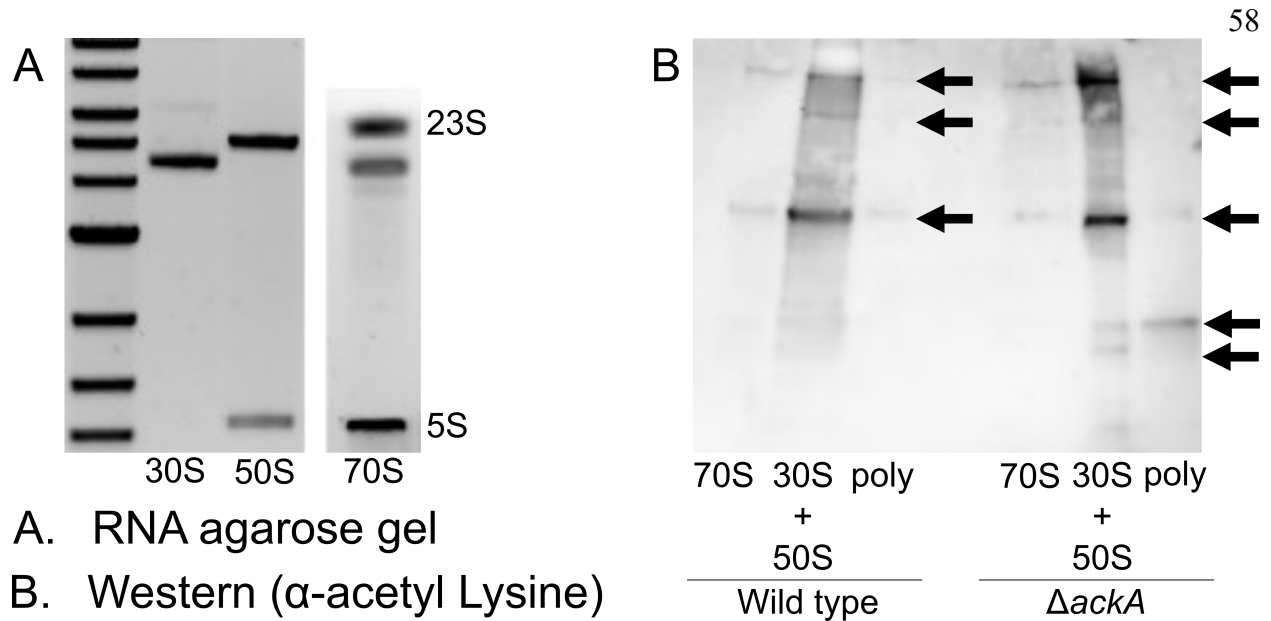


**Figure 7. RNA and Protein Analysis of Polysomal Gradient Profiling Fractions.** (A) Agarose RNA gel for 30S, 50S, and 70S peak fractions collected from polysome profile of wild type BW25113 grown for 10 hours in TB7 + 0.4% glucose. (B) Western blot using anti-acetyllysine protein antibody for the 30S+50S, 70S, and polysome peak fractions collected from polysome profiles of wild type BW25113 and its isogenic  $\Delta ackA$  mutant grown for 10 hours in TB7 + 0.4% glucose.

### Summary

I set out to identify possible areas where an effect from nonenzymatic lysine acetylation on bacterial translation could be observed. I demonstrated that the addition of acetyl donors causes a translation-specific defect in cell-free transcription-translation reactions. This defect is dose-dependent at physiologically relevant concentration of AcP.

To determine if nonenzymatic acetylation altered the ribosome population within cells, I collected polysome profiles of a series of isogenic mutants that promote or ablate nonenzymatic acetylation. Under the conditions tested, the  $\Delta ackA$  mutant (high acetylation) skewed towards dissociated ribosome subunits over 70S ribosome complexes. This skew was not observed in the wild-type strain or its  $\Delta pta$  mutant (low acetylation) mutant. Anti-acetyllysine Western blots of pooled fractions from the wild type strain and its  $\Delta ackA$  mutant showed an increase in

acetylation in the pooled 30S and 50S fractions compared to the 70S fractions for both strains, although this increase was more intense in the  $\Delta ackA$  mutant. These results suggest that acetylated subunits are less likely to be found in 70S ribosomes and may indicate that acetylation interferes with subunit association.

## **Acetyl Phosphate-Dependent Acetylation Does Not Impact Translation Elongation Rate in Stationary Phase**

### **Introduction**

Previous experiments demonstrate that nonenzymatic acetylations impair protein synthesis *in vitro*, but it is not clear how. A defect at the initiation step would prevent subsequent protein synthesis. However, assessing initiation would either require in-depth ribosome profiling and footprinting or rigorous *in vitro* kinetic experiments. As ribosome work is a new avenue of investigation for the Wolfe lab, this area of inquiry is beyond our technical capacities.

A defect in elongation rate could also result in less overall protein synthesis. Elongation rate can be measured using LacZ as a translational reporter, similar to the way it can be used as a transcriptional reporter (125, 299). However, elongation rate is known to correlate with growth rate, and mutations in the Pta-AckA pathway are known to have slight growth defects that could complicate direct comparisons between the wild-type strain and its *ackA* or *pta* mutants. To control for this variation in growth rate, I grew the wild-type strain and its  $\Delta pta$  mutant in MOPS + 0.2% glucose. At 6 hours, half of the cultures were supplemented with 0.27% acetate. This level of acetate was enough to increase acetylation in both strains by 8 hours (**Fig. 3B**) and allowed me to compare wild-type to wild-type and  $\Delta pta$  to  $\Delta pta$ .

## **There is No Difference in Elongation Rate Between *E. coli* Cultured in Low or High**

### **Acetylation Media**

I measured the elongation rate for MG1655 wild-type and an isogenic  $\Delta pta$  mutant after 8 hours of growth in MOPS + 0.2% glucose or MOPS + 0.2% glucose supplemented with 0.27% acetate at 6 hours (**Fig 8A**). While I initially expected the acetate supplementation to increase AcP-dependent acetylation for the  $\Delta pta$  strain alone, the amount of acetate used was enough to also increase acetylation in the wild-type strain (**Fig. 3B**).

As expected, the  $\Delta pta$  mutant had a slight growth defect relative to the wild-type strain, but the addition of acetate did not drastically alter growth (**Fig. 8B**). At 8 hours of growth, there was no difference in the elongation rate of the wild-type strain with or without acetate supplementation (**Fig. 8A**). The same was true for the  $\Delta pta$  mutant.

### **Summary**

I hypothesized that nonenzymatic acetylation might decrease the elongation rate of bacterial ribosomes. Under the conditions investigated, there was no difference in elongation rate between media conditions that increase acetylation and those that do not. However, in addition to increasing acetylation in the  $\Delta pta$  mutant, the amount of acetate used was enough to also increase acetylation in the wild-type strain. This suggests medium choice alone might be sufficient to alter the ribosome population by other measurements.

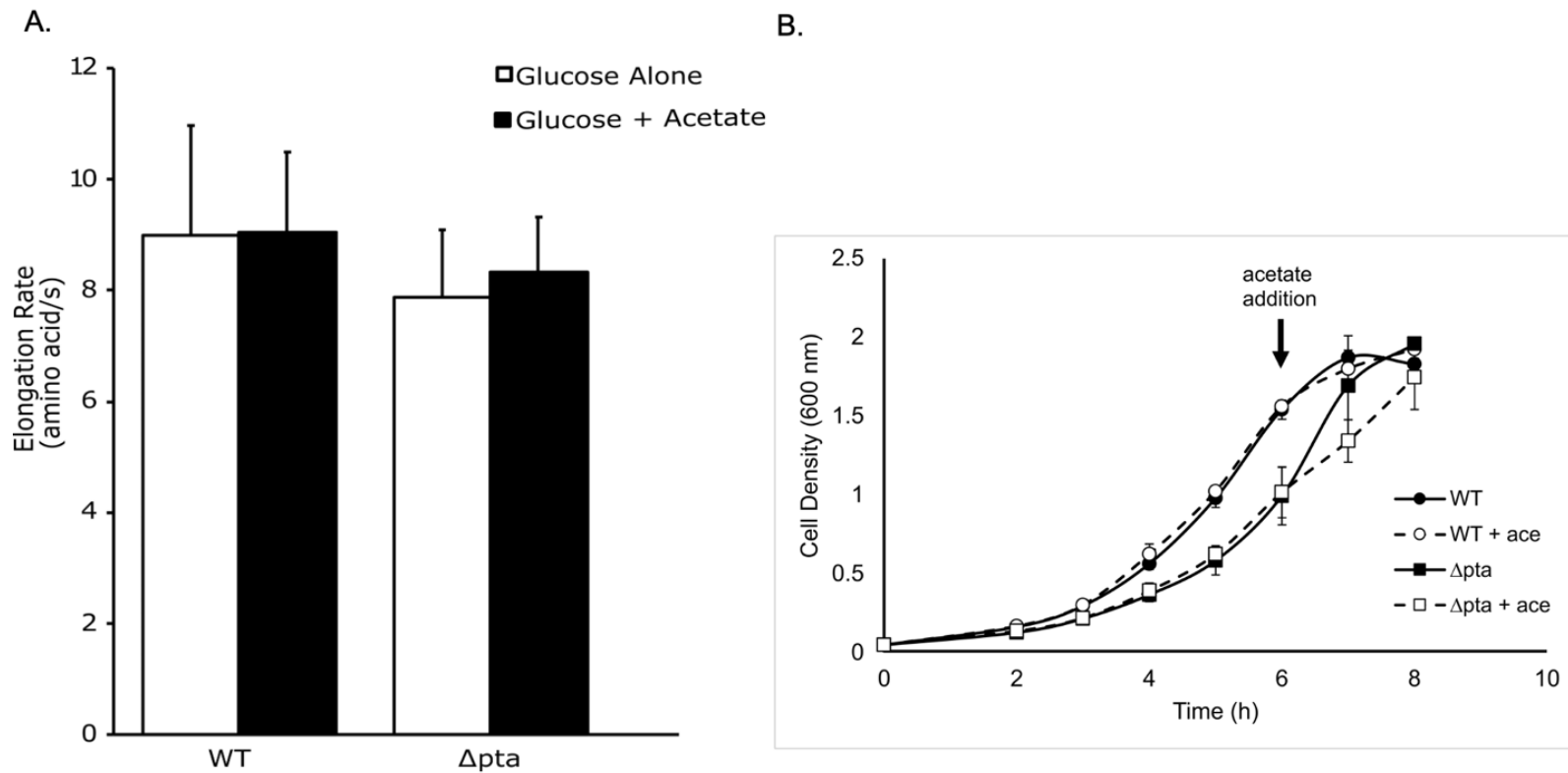


**Figure 8. Elongation Rate is Not Affected by Conditions Promoting Acetylation.** (A) MG1655 wild type and an isogenic  $\Delta$ pta mutant were grown in MOPS + 0.2% glucose (white) or MOPS + 0.2% glucose supplemented with 0.27% acetate at 6 hours (black). At 8 hours,  $\beta$ -galactosidase activity was induced and used to calculate the elongation rate in amino acids/s (aa/s). Error bars represent the standard deviation from three biological replicates. (B) MG1655 wild type and an isogenic  $\Delta$ pta mutant were grown in MOPS + 0.2% glucose (closed markers) or MOPS + 0.2% glucose supplemented with 0.27% acetate at 6 hours (open markers, acetate addition noted by arrow). Optical density was measured at 600 nm. Each time point is the average of 3 biological replicates with error bars representing the standard deviation.

## Subunit Skew Is Dependent on Central Metabolic Flux and Growth Phase of Culture

### Introduction

AcP levels and nonenzymatic acetylation levels are intrinsically linked to central carbon flux. They accumulate when there is excess carbon available for the EMP as other nutrients become limiting. An accumulation of AcP and nonenzymatic acetylations can also occur when there is excess extracellular acetate, prompting acetate assimilation by the Pta-AckA pathway. In fact, I have observed that excess extracellular acetate is sufficient to increase acetylation in wild-type *E. coli* (Fig. 3B). Therefore, if the shift towards the subunits I previously observed in the  $\Delta ackA$  mutant polysome profiles is truly due to AcP levels and nonenzymatic acetylation, I expect wild-type and  $\Delta pta$  cultures to have profiles that favor dissociated subunits if they are supplemented with acetate.

Nonenzymatic acetylations are also known to be more prevalent during stationary phase, particularly when glucose is in excess. This is due to a decrease in protein turnover, meaning acetylated proteins are not replaced by unacetylated proteins, and a decrease in bacterial cell division, meaning acetylated proteins and the AcP to acetylate them are not diluted into a growing bacterial cell population. This suggests the shift towards subunits observed in the  $\Delta ackA$  mutant will be dependent on growth phase.

### Media Conditions that Favor Nonenzymatic Acetylation Alter Polysome Profiles

To determine if the shift towards subunits observed in the  $\Delta ackA$  mutant polysome profiles when grown in TB7 + 0.4% glucose occurs in other conditions that favor nonenzymatic acetylation, I repurposed the media conditions used in my elongation rate experiments. For these polysome profiles, wild-type *E. coli* (BW25113) and isogenic  $\Delta pta$  and  $\Delta ackA$  mutants were

cultured for in MOPS + 0.2% glucose or MOPS + 0.2% glucose supplemented with 0.27% sodium acetate.

I observed a decrease in the 70S ribosome peak and an increase in the 30S and 50S subunit peaks for the wild-type strain and its  $\Delta pta$  mutant when given acetate (**Fig. 9**). As the  $\Delta ackA$  mutant is already acetylation high when grown in glucose, it was predictably less affected by the acetate supplement (**Fig. 9**). In addition to providing further evidence that acetylation favors dissociated subunits, these results demonstrate that wild-type *E. coli* can experience high enough levels of acetylation to have an observable shift towards dissociated subunits in their polysome profile.

### **The Emergence of Increased Ribosome Dissociation Occurs as Cultures Exit Exponential Growth**

Because nonenzymatic acetylations accumulate during stationary phase, I hypothesized that differences in the polysome profiles would not be observable in earlier growth phases. To test this hypothesis, I profiled wild-type *E. coli* (BW25113) and its  $\Delta ackA$  mutant grown in TB7 + 0.4% glucose over time, starting in late exponential growth (**Fig. 10A**). During exponential growth, the profiles for the wild-type strain and its  $\Delta ackA$  mutant were similar, but as the cultures exited exponential phase, they diverged (**Fig. 10**). As seen in earlier experiments, for the  $\Delta ackA$  mutant the peak associated with the 70S ribosome was reduced and the peaks associated with the 30S and 50S subunits increased. These differences between wild-type and  $\Delta ackA$  continued into stationary phase.

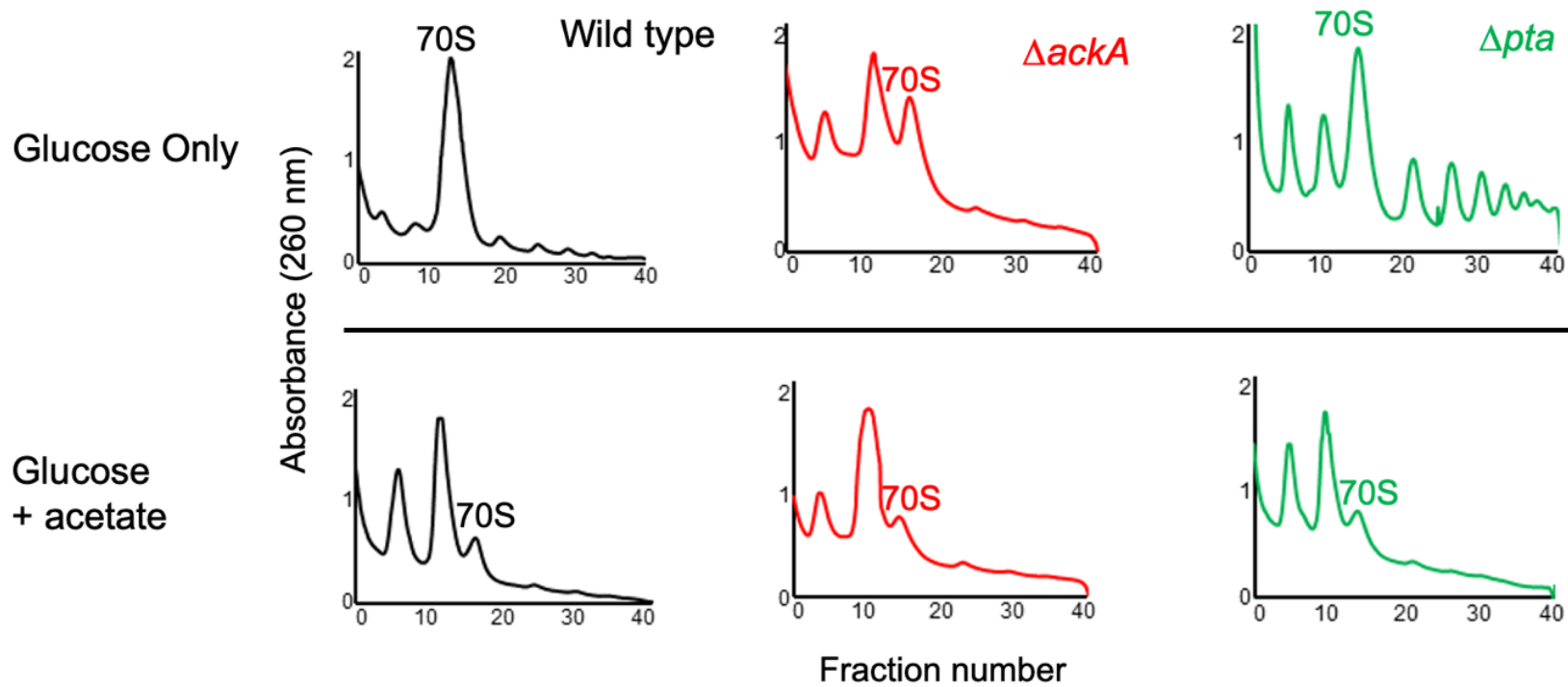


**Figure 9. Growth on Acetate Favors Dissociated Ribosomes.** Polysome profiles of wild type BW25113 and a series of isogenic mutants grown for a total of 10 hours in M9 + 0.4% glucose or M9 + 0.4% glucose supplemented with 0.27% acetate after 6 hours.

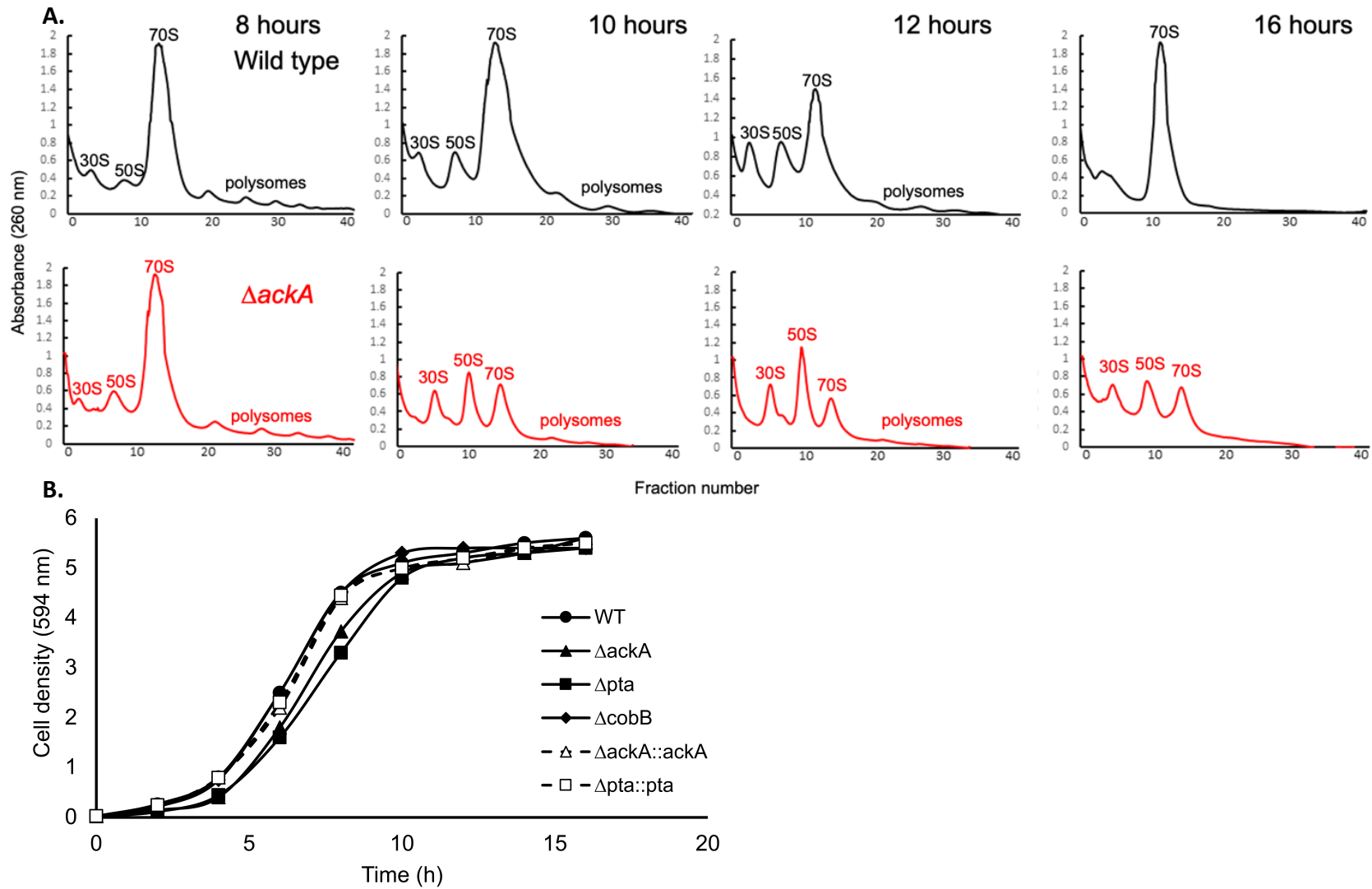


**Figure 10. The Acetylation-Associated Increase in Dissociated Subunits is Specific to Post-Exponential Growth.** (A) Polysome profiles of wild-type BW25113 and an isogenic  $\Delta ackA$  mutant grown in TB7 + 0.4% glucose over times noted. (B) Wild-type BW25113 and a series of isogenic mutants grown for 16 hours in TB7 + 0.4% glucose. Optical density was measured at 594 nm.

Interestingly, there was a transient increase in the subunit peaks and a decrease in 70S peak in the wild-type strain. This is apparent visually from the polysome profiles (**Fig. 10A**) but can be seen most clearly when area under the curve analysis is used to determine the portion of the ribosome population in the 30S, 50S, and 70S fractions (**Table 4**). At 12 hours, there was a noticeable drop in the level of wild-type 70S, but it recovered by 16 hours. For the  $\Delta ackA$  mutant, the level of 70S decreased at 10 hours, while the level of 30S and 50S increased, and like the polysome profiles, this change persisted.

**Table 4. Portion of Ribosomes in 30S, 50S, and 70S Fractions Over Time**

Time	Strain	30S	50S	70S
8 hours	Wild type	7.9%	8.4%	41.1%
	$\Delta ackA$	10.1%	6.7%	48
10 hours	Wild type	7%	9.1%	44%
	$\Delta ackA$	18.5%	18.2%	21.9%
12 hours	Wild type	10.7%	14.2%	27.4%
	$\Delta ackA$	13.7%	24.8%	17.1%
16 hours	Wild type	17.5%		46.9%
	$\Delta ackA$	21.2%	17.7%	18.5%

### Summary

Consistent with a mechanism whereby nonenzymatic acetylation levels influence the bacterial ribosome function, media conditions alone are sufficient to induce an increase in dissociated 30S and 50S subunits (**Fig. 9**). When grown on glucose alone, I observe an increased level of dissociated subunits in the polysome profile of the  $\Delta ackA$  mutant, which is acetylation high when grown on glucose, while the wild-type strain and its  $\Delta pta$  mutant do not show this subunit skewing. However, when the cultures are supplemented with 0.27% sodium acetate, which induces nonenzymatic acetylation in the wild-type strain and its  $\Delta pta$  mutant (**Fig. 3B**), there was a decrease in the 70S peak and an increase in the 30S and 50S peaks for the wild-type strain and its  $\Delta pta$  mutant.

Consistent with the known timing of AcP and nonenzymatic acetylation accumulation, the increase in subunit-associated peaks for the  $\Delta ackA$  mutant grown in TB7 + 0.4% glucose was first observed as the cultures exited exponential growth. Prior to stationary phase, polysome profiles from the  $\Delta ackA$  mutant resembled polysome profiles from wild-type *E. coli* (**Fig. 10**). Interestingly, I also observed a transient increase in the subunit peaks and a decrease in the 70S peak at 12 hours growth for the wild-type strain. By 16 hours, the 70S peak recovers. It is unclear if this transient shift is related to acetylation. While Western blot analysis suggests dissociated subunits are more acetylated than 70S ribosomes even in the wild-type strain (**Fig. 7B**), the acetylation-associated increase in dissociated subunits was not transient in the high acetylation mutant  $\Delta ackA$ . Once the cultures exited exponential growth, the polysome profiles were skewed towards dissociated subunits up to 16 hours.

Taken together, these experiments strengthen my initial observations using high and low acetylation mutants in TB7 + 0.4% glucose. If the increase in dissociated subunits observed in the  $\Delta ackA$  polysome profiles were independent of acetylation, it is unlikely I would observe the same pattern in polysome profiles taken from the wild-type and  $\Delta pta$  strains grown in glucose medium supplemented with acetate. The onset of the  $\Delta ackA$  skew towards subunits at stationary phase is also consistent with an acetylation-dependent effect.

## **CobB-Sensitive Acetylated Lysine Residues Contribute to Some, But Not All, Observed Acetylation-Dependent Changes in Translation Function**

### **Introduction**

Roughly 10% of lysine acetylations in *E. coli* are sensitive to deacetylation by the sirtuin CobB (4, 193, 205, 241). While certain factors seem to make a residue more likely to be CobB-sensitive, including a neighboring aromatic amino acid (Trp, Phe, Tyr) or arginine and a

favorable, accessible location on the three-dimensional structure of the protein, there is not an identified targeting method for CobB (205, 301). This is consistent with the functional promiscuity of CobB, which can act as a general deacylase, though typically with less efficiency than its deacetylase activity (212-216).

Certain acetylated residues on the ribosome have been identified as CobB-sensitive (4, 205, 241). Because studies about the effect of lysine acetylation on the ribosome are uncommon, it is unclear if the potential deacetylation of these residues contribute to the translation effects I have already observed. To this end, I designed experiments to investigate the relevance of CobB in the *in vitro* system and in the polysome profiling system.

### **Purified CobB Does Not Restore Translation Function to Acetylated *in vitro* Transcription-Translation Reactions**

To determine if CobB-sensitive lysine residues are involved in the AcP-dependent inhibition of translation observed in the *in vitro* TXTL reactions, I purified His6-CobB under native conditions (**Fig. 11A**). Incubating the purified CobB with specifically acetylated RcsB AcK154 purified by a previous member of the lab demonstrated that the purified CobB is an active deacetylase (**Fig. 11B**).

I set up a series of *in vitro* TXTL reactions, incubating the system with no AcP, 5 mM AcP, 5 mM AcP + CobB + 10mM NAD<sup>+</sup> (a necessary substrate for CobB), and 5 mM AcP + CobB (**Fig 12**). Without added NAD<sup>+</sup>, the CobB cannot catalyze the deacetylation reaction. If the acetylations that inhibit translation are sensitive to CobB, then the addition of CobB and NAD<sup>+</sup> should restore GFP synthesis to the system.

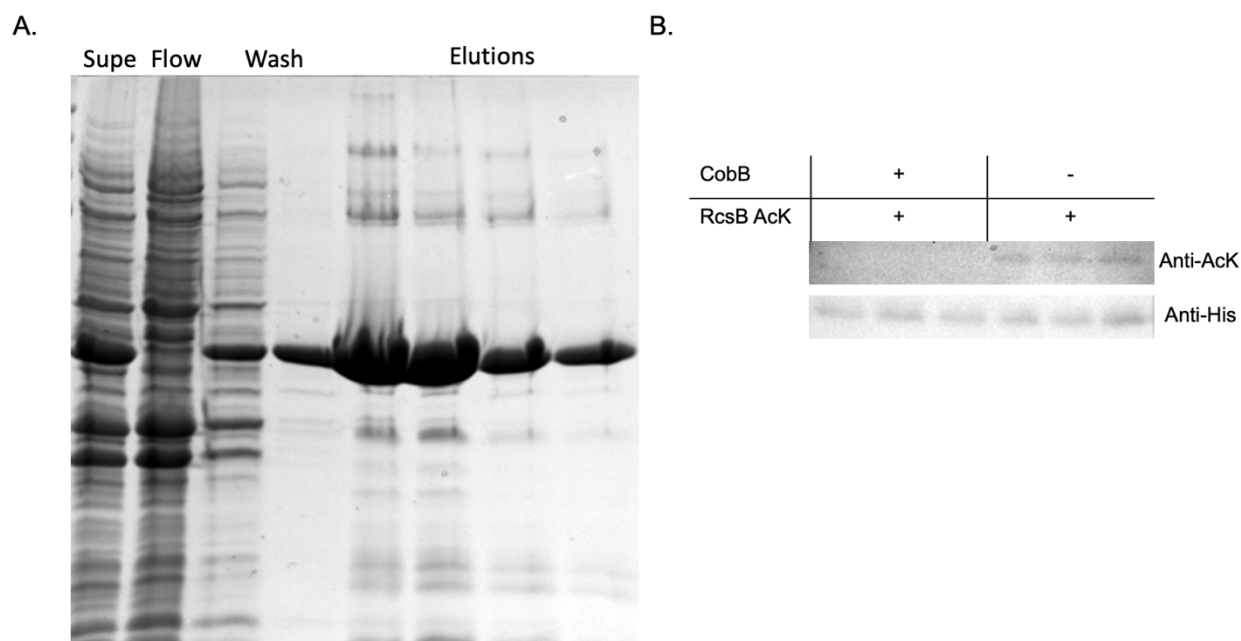


**Figure 11. Purification of Active CobB.** (A) BL21 (DE3) *E. coli* containing a plasmid encoding an IPTG-inducible 6xHis-CobB was subcultured at an  $OD_{600}$  of 0.1 in LB broth and grown at 37 °C aerated at 225 rpm. When culture reached approximately an  $OD_{600}$  of 0.4, expression of CobB was induced with 1 mM IPTG and growth was continued for 4 hours. Cells were pelleted, lysed, and 6xHis-CobB was purified using a Ni<sup>+</sup> column under native conditions. The purification was assessed by SDS-PAGE of the lysed supernatant, initial column flow through, two washes, and four elutions with increasing concentration of imidazole. (B) Deacetylation reactions were prepared in deacetylase buffer and 1 mM NAD<sup>+</sup>. Reactions received 2.7  $\mu$ g of CobB and 16  $\mu$ g of RcsB or 16  $\mu$ g of RcsB alone. A faint RcsB signal is likely due to the high proportion of His-tagged truncated RcsB generated by the synthesis of specifically acetylated protein (data not shown). Reactions were assessed by Western blot using anti-acetyllysine and anti-6xHis antibodies. Acetylation and His-tag blots for full-length RcsB are shown.

Given that several ribosome acetylations have been reported to be sensitive to CobB, I was surprised to see no difference between the reactions that received AcP alone, AcP + CobB + 10 mM NAD<sup>+</sup>, and AcP + CobB (Fig. 12A). Only reactions that received no acetyl donor were able to synthesize GFP.

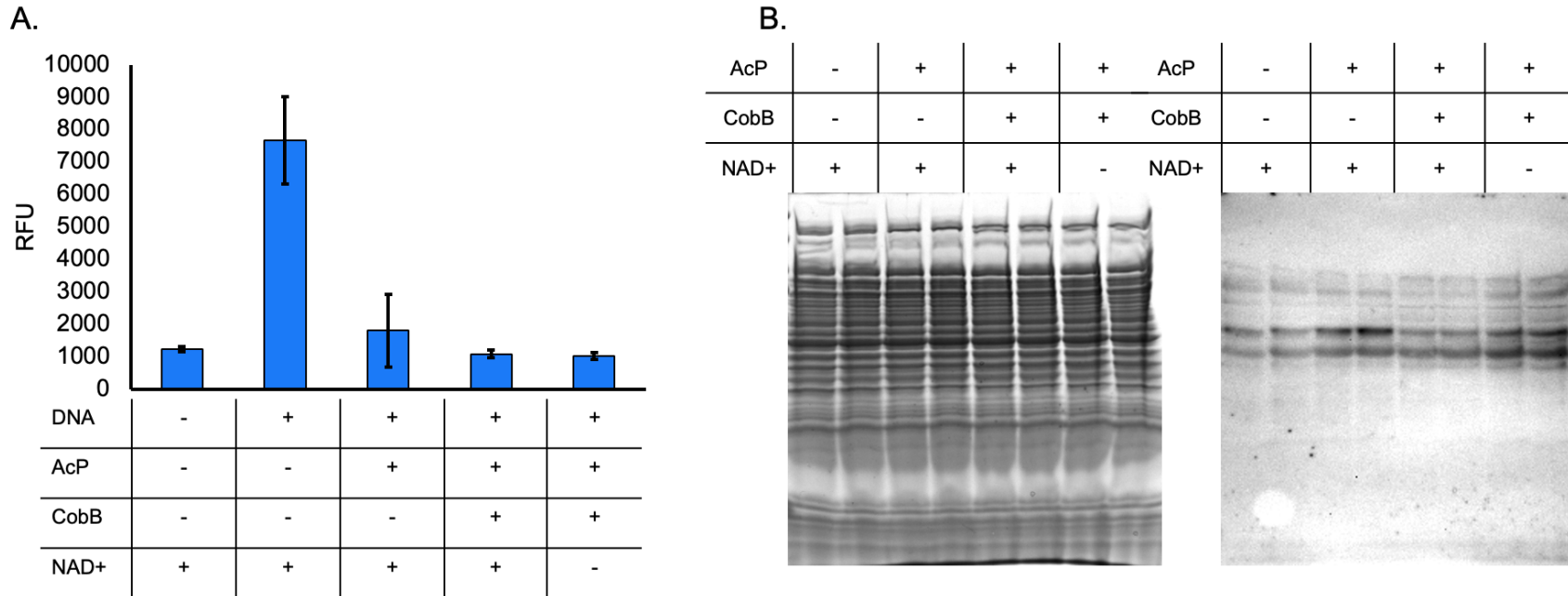


**Figure 12. Addition of Active CobB Does Not Restore Translation Function to Acetylated *in vitro* TXTL Reactions.** (A) GFP synthesis by a cell-free transcription-translation system was measured in the presence of 1 mM NAD<sup>+</sup>, 5 mM AcP + 1 mM NAD<sup>+</sup>, 5 mM AcP + 1.2 μg CobB + 1 mM NAD<sup>+</sup>, and 5 mM AcP + 1.2 μg CobB. Reactions were incubated for 18 hours at 28°C. Error bars represent the standard deviation from three technical replicates. (B) SDS-PAGE Coomassie and anti-acetyllysine Western blot for transcription translation reactions as previously described. 5 μL of reaction from two technical replicates were loaded onto each gel.

To confirm CobB was functional once added to the TXTL reactions, I prepared duplicate reactions for SDS-PAGE analysis. A Coomassie stain for protein was used to ensure consistent loading and an anti-acetyllysine Western blot was used to check for CobB deacetylase activity (**Fig 12B**). The addition of AcP slightly increased several bands of acetylation, while the addition of AcP alongside CobB and NAD<sup>+</sup> did not. Adding CobB without additional NAD<sup>+</sup> did not reduce AcP-dependent acetylation, indicating that this condition is a reasonable proxy for inactive CobB. This demonstrates that CobB can exert its deacetylase function in the context of the *in vitro* transcription-translation reaction.

Taken together, these experiments suggest that the AcP-dependent acetylations that inhibit translation in the *in vitro* transcription-translation reactions are not sensitive to the CobB deacetylase.

### **CobB-Sensitive Lysine Residues Contribute to the Acetylation-Dependent Changes Observed in Polysome Profiles**

I have previously observed an increase in dissociated subunits in the polysome profiles from high acetylation cultures, but it was unknown if CobB was involved. To begin, I returned to my initial polysome profiling conditions. When grown in TB7 + 0.4% glucose for 10 hours, the  $\Delta cobB$  mutant had an intermediate polysome profile pattern when compared to the wild-type strain and its  $\Delta ackA$  mutant (**Fig. 13**). This suggests that some, but perhaps not all, of the acetylations that contribute to the subunit skew pattern are reversible, a departure from the *in vitro* system.

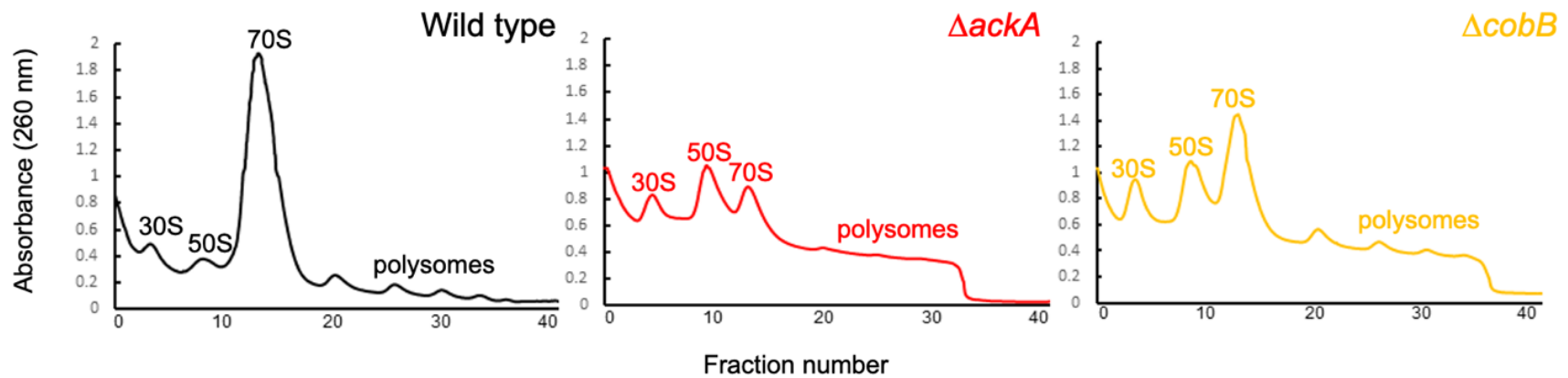


**Figure 13. The Loss of *cobB* Alters the Ribosome Population from Wild-Type but Not to the Extent of the  $\Delta ackA$  Mutant.** Polysome profiles of wild-type BW25113 and isogenic  $\Delta ackA$  and  $\Delta cobB$  mutants grown for 10 hours in TB7 + 0.4% glucose. 30S and 50S subunit peaks, 70S monosome peak, and polysome peaks are marked. Identity of each peak was confirmed by RNA gel (Figure 7A and data not shown).

As I had previously established that the high acetylation shift towards dissociated subunits was not observed in exponentially growing cultures, I collected a series of polysome profiles from cultures of  $\Delta cobB$  *E. coli* grown in TB7 + 0.4% glucose, using the time points previously used for the wild-type strain and its  $\Delta ackA$  mutant (**Fig. 14**). Unexpectedly, I observed that the  $\Delta cobB$  time course exhibited an increase in dissociated subunits at the 8-hour time point and over the entire time course resembled the  $\Delta ackA$  mutant more closely than it did in the initial polysome profiling of the  $\Delta cobB$  mutant. While this could suggest that reversible acetylations are particularly relevant in favoring dissociated ribosomes, I was suspicious of this deviation from the previously observed intermediate pattern for  $\Delta cobB$  and the deviation from the previously observed timing. In particular, I was concerned something might be different in the batch of TB7 used for the  $\Delta cobB$  time course.

### **There is Variability in the Length of Exponential Phase in TB7 Prepared with Different Lots of Tryptone**

Because of elapsed time between the collection of the wild-type and  $\Delta ackA$  time courses and the collection of the  $\Delta cobB$  time course, the TB7 + 0.4% glucose medium prepared for the cultures was made with a new lot of tryptone digest. TB7 is an undefined medium, meaning the precise measures of certain components vary between preparations. In TB7, the tryptone digest can have varying proportions of the amino acids that compose it.

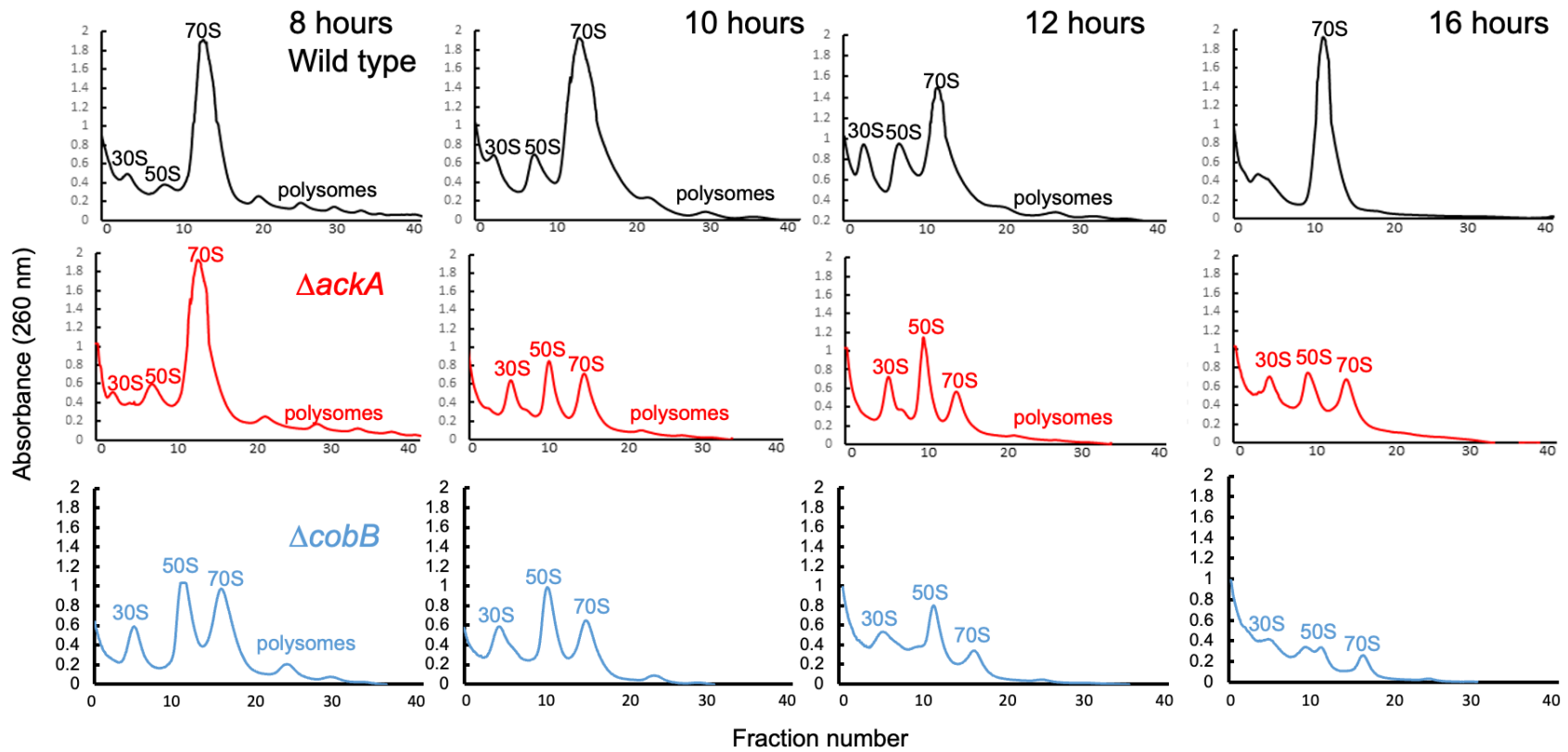


**Figure 14. The Loss of *cobB* Shifts the Ribosome Population in a Pattern that Resembles the Loss of *ackA* Over Time.** Polysome profiles of wild-type BW25113 and isogenic  $\Delta ackA$  and  $\Delta cobB$  mutants grown in TB7 + 0.4% glucose at 37°C over the times noted. Peaks associated with 30S and 50S subunits, 70S ribosomes, and polysomes are noted.

The amino acids in the tryptone are the main carbon source for *E. coli* grown in TB7, and they are consumed in a specific order: L-serine and L-aspartate (acetogenic amino acids) during exponential growth, then L-tryptophan (a non-acetogenic amino acid) as they enter stationary phase, and finally L-threonine, L-alanine, and L-glutamate (a mixture of acetogenic and non-acetogenic amino acids) further into stationary phase (133). Differences in the amino acid composition could alter how a particular batch of TB7 performs. In fact, when I monitored the growth of wild-type *E. coli* in TB7 + 0.4% glucose prepared with the new lot of tryptone, I found that the cultures reached stationary phase after 6 hours of growth (**Fig. 15**), which is 4 hours earlier than what was observed for cultures grown in media prepared with the previous lot of tryptone (**Fig. 10B**).

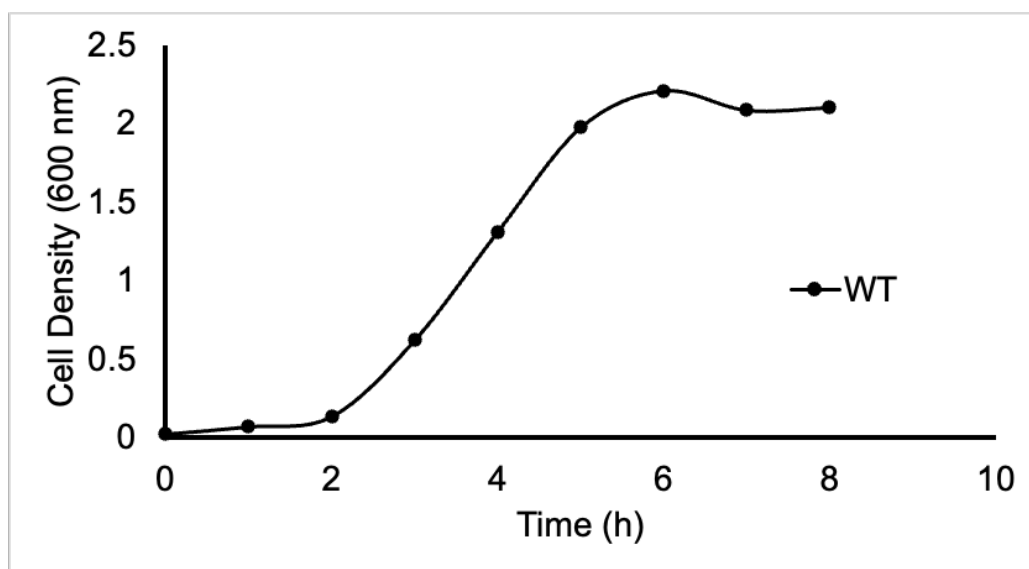


**Figure 15. Exponential Phase is Shorter in TB7 + 0.4% Glucose Prepared with Different Lot of Tryptone.** Wildtype *E. coli* BW25113 was grown for 8 hours in TB7 + 0.4% glucose. Optical density was measured at 600 nm. Differences in cell densities between **Fig. 15** and **Fig. 10B** are due to the use of different spectrophotometers and slightly altered parameters.

To eliminate variability between tryptone lots, moving forward I would recommend focusing on polysome profiling from cultures grown in a defined medium, M9 minimal medium

+ 0.4% glucose or MOPS + 0.4% glucose. Although I have begun this work, due to the time constraints of the project, I do not have adequate polysome profiles for comparison yet.

## Summary

These experiments suggest the contribution of the CobB deacetylase to the regulation of lysine acetylation on the ribosome is layered. Whichever acetylations lead to the inhibition of translation in the *in vitro* transcription-translation system are not sensitive to CobB, despite CobB being functional when added to the system. On the other hand, CobB is, at a minimum, able to target some of the acetylated lysines that contribute to the increase in dissociated subunits observed in polysome profiles. While early polysome profiling of a  $\Delta cobB$  mutant had a more intermediate increase in dissociated subunits relative to a  $\Delta ackA$  mutant, later polysome profiles of  $\Delta cobB$  showed a shift more similar to  $\Delta ackA$ . While it is safe to say that CobB contributes in some way to the subunit skew, it is unclear if CobB-sensitive residues are the primary cause of the increase in dissociated subunits or if the effect is due to a combination of CobB-sensitive and CobB-insensitive residues.

At this time, I can only speculate as to why CobB seems relevant to the dissociated subunit effect but not the *in vitro* inhibition of translation. I hypothesize that this difference in the contribution of CobB is due to which translation-associated acetylations are CobB-sensitive. This hypothesis is elaborated on in more detail in the Discussion.

## **Preliminary Mass Spectrometry Data Identify Several Conserved Acetylation Sites Specific to Wild-Type Subunit Fractions**

### **Introduction**

Mass spectrometry is a commonly used technique to identify acetyllysine sites (see **Table 1** for examples). My data suggest there are differences in acetylation between the 30S/50S

subunit fractions and 70S ribosome fractions in both wild-type and  $\Delta ackA$  mutant *E. coli*, with this difference intensified in the high acetylation mutant. Therefore, a mass spectrometry analysis of these fractions could allow me to identify lysine residues specific to or more common to the subunit fractions. Triplicate samples of 30S, 50S, and 70S fractions collected from the wild-type strain and its  $\Delta ackA$  mutant grown in TB7 + 0.4% glucose were submitted for mass spectrometry analysis by my collaborators at the Pacific Northwest National Laboratory.

### **Mass Spectrometry Identifies Several Acetylations Unique to the Subunit Fractions in Wild-Type *E. coli***

With mass spectrometry, 166 acetylated peptides from 47 ribosomal proteins and elongation factors were detected. Unfortunately, due to the low abundance, digested peptide concentration was below the limit of quantification of the BCA assay. Therefore, samples could not be normalized prior to loading. If the protein in the samples was likely to be present in similar amounts, this would not be an issue, but the  $\Delta ackA$  samples have an accumulation of 30S and 50S subunits higher than their wild-type counterparts. Subsequent normalization based on signal between samples was not possible because of the difference in intensity magnitude. This is particularly limiting for the  $\Delta ackA$  samples, as the high level of global acetylation resulted in acetylated residues that were detected in both the subunit and 70S fractions for all observed acetylations. I am unable to determine if an acetylation was more prevalent in the subunit fraction or the 70S fraction for these samples.

However, for the wild-type fractions, 18 acetylated peptides were observed only in the subunit fractions (**Table 5**). Of the 18 residues unique to the wild-type subunit fractions, 10 have some degree of conservation, and 5 have evidence of functional relevance in the literature.

**Table 5. Acetylated Residues Unique to Wild Type *E. coli* Subunit Fractions.**

<b>Protein</b>	<b>Acetylated residues unique to WT subunit fractions</b>	<b>Highly conserved acetylated residues*</b>	<b>Residues with identified function in the literature</b>
<b>uS3</b>	K80	Positive charged conserved	No
<b>uS7</b>	K35, K136	K35, K136	K35, K136 (302, 303)
<b>uS19</b>	K29	Positive charge conserved	No
<b>uL1</b>	K141	K141	No
<b>uL3</b>	K190	K190	No
<b>uL5</b>	K120	No	No
<b>uL6</b>	K86	No	No
<b>uL10</b>	K101	K101	No
<b>bL12</b>	K71, K85, K101	K71, K85, K101	K71, K85, K101 (23, 304)
<b>bL9</b>	K42	No	No
<b>bL17</b>	K35	No	No
<b>uL18</b>	K88	No	No
<b>uL22</b>	K41	No	No
<b>uL29</b>	K54, K60	No	No

\*Based on data from Nakayasu et al., 2017 (2)

Perhaps unsurprisingly, residues that did not meet the threshold to be considered highly conserved do not appear to have functional significance. Of the highly conserved residues identified, residues on uS7 and bL12 could be impacted by acetylation. K35 30S protein uS7 seems to be important for uS7 to properly integrate in the 30S subunit, and K35 and K136 mutants have reduced affinity for 16S rRNA (302, 303). bL12 is a critical component of the flexible ribosome stalk, and K71, K85, and K101 are all located in the binding helices responsible for interactions between the stalk and the various translation factors that bind to it (304). Charge-charge interactions between K71 and K85 and IF2 have specifically been implicated in rapid subunit association (23).

### Summary

While not as successful as hoped for, the mass spectrometry data provide some insight into residues on dissociated subunits that become acetylated during stationary phase in wild-type

*E. coli*. Several of these residues are highly conserved, and residues on uS7 and bL12 have roles that suggest acetylations at those residues could affect the ability of the subunits to properly form or interact with each other. The preliminary data suggest a possible higher level of acetylation in the 30S and 50S subunits compared to the 70S ribosome. However, larger sample preparations will be required to robustly quantify the acetylation sites in different ribosomal fractions.

## CHAPTER FOUR

### DISCUSSION

#### Overall Summary

My dissertation work has demonstrated that nonenzymatic lysine acetylation is a relevant post-translational modification of the bacterial ribosome in *E. coli*. I have demonstrated that nonenzymatic acetylation is able to alter the function of the ribosome *in vitro* by impairing translation function (**Fig. 5** and **Fig. 12**). Nonenzymatic acetylation also exerts an *in vivo* effect altering the distribution of the ribosome population; polysome profiling of high acetylation mutants or high acetylation media conditions reveal an increase in free 30S and 50S subunits relative to the 70S ribosome (**Fig. 6, Fig. 9, Fig. 10, Fig. 13, Fig. 14, and Table 4**). I have observed that in stationary phase, subunit fractions taken from the wild-type strain and its isogenic  $\Delta ackA$  (high acetylation) mutant are more acetylated than their 70S counterparts, with a more dramatic difference in the high acetylation mutant (**Fig. 7**). When grown in minimal glucose conditions, increasing nonenzymatic acetylation by acetate supplementation does not alter the elongation rate of the bacteria, although this condition is sufficient to produce the subunit skew (**Fig. 8** and **Fig. 9**).

CobB, the *E. coli* deacetylase, contributes to some of the effects I have observed but not all of them. The addition of CobB does not restore translation function to the *in vitro* transcription-translation reaction (**Fig. 12**). However,  $\Delta cobB$  mutants do exhibit a subunit skew in their polysome profiles, although it is not clear if it is to a similar extent as the  $\Delta ackA$  mutant (**Fig. 13** and **Fig. 14**).

Finally, preliminary mass spectrometry has identified 18 residues that are acetylated in the wild-type subunit fractions but not the wild-type 70S fractions. The residues on uS7 and bL12 could be areas of further exploration based on the location and conservation of their acetylations.

Overall, my dissertation work provides a foundation for further explorations into how lysine acetylations affect the bacterial ribosome. My work established that these modifications do affect the ribosome, and that the impact of nonenzymatic lysine acetylation on the ribosome is tied both to nutrient availability (**Fig. 9**) and growth phase (**Fig. 14**). However, many questions remain regarding the specific impacts of lysine acetylation. The extent that CobB-sensitive lysine acetylations affect the ribosome is an open question. The role of specific lysine acetylations is a ripe area for further exploration. In this discussion, I will explore the conclusions that can be drawn from my dissertation work, offer speculation into possible explanations for some unresolved questions, and discuss how my work relates to other published studies on bacterial ribosome acetylation.

### **Which Step of Translation is Affected by Non-Enzymatic Lysine Acetylation?**

While a recent study observed an impact on the rate of elongation under high acetylation conditions (305), this is not what I observed under my conditions (**Fig. 8**). My polysome profiling data suggest a mechanism involving ribosome association. Although I do not have evidence for a specific mechanism, the simplest explanation is that acetylation inhibits translation initiation, the process of the 30S and 50S subunits associating with initiation factors, tRNA, and mRNA to form the 70S complex. This proposed mechanism might explain the detection of acetylated bL12 residues in the wild-type subunit fractions (**Table 4**). During initiation, IF2 binds at a pair of highly conserved helices on bL12 (304). Charge-charge

interactions between K71 and K85 on bL12 and aspartic acid and glutamic acid residues on IF2 are key for rapid subunit association (23). Acetylations on the lysine residues throughout the binding helices are common and conserved (2). Therefore, a possible explanation for the observed subunit skew is that as AcP accumulates, more bL12 becomes acetylated. This acetylated bL12 is less able to recruit IF2 than unacetylated bL12 and is less effective at forming the 70S complex.

While a plausible argument for an initiation defect can be made, other observations have suggested lysine acetylation impacts elongation. The disparate observations concerning elongation between my work and Zhang and co-authors may be related to the differences in growth conditions used. In my experiments, I grew wild-type and  $\Delta$ *pta* *E. coli* in MOPS + 0.2% glucose with or without acetate supplementation. This choice was meant to address the known growth difference between the wild-type strain and its  $\Delta$ *pta* mutant by allowing me to compare the wild-type strain without acetate to the wild-type strain with acetate and the  $\Delta$ *pta* mutant without acetate to the  $\Delta$ *pta* mutant with acetate. In their 2020 paper, Zhang and colleagues grew their wild-type strain and its  $\Delta$ *pta* mutant in minimal acetate medium and used their growth curve measurements to select time points at the entrance to stationary phase (305). It may be that the minimal acetate conditions increase acetylation to a greater extent than my acetate supplementation conditions. The growth of wild-type and  $\Delta$ *pta* cells is not as robust in minimal acetate as in minimal glucose, and it may be that the lower growth rate of the  $\Delta$ *pta* mutant in minimal acetate makes the strain more sensitive to acetylations that affect elongation rate than the conditions I used. Zhang and co-authors also demonstrated that an acetylated residue on EF-G decreased elongation rate by overexpressing EF-G K618Q (an acetyl mimic mutation), K618R

(an acetyl ablative mutation), and K618A. While overexpression of EF-G K618Q and K618A reduced the elongation rate, overexpression of K618R did not (305).

The different observations in my work and in the work of Zhang and colleagues highlight the sensitivity of acetylation effects to growth conditions. This is unsurprising when considering the close ties between carbon metabolism and accumulation of acetylation. Taken together, this suggests that acetylation impacts translation at multiple points. In fact, in 2022, Zhang and co-authors published another article that provided evidence that acetylations on bS1 alter the selectivity of the ribosome for certain mRNA, in particular preferring transcripts related to nitrogen assimilation and amino acid degradation and other stress response transcripts (306). This effect could be induced by nitrogen starvation, a condition that favors acetate overflow (133, 307, 308).

The growing body of evidence suggests the impact of acetylation is not limited to a specific step of translation. Instead, the way acetylation alters translation function is likely determined by the sensitivity of different residues to acetylation, deacetylation, the overall level of AcP in the cell, and the growth state of the cell.

### **The Reversibility of Ribosomal Lysine Acetylation**

While the lysine acetylations that contribute to the observed subunit skew in the polysome profiles have some sensitivity to CobB (**Fig. 13** and **Fig. 14**), at least some of the lysine acetylations that impair *in vitro* translation are not affected by CobB (**Fig. 12**). When I initially designed these experiments, I expected that the *in vitro* and *in vivo* results would be similar. If CobB contributed to the subunit skew, then CobB would also contribute to the *in vitro* translation inhibition. I assumed that whatever acetylations mechanistically caused the subunit skew, whether at initiation or elongation, those acetylations were responsible for inhibited

translation *in vitro* as well. I interpreted the lack of polysomes in high acetylation conditions (**Fig. 6, Fig. 9, Fig. 13, and Fig. 14**) as an indication that translation was suppressed. While this is not an unreasonable interpretation of the polysome profiling, the technique does not directly measure translational output. Currently, there are no published studies that investigate the effect of acetylation on global translational output. However, I do think it likely that acetylation of the ribosome has a broadly suppressive effect on translation, despite the results of my *in vitro* experiments.

There are several reasons that may explain the differences in CobB sensitivity between the *in vivo* and *in vitro* experiments. It may be that the *in vitro* experimental design was suboptimal for observing the impact of CobB, or it may be that the *in vitro* assay is detecting acetylations that affect a step in the process other than subunit association. Ultimately, the behavior of *in vitro* systems does not perfectly mirror the *in vivo* system. CobB is a promiscuous deacetylase, but it is possible that within cells there is some sort of compartmentalization that can direct CobB towards ribosomes. This would be lacking in the *in vitro* system. Alternatively, the *in vitro* system may be enriched for CobB targets that pull the deacetylase away from ribosomal acetylations, as AcP is known to acetylate both metabolic enzymes that make up the energy generation components and the RNA polymerase (170, 287). Possibly supporting this explanation, others have been able to restore *in vitro* translation function to an acetylated transcription-translation system with CobB using a different commercial transcription-translation kit (305). The composition of the proprietary energy regenerating system is likely to vary between the kits.

While I did not observe a restoration of translation function when adding active CobB to the acetylated myTXTL kit (**Fig.12**), the addition of CobB to the acetylated Invitrogen

Expressway kit resulted in a partial restoration of translation (305). In addition to differences in the energy regenerating systems, the protocols for the kits have major differences in recommended reaction volume, incubation temperature, incubation time, and whether the reaction is shaken. Characterization of the kits suggests there are functional differences between the two as well (309). It is also worth noting that in my hands, the addition of 5 mM AcP severely inhibits translation in the myTXTL kit, while 10 mM AcP significantly, but not as drastically, inhibited the Expressway kit in work performed by Zhang and colleagues (305). However, addition of CobB did not fully restore translation function to the Expressway kit, suggesting that there are lysine acetylations that impair global translation that are not sensitive to CobB.

One promising, CobB-insensitive candidate is the acetylation of EF-G K618. As discussed above, overexpression of EF-G K618Q, an acetyl mimic mutant, reduced the elongation rate, while overexpression of EF-G K618R, an acetyl ablative mutant, did not affect the elongation rate (305). In *E. coli*, this acetylation is AcP-dependent, and it has not been identified as a target of CobB (3, 4, 170, 201, 205). It is unlikely to be a contributor to the subunit skew pattern observed in polysome profiling, although it may be that acetylations on EF-G cause ribosomes to dissociate from mRNA transcripts. This, however, is purely speculation.

Operating under the assumption that the main culprit for the *in vitro* inhibition of translation are acetylations that are not sensitive to CobB, I also assume that the major contributors to the increase in dissociated subunits observed in the polysome profiles are acetylations that are sensitive to CobB. The increase in dissociated subunits is the major effect measured by the polysome profiling. Whereas the polysome profiling technique does not give insight into elongation rate, the number and intensity of polysome peaks can be a proxy for

active translation. While there is a noticeable loss of polysome peaks in high acetylation polysome profiles compared to basal or low acetylation polysome profiles, the polysomes are not lost entirely. This suggests some translational capacity is maintained.

When considering a mechanism for the increase in dissociated subunits, the lysine acetylations on bL12 are promising candidates. Mass spectrometry data from this project indicate that ribosomal protein bL12, a critical component of the ribosome stalk that binds various initiation factors, elongation factors, and recycling factors, is acetylated on its binding helices in the 50S subunit fraction. bL12 acetylations have also been observed in a variety of other acetylomes, and several studies have indicated at least some of the acetylations on the binding helices are sensitive to CobB (2, 4, 201, 205, 222). This is of particular interest, because interactions between bL12 and IF2 require K71 and K85 (23). Residues on bL12 are a plausible, CobB-sensitive, contributor to the polysome profile subunit skew. However, these acetylations could easily be relevant during elongation as well, as they are part of the binding site for EF-G and EF-Tu (304).

Ultimately, the role of reversible lysine acetylations on the ribosome is likely to be complicated. My work suggests that CobB-sensitive residues contribute to the increase in dissociated subunits observed in polysome profiles but not to the inhibition of *in vitro* translation. Work from another group revealed an *in vitro* effect from CobB, albeit in a different *in vitro* transcription-translation system (305).

As a simplistic model, it is likely that there is a basal level of acetylation that is normal for wild-type bacteria. This is consistent with the slight difference observed between wild-type and  $\Delta pta$  polysome profiles under conditions where  $\Delta pta$  mutants have low levels of acetylation.

Deviations from this level of acetylation result in changes in ribosome function. CobB contributes to the maintenance of homeostatic ribosome acetylation.

### **Lysine Acetylations Link Ribosome Function to Central Carbon Metabolism**

Although many areas of exploration regarding the precise mechanistic effects of lysine acetylation on the bacterial ribosome remain, there is a growing body of evidence to support the argument that lysine acetylation is a relevant post-translational modification for the bacterial ribosome. In addition to asking how lysine acetylation affects the ribosome, it is important to consider why lysine acetylations affect the ribosome. I propose the purpose of lysine acetylation on the bacterial ribosome is to modify translation in response to changes in carbon flux.

The idea that lysine acetylations alter protein function in response to changes in central metabolism has been investigated for other proteins. It has been speculated that nonenzymatic acetylations are a response to global carbon flux, accumulating when there is an imbalance between available carbon and other nutrients (2, 310). Indeed, alleviating carbon-nutrient imbalances can reduce levels of nonenzymatic acetylation (202). More recently, it was demonstrated that *E. coli* GapA and GpmA are acetylated to a high stoichiometry by AcP, and the acetylation of these enzymes reduced the activity of glycolysis (291). This type of metabolic sensing is not limited to nonenzymatic acetylations; for example, in *Salmonella enterica*, glucose-induced acetylations by the acetyltransferase Pat on glutamine synthetase and glutamate dehydrogenase link carbon flux to the fine-tuning of ammonium assimilation (311).

In particular, the observed increase in dissociated subunits in the polysome profiles of wild-type *E. coli* grown in minimal glucose medium supplemented with acetate relative to wild-type *E. coli* grown in the same medium without acetate supplementation (**Fig. 9**) suggests that shifts in metabolic flux alone are sufficient for acetylation to exert an effect on the ribosome. The

apparent sensitivity of the subunit skew observed in a  $\Delta cobB$  mutant to differing lots of tryptone (**Fig. 13 and 14**) also suggests that metabolic flux is a key player, as a likely explanation for this sensitivity is variation in the concentration of acetogenic and non-acetogenic amino acids between tryptone lots. This is also supported by work demonstrating that nitrogen limitation can induce nonenzymatic acetylation of ribosomal protein bS1, changing the preference of the ribosome for certain mRNA ribosome binding sites (306).

There is support for the broad argument that lysine acetylations tune protein function to carbon flux in some of my *in vitro* experiments. The inhibition of *in vitro* translation by AcP itself is dose-dependent (**Fig. 5B**). Although not explored in-depth due to my focus on translation, qRT-PCR data showed an increase in *deGFP* transcript at lower concentrations of AcP relative to the no AcP control (**Fig. 5C**). At 5 mM AcP, however, transcript levels returned to levels similar to the no AcP control. This suggests lysines acetylated on RNA polymerase at lower concentrations of AcP can enhance basal transcription of  $\sigma^{70}$  promoters, while lysines acetylated at higher concentrations suppress that effect. This is similar to the interplay between YfiQ-induced acetylation of RNA polymerase enhancing *cpxP* transcription in 0.4% glucose, but the AcP-induced acetylation of RNA polymerase repressing *cpxP* transcription in 4% glucose (**Fig. 4**). These observations suggest that different levels of carbon flux produce different acetylation-dependent effects.

Synthesizing my dissertation data with the results of other studies of bacterial ribosome acetylation, I propose that nonenzymatic lysine acetylation has a homeostatic role on the bacterial ribosome. When the level of AcP in the cell exceeds a certain threshold, acetylations occur on the ribosome that alter its function. These changes seem to have multiple effects, such as increasing the level of dissociated subunits, decreasing the rate of elongation, and altering the

preference of the ribosome for certain mRNAs (292, 305, 306). By utilizing a post-translational modification that is more or less prevalent depending on carbon flux and growth state, the ribosome can rapidly adjust to dynamic nutrient availability.

### **Future Directions**

Many questions remain regarding the role of lysine acetylation on the bacterial ribosome, and this is a rich area for further study. In this section, I highlight three areas I find particularly compelling, but this should not be considered exhaustive. Rather it is a suggestion of what I consider to be the most logical next steps.

As I have already alluded to, questions remain about the contribution of CobB-sensitive lysine acetylations. This area may be best served by targeting specific lysine acetylations likely to alter ribosome function and assessing the sensitivity of the residues to CobB. As I found in my work, the interplay between central metabolism, nonenzymatic acetylation, and CobB activity makes it challenging to separate out the effect of CobB. While the use of defined rather than undefined media may improve results for the global approach I have used, a targeted approach could be more effective. An epistatic approach guided by mass spectrometry of ribosomes from the wild-type strain and its isogenic  $\Delta ackA$ ,  $\Delta cobB$ , and  $\Delta ackA\Delta cobB$  mutants would allow for the identification and targeting of residues that are sensitive to AcP, CobB, or both.

One area of translation where lysine acetylation may be relevant is hibernation, as the formation of 100S ribosomes occurs under conditions that favor the accumulation of acetylations. In fact, RaiA, a stationary phase factor that promotes the formation of inactive 70S monomers over 100S dimers, is nonenzymatically acetylated (3, 4, 98-101, 221). One might speculate that the extent of RaiA acetylation may correlate to the ratio of 100S dimers to inactive 70S monomers. The resolution of 100S ribosomes by polysome profiling requires considerations

that I did not include in my experiments, as the dimers can easily dissociate to 70S monomers without proper treatment (87). Further work could resolve 100S ribosomes in high and low acetylation conditions and investigate the acetylation of RaiA specifically should there be differences.

Much of the work currently published on lysine acetylation of the ribosome has focused on the effect of nonenzymatic lysine acetylation. However, roughly 50% of lysine acetylations on the *E. coli* ribosome are KAT-dependent enzymatic acetylations (170). It is unclear if these acetylations contribute to any of the effects that have been observed for nonenzymatic acetylations, but it is likely that some of them have unique impacts. One particularly interesting example is the difference in acetylation mechanisms between acetylations on elongation factors and initiation factors. The elongation factors are primarily nonenzymatically acetylated while the initiation factors are primarily enzymatically acetylated (170). The interplay between enzymatic and nonenzymatic acetylation on the ribosome could be a rich area for exploration. An *in vivo* approach would involve overexpressing specific KATs to explore effects on polysome profiles, elongation rates, and transcript preference. An *in vitro* approach might involve purifying the KATs and the elongation and initiation factors as well as ribosomes for variety of *in vitro* experiments including subunit association experiments and *in vitro* transcription-translation experiments. These types of *in vitro* experiments, particularly those regarding the initiation factors and subunit association, would be best undertaken by a group with a primary focus on the ribosome, but the *in vivo* experiments are within the capabilities of a more acetylation-focused group.

### Concluding Remarks

Although the acetylation of the bacterial ribosome has been evident since the modification was first acknowledged as prevalent in bacteria, it is only recently that any work has been done to determine how the post-translational modification affects the ribosome. My work represents preliminary explorations into an area of bacterial biology that is likely to be vast and complicated.

Data from my work suggest that the impact of lysine acetylation on the bacterial ribosome is tied to carbon flux as well as to the growth state of the cell. In combination with the handful of other studies available, it is reasonable to propose that lysine acetylation affects a broad range of ribosome functions. The breadth of observed acetylation impacts combined with the clear connection between lysine acetylation and central metabolism lead me to propose that lysine acetylation is a homeostatic mechanism that allows the ribosome to sense flux through central carbon metabolism.

At basal levels of acetylation, the ribosome functions as normal. However, as acetylations increase, several changes in ribosome function, including increases in dissociated subunits, decreases in elongation rate, and decreases in global translational are observed. My work and the work of others suggests that while some of these changes are consistent with expected changes in ribosome function during stationary phase, there does seem to be an acetylation-specific contribution. Acetylation is a part of the multiple layers of regulation that govern the bacterial ribosome.

Over the course of my dissertation work, I have been excited to see other groups investigating the effect of lysine acetylation on the ribosome from various angles, and I hope that

in the future, a better understanding of how lysine acetylation mediates its effects on the ribosome can be reached.

## REFERENCE LIST

1. Simsek D, Barna M. 2017. An emerging role for the ribosome as a nexus for post-translational modifications. *Current opinion in cell biology* 45:92-101.
2. Nakayasu ES, Burnet MC, Walukiewicz HE, Wilkins CS, Shukla AK, Brooks S, Plutz MJ, Lee BD, Schilling B, Wolfe AJ, Müller S, Kirby JR, Rao CV, Cort JR, Payne SH. 2017. Ancient regulatory role of lysine acetylation in central metabolism. *mBio* 8:e01894-17.
3. Weinert BT, Iesmantavicius V, Wagner SA, Schölz C, Gummesson B, Beli P, Nyström T, Choudhary C. 2013. Acetyl-phosphate is a critical determinant of lysine acetylation in *E. coli*. *Molecular cell* 51:265-272.
4. Kuhn ML, Zemaitaitis B, Hu LI, Sahu A, Sorensen D, Minasov G, Lima BP, Scholle M, Mrksich M, Anderson WF, Gibson BW, Schilling B, Wolfe AJ. 2014. Structural, kinetic and proteomic characterization of acetyl phosphate-dependent bacterial protein acetylation. *PloS one* 9:e94816.
5. Post DMB, Schilling B, Reinders LM, D'Souza AK, Ketterer MR, Kiel SJ, Chande AT, Apicella MA, Gibson BW. 2017. Identification and characterization of AckA-dependent protein acetylation in *Neisseria gonorrhoeae*. *PloS one* 12:e0179621.
6. Schilling B, Basisty N, Christensen DG, Sorensen D, Orr JS, Wolfe AJ, Rao CV. 2019. Global lysine acetylation in *Escherichia coli* results from growth conditions that favor acetate fermentation. *Journal of Bacteriology* 201:e00768-18. Print 2019 May 1.
7. Gao H, Sengupta J, Valle M, Korostelev A, Eswar N, Stagg SM, Van Roey P, Agrawal RK, Harvey SC, Sali A, Chapman MS, Frank J. 2003. Study of the structural dynamics of the *E. coli* 70S ribosome using real-space refinement. *Cell* 113:789-801.

8. Ban N, Beckmann R, Cate JH, Dinman JD, Dragon F, Ellis SR, Lafontaine DL, Lindahl L, Liljas A, Lipton JM, McAlear MA, Moore PB, Noller HF, Ortega J, Panse VG, Ramakrishnan V, Spahn CM, Steitz TA, Tchorzewski M, Tollervey D, Warren AJ, Williamson JR, Wilson D, Yonath A, Yusupov M. 2014. A new system for naming ribosomal proteins. *Curr Opin Struct Biol* 24:165-9.9.
9. Weiner J, 3rd, Herrmann R, Browning GF. 2000. Transcription in *Mycoplasma pneumoniae*. *Nucleic Acids Res* 28:4488-96.
10. Ma J, Campbell A, Karlin S. 2002. Correlations between Shine-Dalgarno sequences and gene features such as predicted expression levels and operon structures. *J Bacteriol* 184:5733-45.
11. Chang B, Halgamuge S, Tang SL. 2006. Analysis of SD sequences in completed microbial genomes: non-SD-led genes are as common as SD-led genes. *Gene* 373:90-9.
12. Milon P, Rodnina MV. 2012. Kinetic control of translation initiation in bacteria. *Crit Rev Biochem Mol Biol* 47:334-48.
13. Duval M, Simonetti A, Caldelari I, Marzi S. 2015. Multiple ways to regulate translation initiation in bacteria: mechanisms, regulatory circuits, dynamics. *Biochimie* 114:18-29.
14. Gualerzi CO, Pon CL. 2015. Initiation of mRNA translation in bacteria: structural and dynamic aspects. *Cell Mol Life Sci* 72:4341-67.
15. Milon P, Maracci C, Filonava L, Gualerzi CO, Rodnina MV. 2012. Real-time assembly landscape of bacterial 30S translation initiation complex. *Nat Struct Mol Biol* 19:609-15.
16. Studer SM, Joseph S. 2006. Unfolding of mRNA secondary structure by the bacterial translation initiation complex. *Mol Cell* 22:105-15.
17. Qin D, Liu Q, Devaraj A, Fredrick K. 2012. Role of helix 44 of 16S rRNA in the fidelity of translation initiation. *RNA* 18:485-95.
18. Elvekrog MM, Gonzalez RL, Jr. 2013. Conformational selection of translation initiation factor 3 signals proper substrate selection. *Nat Struct Mol Biol* 20:628-33.

19. Hussain T, Llacer JL, Wimberly BT, Kieft JS, Ramakrishnan V. 2016. Large-scale movements of IF3 and tRNA during bacterial translation initiation. *Cell* 167:133-144 e13.
20. Antoun A, Pavlov MY, Lovmar M, Ehrenberg M. 2006. How initiation factors tune the rate of initiation of protein synthesis in bacteria. *EMBO J* 25:2539-50.
21. Milon P, Konevega AL, Gualerzi CO, Rodnina MV. 2008. Kinetic checkpoint at a late step in translation initiation. *Mol Cell* 30:712-20.
22. Goyal A, Belardinelli R, Maracci C, Milon P, Rodnina MV. 2015. Directional transition from initiation to elongation in bacterial translation. *Nucleic Acids Res* 43:10700-12.
23. Ge X, Mandava CS, Lind C, Åqvist J, Sanyal S. 2018. Complementary charge-based interaction between the ribosomal-stalk protein L7/12 and IF2 is the key to rapid subunit association. *Proceedings of the National Academy of Sciences of the United States of America* 115:4649-4654.
24. Grigoriadou C, Marzi S, Kirillov S, Gualerzi CO, Cooperman BS. 2007. A quantitative kinetic scheme for 70 S translation initiation complex formation. *J Mol Biol* 373:562-72.
25. Fabbretti A, Pon CL, Hennelly SP, Hill WE, Lodmell JS, Gualerzi CO. 2007. The real-time path of translation factor IF3 onto and off the ribosome. *Mol Cell* 25:285-96.
26. Chen B, Kaledhonkar S, Sun M, Shen B, Lu Z, Barnard D, Lu TM, Gonzalez RL, Jr., Frank J. 2015. Structural dynamics of ribosome subunit association studied by mixing-spraying time-resolved cryogenic electron microscopy. *Structure* 23:1097-105.
27. Goyal A, Belardinelli R, Rodnina MV. 2017. Non-canonical binding site for bacterial initiation factor 3 on the large ribosomal subunit. *Cell Rep* 20:3113-3122.
28. Liu Q, Fredrick K. 2015. Roles of helix H69 of 23S rRNA in translation initiation. *Proc Natl Acad Sci U S A* 112:11559-64.
29. MacDougall DD, Gonzalez RL, Jr. 2015. Translation initiation factor 3 regulates switching between different modes of ribosomal subunit joining. *J Mol Biol* 427:1801-18.

30. Rodnina MV. 2018. Translation in prokaryotes. Cold Spring Harbor perspectives in biology 10:a032664. doi: 10.1101/cshperspect.a032664.
31. Dever TE, Dinman JD, Green R. 2018. Translation elongation and recoding in eukaryotes. Cold Spring Harb Perspect Biol 10.
32. Polikanov YS, Steitz TA, Innis CA. 2014. A proton wire to couple aminoacyl-tRNA accommodation and peptide-bond formation on the ribosome. Nat Struct Mol Biol 21:787-93.
33. Zaher HS, Shaw JJ, Strobel SA, Green R. 2011. The 2'-OH group of the peptidyl-tRNA stabilizes an active conformation of the ribosomal PTC. EMBO J 30:2445-53.
34. Erlacher MD, Lang K, Wotzel B, Rieder R, Micura R, Polacek N. 2006. Efficient ribosomal peptidyl transfer critically relies on the presence of the ribose 2'-OH at A2451 of 23S rRNA. J Am Chem Soc 128:4453-9.
35. Hersch SJ, Wang M, Zou SB, Moon KM, Foster LJ, Ibba M, Navarre WW. 2013. Divergent protein motifs direct elongation factor P-mediated translational regulation in *Salmonella enterica* and *Escherichia coli*. mBio 4:e00180-13.
36. Peil L, Starosta AL, Lassak J, Atkinson GC, Virumae K, Spitzer M, Tenson T, Jung K, Remme J, Wilson DN. 2013. Distinct XPPX sequence motifs induce ribosome stalling, which is rescued by the translation elongation factor EF-P. Proc Natl Acad Sci U S A 110:15265-70.
37. Woolstenhulme CJ, Parajuli S, Healey DW, Valverde DP, Petersen EN, Starosta AL, Gydosh NR, Johnson WE, Wilson DN, Buskirk AR. 2013. Nascent peptides that block protein synthesis in bacteria. Proc Natl Acad Sci U S A 110:E878-87.
38. Ude S, Lassak J, Starosta AL, Kraxenberger T, Wilson DN, Jung K. 2013. Translation elongation factor EF-P alleviates ribosome stalling at polyproline stretches. Science 339:82-5.
39. Doerfel LK, Wohlgemuth I, Kothe C, Peske F, Urlaub H, Rodnina MV. 2013. EF-P is essential for rapid synthesis of proteins containing consecutive proline residues. Science 339:85-8.

40. Gutierrez E, Shin BS, Woolstenhulme CJ, Kim JR, Saini P, Buskirk AR, Dever TE. 2013. eIF5A promotes translation of polyproline motifs. *Mol Cell* 51:35-45.
41. Katoh T, Wohlgemuth I, Nagano M, Rodnina MV, Suga H. 2016. Essential structural elements in tRNA(Pro) for EF-P-mediated alleviation of translation stalling. *Nat Commun* 7:11657.
42. Schuller AP, Wu CC, Dever TE, Buskirk AR, Green R. 2017. eIF5A functions globally in translation elongation and termination. *Mol Cell* 66:194-205 e5.
43. Rexroad G, Donohue JP, Lancaster L, Noller HF. 2022. The role of GTP hydrolysis by EF-G in ribosomal translocation. *Proc Natl Acad Sci U S A* 119:e2212502119.
44. Guo Z, Noller HF. 2012. Rotation of the head of the 30S ribosomal subunit during mRNA translocation. *Proc Natl Acad Sci U S A* 109:20391-4.
45. Belardinelli R, Sharma H, Peske F, Wintermeyer W, Rodnina MV. 2016. Translocation as continuous movement through the ribosome. *RNA Biol* 13:1197-1203.
46. Wasserman MR, Alejo JL, Altman RB, Blanchard SC. 2016. Multiperspective smFRET reveals rate-determining late intermediates of ribosomal translocation. *Nat Struct Mol Biol* 23:333-41.
47. Savelsbergh A, Katunin VI, Mohr D, Peske F, Rodnina MV, Wintermeyer W. 2003. An elongation factor G-induced ribosome rearrangement precedes tRNA-mRNA translocation. *Mol Cell* 11:1517-23.
48. Savelsbergh A, Mohr D, Kothe U, Wintermeyer W, Rodnina MV. 2005. Control of phosphate release from elongation factor G by ribosomal protein L7/12. *EMBO J* 24:4316-23.
49. Adio S, Senyushkina T, Peske F, Fischer N, Wintermeyer W, Rodnina MV. 2015. Fluctuations between multiple EF-G-induced chimeric tRNA states during translocation on the ribosome. *Nat Commun* 6:7442.
50. Belardinelli R, Sharma H, Caliskan N, Cunha CE, Peske F, Wintermeyer W, Rodnina MV. 2016. Choreography of molecular movements during ribosome progression along mRNA. *Nat Struct Mol Biol* 23:342-8.

51. Korostelev A, Zhu J, Asahara H, Noller HF. 2010. Recognition of the amber UAG stop codon by release factor RF1. *EMBO J* 29:2577-85.
52. Weixlbaumer A, Jin H, Neubauer C, Voorhees RM, Petry S, Kelley AC, Ramakrishnan V. 2008. Insights into translational termination from the structure of RF2 bound to the ribosome. *Science* 322:953-6.
53. Hellen CUT. 2018. Translation termination and ribosome recycling in eukaryotes. *Cold Spring Harb Perspect Biol* 10.
54. Korostelev A, Asahara H, Lancaster L, Laurberg M, Hirschi A, Zhu J, Trakhanov S, Scott WG, Noller HF. 2008. Crystal structure of a translation termination complex formed with release factor RF2. *Proc Natl Acad Sci U S A* 105:19684-9.
55. Laurberg M, Asahara H, Korostelev A, Zhu J, Trakhanov S, Noller HF. 2008. Structural basis for translation termination on the 70S ribosome. *Nature* 454:852-7.
56. Santos N, Zhu J, Donohue JP, Korostelev AA, Noller HF. 2013. Crystal structure of the 70S ribosome bound with the Q253P mutant form of release factor RF2. *Structure* 21:1258-63.
57. Rodnina MV. 2013. The ribosome as a versatile catalyst: reactions at the peptidyl transferase center. *Curr Opin Struct Biol* 23:595-602.
58. Zavialov AV, Buckingham RH, Ehrenberg M. 2001. A posttermination ribosomal complex is the guanine nucleotide exchange factor for peptide release factor RF3. *Cell* 107:115-24.
59. Zavialov AV, Mora L, Buckingham RH, Ehrenberg M. 2002. Release of peptide promoted by the GGQ motif of class 1 release factors regulates the GTPase activity of RF3. *Mol Cell* 10:789-98.
60. Koutmou KS, McDonald ME, Brunelle JL, Green R. 2014. RF3:GTP promotes rapid dissociation of the class 1 termination factor. *RNA* 20:609-20.
61. Peske F, Kuhlenkoetter S, Rodnina MV, Wintermeyer W. 2014. Timing of GTP binding and hydrolysis by translation termination factor RF3. *Nucleic Acids Res* 42:1812-20.

62. Shi X, Joseph S. 2016. Mechanism of translation termination: RF1 dissociation follows dissociation of RF3 from the ribosome. *Biochemistry* 55:6344-6354.
63. Adio S, Sharma H, Senyushkina T, Karki P, Maracci C, Wohlgemuth I, Holtkamp W, Peske F, Rodnina MV. 2018. Dynamics of ribosomes and release factors during translation termination in *E. coli*. *Elife* 7.
64. Svidritskiy E, Demo G, Loveland AB, Xu C, Korostelev AA. 2019. Extensive ribosome and RF2 rearrangements during translation termination. *Elife* 8.
65. Gao N, Zavialov AV, Li W, Sengupta J, Valle M, Gursky RP, Ehrenberg M, Frank J. 2005. Mechanism for the disassembly of the posttermination complex inferred from cryo-EM studies. *Molecular cell* 18:663-674.
66. Hirokawa G, Nijman RM, Raj VS, Kaji H, Igarashi K, Kaji A. 2005. The role of ribosome recycling factor in dissociation of 70S ribosomes into subunits. *RNA (New York, NY)* 11:1317-1328.
67. Zavialov AV, Hauryliuk VV, Ehrenberg M. 2005. Splitting of the posttermination ribosome into subunits by the concerted action of RRF and EF-G. *Molecular cell* 18:675-686.
68. Dunkle JA, Wang L, Feldman MB, Pulk A, Chen VB, Kapral GJ, Noeske J, Richardson JS, Blanchard SC, Cate JH. 2011. Structures of the bacterial ribosome in classical and hybrid states of tRNA binding. *Science* 332:981-4.
69. Seo HS, Kiel M, Pan D, Raj VS, Kaji A, Cooperman BS. 2004. Kinetics and thermodynamics of RRF, EF-G, and thiostrepton interaction on the *Escherichia coli* ribosome. *Biochemistry* 43:12728-40.
70. Savelsbergh A, Rodnina MV, Wintermeyer W. 2009. Distinct functions of elongation factor G in ribosome recycling and translocation. *RNA* 15:772-80.
71. Borg A, Pavlov M, Ehrenberg M. 2016. Mechanism of fusidic acid inhibition of RRF- and EF-G-dependent splitting of the bacterial post-termination ribosome. *Nucleic acids research* 44:3264-3275.
72. Prabhakar A, Capece MC, Petrov A, Choi J, Puglisi JD. 2017. Post-termination ribosome intermediate acts as the gateway to ribosome recycling. *Cell reports* 20:161-172.

73. Fu Z, Kaledhonkar S, Borg A, Sun M, Chen B, Grassucci RA, Ehrenberg M, Frank J. 2016. Key intermediates in ribosome recycling visualized by time-resolved cryoelectron microscopy. *Structure* 24:2092-2101.
74. Chen Y, Kaji A, Kaji H, Cooperman BS. 2017. The kinetic mechanism of bacterial ribosome recycling. *Nucleic acids research* 45:10168-10177.
75. Iwakura N, Yokoyama T, Quaglia F, Mitsuoka K, Mio K, Shigematsu H, Shirouzu M, Kaji A, Kaji H. 2017. Chemical and structural characterization of a model Post-Termination Complex (PoTC) for the ribosome recycling reaction: evidence for the release of the mRNA by RRF and EF-G. *PLoS One* 12:e0177972.
76. Prossliner T, Skovbo Winther K, Sørensen MA, Gerdes K. 2018. Ribosome hibernation. *Annual Review of Genetics* 52:321-348.
77. Franken LE, Oostergetel GT, Pijning T, Puri P, Arkhipova V, Boekema EJ, Poolman B, Guskov A. 2017. A general mechanism of ribosome dimerization revealed by single-particle cryo-electron microscopy. *Nature communications* 8:722-x.
78. Ueta M, Wada C, Daifuku T, Sako Y, Bessho Y, Kitamura A, Ohniwa RL, Morikawa K, Yoshida H, Kato T, Miyata T, Namba K, Wada A. 2013. Conservation of two distinct types of 100S ribosome in bacteria. *Genes Cells* 18:554-74.
79. Yoshida H, Wada A. 2014. The 100S ribosome: ribosomal hibernation induced by stress. *Wiley Interdiscip Rev RNA* 5:723-32.
80. Krokowski D, Gaccioli F, Majumder M, Mullins MR, Yuan CL, Papadopoulou B, Merrick WC, Komar AA, Taylor D, Hatzoglou M. 2011. Characterization of hibernating ribosomes in mammalian cells. *Cell Cycle* 10:2691-702.
81. Sharma MR, Donhofer A, Barat C, Marquez V, Datta PP, Fucini P, Wilson DN, Agrawal RK. 2010. PSRP1 is not a ribosomal protein, but a ribosome-binding factor that is recycled by the ribosome-recycling factor (RRF) and elongation factor G (EF-G). *J Biol Chem* 285:4006-4014.
82. Tissieres A, Watson JD. 1958. Ribonucleoprotein particles from *Escherichia coli*. *Nature* 182:778-80.

83. Hall C, Slayter H. 1959. Electron microscopy of ribonucleoprotein particles from *E. coli*. *Journal of Molecular Biology* 1:329-IN1.
84. McCarthy B. 1960. Variations in bacterial ribosomes. *Biochimica et biophysica acta* 39:563-564.
85. Beckert B, Turk M, Czech A, Berninghausen O, Beckmann R, Ignatova Z, Plitzko JM, Wilson DN. 2018. Structure of a hibernating 100S ribosome reveals an inactive conformation of the ribosomal protein S1. *Nature microbiology* 3:1115-1121.
86. Ortiz JO, Brandt F, Matias VR, Sennels L, Rappsilber J, Scheres SH, Eibauer M, Hartl FU, Baumeister W. 2010. Structure of hibernating ribosomes studied by cryoelectron tomography *in vitro* and *in situ*. *Journal of Cell Biology* 190:613-621.
87. Wada A, Yamazaki Y, Fujita N, Ishihama A. 1990. Structure and probable genetic location of a "ribosome modulation factor" associated with 100S ribosomes in stationary-phase *Escherichia coli* cells. *Proceedings of the National Academy of Sciences* 87:2657-2661.
88. Yoshida H, Maki Y, Kato H, Fujisawa H, Izutsu K, Wada C, Wada A. 2002. The ribosome modulation factor (RMF) binding site on the 100S ribosome of *Escherichia coli*. *The journal of biochemistry* 132:983-989.
89. Kato T, Yoshida H, Miyata T, Maki Y, Wada A, Namba K. 2010. Structure of the 100S ribosome in the hibernation stage revealed by electron cryomicroscopy. *Structure (London, England : 1993)* 18:719-724.
90. Wada A. 1998. Growth phase coupled modulation of *Escherichia coli* ribosomes. *Genes to Cells* 3:203-208.
91. Wada A, Mikkola R, Kurland CG, Ishihama A. 2000. Growth phase-coupled changes of the ribosome profile in natural isolates and laboratory strains of *Escherichia coli*. *Journal of bacteriology* 182:2893-2899.
92. Shcherbakova K, Nakayama H, Shimamoto N. 2015. Role of 100S ribosomes in bacterial decay period. *Genes to Cells* 20:789-801.

93. Aiso T, Yoshida H, Wada A, Ohki R. 2005. Modulation of mRNA stability participates in stationary-phase-specific expression of ribosome modulation factor. *Journal of bacteriology* 187:1951-1958.
94. Yamagishi M, Matsushima H, Wada A, Sakagami M, Fujita N, Ishihama A. 1993. Regulation of the *Escherichia coli* *rmf* gene encoding the ribosome modulation factor: growth phase- and growth rate-dependent control. *The EMBO journal* 12:625-630.
95. Ueta M, Ohniwa RL, Yoshida H, Maki Y, Wada C, Wada A. 2008. Role of HPF (hibernation promoting factor) in translational activity in *Escherichia coli*. *Journal of biochemistry* 143:425-433.
96. Ueta M, Yoshida H, Wada C, Baba T, Mori H, Wada A. 2005. Ribosome binding proteins YhbH and YfiA have opposite functions during 100S formation in the stationary phase of *Escherichia coli*. *Genes to Cells* 10:1103-1112.
97. Wada A, Igarashi K, Yoshimura S, Aimoto S, Ishihama A. 1995. Ribosome modulation factor: stationary growth phase-specific inhibitor of ribosome functions from *Escherichia coli*. *Biochemical and biophysical research communications* 214:410-417.
98. Agafonov DE, Kolb VA, Nazimov IV, Spirin AS. 1999. A protein residing at the subunit interface of the bacterial ribosome. *Proceedings of the National Academy of Sciences* 96:12345-12349.
99. Vila-Sanjurjo A, Schuwirth B-S, Hau CW, Cate JH. 2004. Structural basis for the control of translation initiation during stress. *Nature structural & molecular biology* 11:1054-1059.
100. Sato A, Watanabe T, Maki Y, Ueta M, Yoshida H, Ito Y, Wada A, Mishima M. 2009. Solution structure of the *E. coli* ribosome hibernation promoting factor HPF: Implications for the relationship between structure and function. *Biochem Biophys Res Commun* 389:580-5.
101. Polikanov YS, Blaha GM, Steitz TA. 2012. How hibernation factors RMF, HPF, and YfiA turn off protein synthesis. *Science* 336:915-918.
102. Akanuma G, Kazo Y, Tagami K, Hiraoka H, Yano K, Suzuki S, Hanai R, Nanamiya H, Kato-Yamada Y, Kawamura F. 2016. Ribosome dimerization is essential for the efficient regrowth of *Bacillus subtilis*. *Microbiology (Reading)* 162:448-458.

103. Kline BC, McKay SL, Tang WW, Portnoy DA. 2015. The *Listeria monocytogenes* hibernation-promoting factor is required for the formation of 100S ribosomes, optimal fitness, and pathogenesis. *J Bacteriol* 197:581-91.
104. Puri P, Eckhardt TH, Franken LE, Fusetti F, Stuart MC, Boekema EJ, Kuipers OP, Kok J, Poolman B. 2014. *Lactococcus lactis* YfiA is necessary and sufficient for ribosome dimerization. *Mol Microbiol* 91:394-407.
105. Ueta M, Wada C, Wada A. 2010. Formation of 100S ribosomes in *Staphylococcus aureus* by the hibernation promoting factor homolog SaHPF. *Genes Cells* 15:43-58.
106. Basu A, Yap MN. 2016. Ribosome hibernation factor promotes Staphylococcal survival and differentially represses translation. *Nucleic Acids Res* 44:4881-93.
107. el-Sharoud WM, Niven GW. 2005. The activity of ribosome modulation factor during growth of *Escherichia coli* under acidic conditions. *Arch Microbiol* 184:18-24.
108. Garay-Arroyo A, Colmenero-Flores JM, Garcarrubio A, Covarrubias AA. 2000. Highly hydrophilic proteins in prokaryotes and eukaryotes are common during conditions of water deficit. *J Biol Chem* 275:5668-74.
109. Izutsu K, Wada A, Wada C. 2001. Expression of ribosome modulation factor (RMF) in *Escherichia coli* requires ppGpp. *Genes Cells* 6:665-76.
110. Moen B, Janbu AO, Langsrud S, Langsrud O, Hobman JL, Constantinidou C, Kohler A, Rudi K. 2009. Global responses of *Escherichia coli* to adverse conditions determined by microarrays and FT-IR spectroscopy. *Can J Microbiol* 55:714-28.
111. Raivio TL, Leblanc SK, Price NL. 2013. The *Escherichia coli* Cpx envelope stress response regulates genes of diverse function that impact antibiotic resistance and membrane integrity. *J Bacteriol* 195:2755-67.
112. Traxler MF, Summers SM, Nguyen HT, Zacharia VM, Hightower GA, Smith JT, Conway T. 2008. The global, ppGpp-mediated stringent response to amino acid starvation in *Escherichia coli*. *Mol Microbiol* 68:1128-48.
113. Durfee T, Hansen AM, Zhi H, Blattner FR, Jin DJ. 2008. Transcription profiling of the stringent response in *Escherichia coli*. *J Bacteriol* 190:1084-96.

114. Drzewiecki K, Eymann C, Mittenhuber G, Hecker M. 1998. The *yvyD* gene of *Bacillus subtilis* is under dual control of sigmaB and sigmaH. *J Bacteriol* 180:6674-80.
115. Tagami K, Nanamiya H, Kazo Y, Maehashi M, Suzuki S, Namba E, Hoshiya M, Hanai R, Tozawa Y, Morimoto T, Ogasawara N, Kageyama Y, Ara K, Ozaki K, Yoshida M, Kuroiwa H, Kuroiwa T, Ohashi Y, Kawamura F. 2012. Expression of a small (p)ppGpp synthetase, YwaC, in the (p)ppGpp(0) mutant of *Bacillus subtilis* triggers YvyD-dependent dimerization of ribosome. *Microbiologyopen* 1:115-34.
116. Potrykus K, Cashel M. 2008. (p)ppGpp: still magical? *Annu Rev Microbiol* 62:35-51.
117. Boutte CC, Crosson S. 2013. Bacterial lifestyle shapes stringent response activation. *Trends Microbiol* 21:174-80.
118. Corrigan RM, Bellows LE, Wood A, Grundling A. 2016. ppGpp negatively impacts ribosome assembly affecting growth and antimicrobial tolerance in Gram-positive bacteria. *Proc Natl Acad Sci U S A* 113:E1710-9.
119. Persky NS, Ferullo DJ, Cooper DL, Moore HR, Lovett ST. 2009. The ObgE/CgtA GTPase influences the stringent response to amino acid starvation in *Escherichia coli*. *Mol Microbiol* 73:253-66.
120. Legault L, Jeantet C, Gros F. 1972. Inhibition of *in vitro* protein synthesis by ppGpp. *FEBS Lett* 27:71-75.
121. Vinogradova DS, Zegarra V, Maksimova E, Nakamoto JA, Kasatsky P, Paleskava A, Konevega AL, Milon P. 2020. How the initiating ribosome copes with ppGpp to translate mRNAs. *PLoS Biol* 18:e3000593.
122. Rojas AM, Ehrenberg M, Andersson SG, Kurland CG. 1984. ppGpp inhibition of elongation factors Tu, G and Ts during polypeptide synthesis. *Mol Gen Genet* 197:36-45.
123. Kihira K, Shimizu Y, Shomura Y, Shibata N, Kitamura M, Nakagawa A, Ueda T, Ochi K, Higuchi Y. 2012. Crystal structure analysis of the translation factor RF3 (release factor 3). *FEBS Lett* 586:3705-9.
124. Ryals J, Little R, Bremer H. 1982. Control of rRNA and tRNA syntheses in *Escherichia coli* by guanosine tetraphosphate. *J Bacteriol* 151:1261-8.

125. Dai X, Zhu M, Warren M, Balakrishnan R, Patsalo V, Okano H, Williamson JR, Fredrick K, Wang YP, Hwa T. 2016. Reduction of translating ribosomes enables *Escherichia coli* to maintain elongation rates during slow growth. *Nature microbiology* 2:16231.
126. Li SH, Li Z, Park JO, King CG, Rabinowitz JD, Wingreen NS, Gitai Z. 2018. *Escherichia coli* translation strategies differ across carbon, nitrogen and phosphorus limitation conditions. *Nature microbiology* 3:939-947.
127. Dai X, Zhu M, Warren M, Balakrishnan R, Okano H, Williamson JR, Fredrick K, Hwa T. 2018. Slowdown of translational elongation in *Escherichia coli* under hyperosmotic stress. *mBio* 9.
128. Pokusaeva K, Fitzgerald GF, van Sinderen D. 2011. Carbohydrate metabolism in *Bifidobacteria*. *Genes Nutr* 6:285-306.
129. Andersen KB, von Meyenburg K. 1980. Are growth rates of *Escherichia coli* in batch cultures limited by respiration? *J Bacteriol* 144:114-23.
130. Hollywood N, Doelle HW. 1976. Effect of specific growth rate and glucose concentration on growth and glucose metabolism of *Escherichia coli* K-12. *Microbios* 17:23-33.
131. Majewski RA, Domach MM. 1990. Simple constrained-optimization view of acetate overflow in *E. coli*. *Biotechnol Bioeng* 35:732-8.
132. Rose IA, Grunberg-Manago M, Corey SR, Ochoa S. 1954. Enzymatic phosphorylation of acetate. *J Biol Chem* 211:737-56.
133. Wolfe AJ. 2005. The acetate switch. *Microbiology and molecular biology reviews* : MMBR 69:12-50.
134. Orr JS, Christensen DG, Wolfe AJ, Rao CV. 2019. Extracellular acidic pH inhibits acetate consumption by decreasing gene transcription of the tricarboxylic acid cycle and the glyoxylate shunt. *J Bacteriol* 201.
135. Christensen DG, Baumgartner JT, Xie X, Jew KM, Basisty N, Schilling B, Kuhn ML, Wolfe AJ. 2019. Mechanisms, detection, and relevance of protein acetylation in prokaryotes. *mBio* 10:e02708-18.

136. Carabetta VJ, Cristea IM. 2017. Regulation, function, and detection of protein acetylation in bacteria. *J Bacteriol* 199.
137. Drazic A, Myklebust LM, Ree R, Arnesen T. 2016. The world of protein acetylation. *Biochimica et biophysica acta* 1864:1372-1401.
138. Ouidir T, Kentache T, Hardouin J. 2016. Protein lysine acetylation in bacteria: Current state of the art. *Proteomics* 16:301-309.
139. Song G, Walley JW. 2016. Dynamic protein acetylation in plant-pathogen interactions. *Front Plant Sci* 7:421.
140. Hentchel KL, Escalante-Semerena JC. 2015. Acylation of biomolecules in prokaryotes: a widespread strategy for the control of biological function and metabolic Stress. *Microbiol Mol Biol Rev* 79:321-46.
141. Liu J, Wang Q, Jiang X, Yang H, Zhao D, Han J, Luo Y, Xiang H. 2017. Systematic analysis of lysine acetylation in the halophilic archaeon *Haloferax mediterranei*. *J Proteome Res* 16:3229-3241.
142. Soppa J. 2010. Protein acetylation in archaea, bacteria, and eukaryotes. *Archaea (Vancouver, BC)* 2010:10.1155/2010/820681.
143. Bell SD, Botting CH, Wardleworth BN, Jackson SP, White MF. 2002. The interaction of Alba, a conserved archaeal chromatin protein, with Sir2 and its regulation by acetylation. *Science* 296:148-51.
144. Narita T, Weinert BT, Choudhary C. 2019. Functions and mechanisms of non-histone protein acetylation. *Nat Rev Mol Cell Biol* 20:156-174.
145. Mukherjee S, Hao YH, Orth K. 2007. A newly discovered post-translational modification--the acetylation of serine and threonine residues. *Trends Biochem Sci* 32:210-6.
146. Plevoda B, Sherman F. 2003. N-terminal acetyltransferases and sequence requirements for N-terminal acetylation of eukaryotic proteins. *Journal of Molecular Biology* 325:595-622.

147. Lee FJ, Lin LW, Smith JA. 1989. N alpha-acetyltransferase deficiency alters protein synthesis in *Saccharomyces cerevisiae*. FEBS Lett 256:139-42.
148. Brown JL. 1979. A comparison of the turnover of alpha-N-acetylated and nonacetylated mouse L-cell proteins. J Biol Chem 254:1447-9.
149. Brown JL, Roberts WK. 1976. Evidence that approximately eighty per cent of the soluble proteins from *Ehrlich ascites* cells are Nalpha-acetylated. J Biol Chem 251:1009-14.
150. Schmidt A, Kochanowski K, Vedelaar S, Ahrne E, Volkmer B, Callipo L, Knoops K, Bauer M, Aebersold R, Heinemann M. 2016. The quantitative and condition-dependent *Escherichia coli* proteome. Nat Biotechnol 34:104-10.
151. Soufi B, Krug K, Harst A, Macek B. 2015. Characterization of the *E. coli* proteome and its modifications during growth and ethanol stress. Front Microbiol 6:103.
152. Favrot L, Blanchard JS, Vergnolle O. 2016. Bacterial GCN5-related N-acetyltransferases: from resistance to regulation. Biochemistry 55:989-1002.
153. Vetting MW, S de Carvalho LP, Yu M, Hegde SS, Magnet S, Roderick SL, Blanchard JS. 2005. Structure and functions of the GNAT superfamily of acetyltransferases. Archives of Biochemistry and Biophysics 433:212-226.
154. Ma KW, Ma W. 2016. YopJ family effectors promote bacterial infection through a unique acetyltransferase activity. Microbiol Mol Biol Rev 80:1011-1027.
155. Lewis JD, Lee A, Ma W, Zhou H, Guttman DS, Desveaux D. 2011. The YopJ superfamily in plant-associated bacteria. Mol Plant Pathol 12:928-37.
156. Tanner KG, Trievel RC, Kuo MH, Howard RM, Berger SL, Allis CD, Marmorstein R, Denu JM. 1999. Catalytic mechanism and function of invariant glutamic acid 173 from the histone acetyltransferase GCN5 transcriptional coactivator. J Biol Chem 274:18157-60.
157. Dyda F, Klein DC, Hickman AB. 2000. GCN5-related N-acetyltransferases: a structural overview. Annu Rev Biophys Biomol Struct 29:81-103.

158. de Diego Puente T, Gallego-Jara J, Castano-Cerezo S, Bernal Sanchez V, Fernandez Espin V, Garcia de la Torre J, Manjon Rubio A, Canovas Diaz M. 2015. The protein acetyltransferase PatZ from *Escherichia coli* is regulated by autoacetylation-induced oligomerization. *J Biol Chem* 290:23077-93.
159. Lu YX, Liu XX, Liu WB, Ye BC. 2017. Identification and characterization of two types of amino acid-regulated acetyltransferases in *Actinobacteria*. *Biosci Rep* 37.
160. Castaño-Cerezo S, Bernal V, Blanco-Catalá J, Iborra JL, Cánovas M. 2011. cAMP-CRP co-ordinates the expression of the protein acetylation pathway with central metabolism in *Escherichia coli*. *Molecular microbiology* 82:1110-1128.
161. Liimatta K, Flaherty E, Ro G, Nguyen DK, Prado C, Purdy AE. 2018. A putative acetylation system in *Vibrio cholerae* modulates virulence in arthropod hosts. *Appl Environ Microbiol* 84.
162. Starai VJ, Escalante-Semerena JC. 2004. Identification of the protein acetyltransferase (Pat) enzyme that acetylates acetyl-CoA synthetase in *Salmonella enterica*. *J Mol Biol* 340:1005-12.
163. Liu W, Tan Y, Cao S, Zhao H, Fang H, Yang X, Wang T, Zhou Y, Yan Y, Han Y, Song Y, Bi Y, Wang X, Yang R, Du Z. 2018. Protein acetylation mediated by YfiQ and CobB is involved in the virulence and stress response of *Yersinia pestis*. *Infect Immun* 86.
164. Crosby HA, Pelletier DA, Hurst GB, Escalante-Semerena JC. 2012. System-wide studies of N-lysine acetylation in *Rhodopseudomonas palustris* reveal substrate specificity of protein acetyltransferases. *J Biol Chem* 287:15590-601.
165. Tucker AC, Taylor KC, Rank KC, Rayment I, Escalante-Semerena JC. 2014. Insights into the specificity of lysine acetyltransferases. *J Biol Chem* 289:36249-62.
166. Ishigaki Y, Akanuma G, Yoshida M, Horinouchi S, Kosono S, Ohnishi Y. 2017. Protein acetylation involved in streptomycin biosynthesis in *Streptomyces griseus*. *J Proteomics* 155:63-72.
167. Thao S, Escalante-Semerena JC. 2011. Biochemical and thermodynamic analyses of *Salmonella enterica* Pat, a multidomain, multimeric N(epsilon)-lysine acetyltransferase involved in carbon and energy metabolism. *mBio* 2.

168. Ren J, Sang Y, Ni J, Tao J, Lu J, Zhao M, Yao YF. 2015. Acetylation regulates survival of *Salmonella enterica* Serovar Typhimurium under acid stress. *Applied and Environmental Microbiology* 81:5675-5682.
169. Ma Q, Wood TK. 2011. Protein acetylation in prokaryotes increases stress resistance. *Biochem Biophys Res Commun* 410:846-51.
170. Christensen DG, Meyer JG, Baumgartner JT, D'Souza AK, Nelson WC, Payne SH, Kuhn ML, Schilling B, Wolfe AJ. 2018. Identification of novel protein lysine acetyltransferases in *Escherichia coli*. *mBio* 9:e01905-18.
171. Xu H, Hegde SS, Blanchard JS. 2011. Reversible acetylation and inactivation of *Mycobacterium tuberculosis* acetyl-CoA synthetase is dependent on cAMP. *Biochemistry* 50:5883-92.
172. Nambi S, Basu N, Visweswariah SS. 2010. cAMP-regulated protein lysine acetylases in *mycobacteria*. *J Biol Chem* 285:24313-23.
173. Liu XX, Liu WB, Ye BC. 2015. Regulation of a protein acetyltransferase in *Myxococcus xanthus* by the coenzyme NADP. *J Bacteriol* 198:623-32.
174. Lee W, VanderVen BC, Walker S, Russell DG. 2017. Novel protein acetyltransferase, Rv2170, modulates carbon and energy metabolism in *Mycobacterium tuberculosis*. *Sci Rep* 7:72.
175. Li Y, Krishnan K, Duncan MJ. 2018. Post-translational regulation of a *Porphyromonas gingivalis* regulator. *J Oral Microbiol* 10:1487743.
176. Gardner JG, Grundy FJ, Henkin TM, Escalante-Semerena JC. 2006. Control of acetyl-coenzyme A synthetase (AcsA) activity by acetylation/deacetylation without NAD(+) involvement in *Bacillus subtilis*. *J Bacteriol* 188:5460-8.
177. You D, Yao LL, Huang D, Escalante-Semerena JC, Ye BC. 2014. Acetyl coenzyme A synthetase is acetylated on multiple lysine residues by a protein acetyltransferase with a single Gcn5-type N-acetyltransferase (GNAT) domain in *Saccharopolyspora erythraea*. *J Bacteriol* 196:3169-78.
178. Marsh VL, Peak-Chew SY, Bell SD. 2005. Sir2 and the acetyltransferase, Pat, regulate the archaeal chromatin protein, Alba. *J Biol Chem* 280:21122-8.

179. Brent MM, Iwata A, Carten J, Zhao K, Marmorstein R. 2009. Structure and biochemical characterization of protein acetyltransferase from *Sulfolobus solfataricus*. *J Biol Chem* 284:19412-9.
180. VanDrisse CM, Parks AR, Escalante-Semerena JC. 2017. A toxin involved in *Salmonella* persistence regulates its activity by acetylating its cognate antitoxin, a modification reversed by CobB sirtuin deacetylase. *mBio* 8.
181. Ghosh S, Padmanabhan B, Anand C, Nagaraja V. 2016. Lysine acetylation of the *Mycobacterium tuberculosis* HU protein modulates its DNA binding and genome organization. *Mol Microbiol* 100:577-88.
182. Green KD, Biswas T, Pang AH, Willby MJ, Reed MS, Stuchlik O, Pohl J, Posey JE, Tsodikov OV, Garneau-Tsodikova S. 2018. Acetylation by Eis and deacetylation by Rv1151c of *Mycobacterium tuberculosis* HupB: biochemical and structural insight. *Biochemistry* 57:781-790.
183. Kim KH, An DR, Song J, Yoon JY, Kim HS, Yoon HJ, Im HN, Kim J, Kim DJ, Lee SJ, Kim KH, Lee HM, Kim HJ, Jo EK, Lee JY, Suh SW. 2012. *Mycobacterium tuberculosis* Eis protein initiates suppression of host immune responses by acetylation of DUSP16/MKP-7. *Proc Natl Acad Sci U S A* 109:7729-34.
184. Zaunbrecher MA, Sikes RD, Jr., Metchock B, Shinnick TM, Posey JE. 2009. Overexpression of the chromosomally encoded aminoglycoside acetyltransferase *eis* confers kanamycin resistance in *Mycobacterium tuberculosis*. *Proc Natl Acad Sci U S A* 106:20004-9.
185. Chen W, Biswas T, Porter VR, Tsodikov OV, Garneau-Tsodikova S. 2011. Unusual regioversatility of acetyltransferase Eis, a cause of drug resistance in XDR-TB. *Proc Natl Acad Sci U S A* 108:9804-8.
186. Vetting MW, Bareich DC, Yu M, Blanchard JS. 2008. Crystal structure of RimI from *Salmonella typhimurium* LT2, the GNAT responsible for N(alpha)-acetylation of ribosomal protein S18. *Protein Sci* 17:1781-90.
187. Isono K, Isono S. 1980. Ribosomal protein modification in *Escherichia coli*. II. Studies of a mutant lacking the N-terminal acetylation of protein S18. *Mol Gen Genet* 177:645-51.

188. Yoshikawa A, Isono S, Sheback A, Isono K. 1987. Cloning and nucleotide sequencing of the genes *rimI* and *rimJ* which encode enzymes acetylating ribosomal proteins S18 and S5 of *Escherichia coli* K12. *Mol Gen Genet* 209:481-8.
189. Pathak D, Bhat AH, Sapehia V, Rai J, Rao A. 2016. Biochemical evidence for relaxed substrate specificity of Nalpha-acetyltransferase (Rv3420c/*rimI*) of *Mycobacterium tuberculosis*. *Sci Rep* 6:28892.
190. Kosono S, Tamura M, Suzuki S, Kawamura Y, Yoshida A, Nishiyama M, Yoshida M. 2015. Changes in the acetylome and succinylome of *Bacillus subtilis* in response to carbon Source. *PLoS one* 10:e0131169.
191. Wang MM, You D, Ye BC. 2017. Site-specific and kinetic characterization of enzymatic and nonenzymatic protein acetylation in bacteria. *Sci Rep* 7:14790.
192. Okanishi H, Kim K, Masui R, Kuramitsu S. 2013. Acetylome with structural mapping reveals the significance of lysine acetylation in *Thermus thermophilus*. *J Proteome Res* 12:3952-68.
193. Castano-Cerezo S, Bernal V, Post H, Fuhrer T, Cappadona S, Sanchez-Diaz NC, Sauer U, Heck AJ, Altelaar AF, Canovas M. 2014. Protein acetylation affects acetate metabolism, motility and acid stress response in *Escherichia coli*. *Mol Syst Biol* 10:762.
194. Bologna FP, Andreo CS, Drincovich MF. 2007. *Escherichia coli* malic enzymes: two isoforms with substantial differences in kinetic properties, metabolic regulation, and structure. *J Bacteriol* 189:5937-46.
195. Starai VJ, Garrity J, Escalante-Semerena JC. 2005. Acetate excretion during growth of *Salmonella enterica* on ethanolamine requires phosphotransacetylase (EutD) activity, and acetate recapture requires acetyl-CoA synthetase (Acs) and phosphotransacetylase (Pta) activities. *Microbiology (Reading)* 151:3793-3801.
196. Sheppard DE, Roth JR. 1994. A rationale for autoinduction of a transcriptional activator: ethanolamine ammonia-lyase (EutBC) and the operon activator (EutR) compete for adenosyl-cobalamin in *Salmonella typhimurium*. *J Bacteriol* 176:1287-96.
197. Marolewski A, Smith JM, Benkovic SJ. 1994. Cloning and characterization of a new purine biosynthetic enzyme: a non-folate glycinamide ribonucleotide transformylase from *E. coli*. *Biochemistry* 33:2531-7.

198. Wolfe AJ. 2015. Glycolysis for microbiome generation. *Microbiol Spectr* 3.
199. Klein AH, Shulla A, Reimann SA, Keating DH, Wolfe AJ. 2007. The intracellular concentration of acetyl phosphate in *Escherichia coli* is sufficient for direct phosphorylation of two-component response regulators. *Journal of Bacteriology* 189:5574-5581.
200. Pruss BM, Wolfe AJ. 1994. Regulation of acetyl phosphate synthesis and degradation, and the control of flagellar expression in *Escherichia coli*. *Mol Microbiol* 12:973-84.
201. Schilling B, Christensen D, Davis R, Sahu AK, Hu LI, Walker-Peddakotla A, Sorensen DJ, Zemaitaitis B, Gibson BW, Wolfe AJ. 2015. Protein acetylation dynamics in response to carbon overflow in *Escherichia coli*. *Molecular microbiology* 98:847-863.
202. Christensen DG, Orr JS, Rao CV, Wolfe AJ. 2017. Increasing growth yield and decreasing acetylation in *Escherichia coli* by optimizing the carbon-to-magnesium ratio in peptide-based media. *Applied and Environmental Microbiology* 83:e03034-16. Print 2017 Mar 15.
203. Yang XJ, Seto E. 2008. The Rpd3/Hda1 family of lysine deacetylases: from bacteria and yeast to mice and men. *Nature reviews Molecular cell biology* 9:206-218.
204. Blander G, Guarente L. 2004. The Sir2 family of protein deacetylases. *Annual Review of Biochemistry* 73:417-435.
205. AbouElfetouh A, Kuhn ML, Hu LI, Scholle MD, Sorensen DJ, Sahu AK, Becher D, Antelmann H, Mrksich M, Anderson WF, Gibson BW, Schilling B, Wolfe AJ. 2015. The *E. coli* sirtuin CobB shows no preference for enzymatic and nonenzymatic lysine acetylation substrate sites. *Microbiologyopen* 4:66-83.
206. Tu S, Guo SJ, Chen CS, Liu CX, Jiang HW, Ge F, Deng JY, Zhou YM, Czajkowsky DM, Li Y, Qi BR, Ahn YH, Cole PA, Zhu H, Tao SC. 2015. YcgC represents a new protein deacetylase family in prokaryotes. *Elife* 4.
207. Kremer M, Kuhlmann N, Lechner M, Baldus L, Lammers M. 2018. Comment on 'YcgC represents a new protein deacetylase family in prokaryotes'. *Elife* 7.

208. Ye Q, Ji QQ, Yan W, Yang F, Wang ED. 2017. Acetylation of lysine  $\epsilon$ -amino groups regulates aminoacyl-tRNA synthetase activity in *Escherichia coli*. *The Journal of biological chemistry* 292:10709-10722.
209. Venkat S, Gregory C, Sturges J, Gan Q, Fan C. 2017. Studying the lysine acetylation of malate dehydrogenase. *J Mol Biol* 429:1396-1405.
210. Zhang Q, Zhou A, Li S, Ni J, Tao J, Lu J, Wan B, Li S, Zhang J, Zhao S, Zhao GP, Shao F, Yao YF. 2016. Reversible lysine acetylation is involved in DNA replication initiation by regulating activities of initiator DnaA in *Escherichia coli*. *Sci Rep* 6:30837.
211. Song L, Wang G, Malhotra A, Deutscher MP, Liang W. 2016. Reversible acetylation on Lys501 regulates the activity of RNase II. *Nucleic Acids Res* 44:1979-88.
212. Colak G, Xie Z, Zhu AY, Dai L, Lu Z, Zhang Y, Wan X, Chen Y, Cha YH, Lin H, Zhao Y, Tan M. 2013. Identification of lysine succinylation substrates and the succinylation regulatory enzyme CobB in *Escherichia coli*. *Mol Cell Proteomics* 12:3509-20.
213. Sun M, Xu J, Wu Z, Zhai L, Liu C, Cheng Z, Xu G, Tao S, Ye BC, Zhao Y, Tan M. 2016. Characterization of protein lysine propionylation in *Escherichia coli*: global profiling, dynamic change, and enzymatic regulation. *J Proteome Res* 15:4696-4708.
214. Garrity J, Gardner JG, Hawse W, Wolberger C, Escalante-Semerena JC. 2007. N-lysine propionylation controls the activity of propionyl-CoA synthetase. *J Biol Chem* 282:30239-45.
215. Rowland EA, Greco TM, Snowden CK, McCabe AL, Silhavy TJ, Cristea IM. 2017. Sirtuin lipoamidase activity is conserved in bacteria as a regulator of metabolic enzyme complexes. *mBio* 8.
216. Mei XY, He XD, Huang L, Qi DS, Nie J, Li Y, Si W, Zhao SM. 2016. Dehomocysteinylation is catalysed by the sirtuin-2-like bacterial lysine deacetylase CobB. *FEBS J* 283:4149-4162.
217. Doll S, Burlingame AL. 2015. Mass spectrometry-based detection and assignment of protein posttranslational modifications. *ACS Chem Biol* 10:63-71.

218. Ong SE, Blagoev B, Kratchmarova I, Kristensen DB, Steen H, Pandey A, Mann M. 2002. Stable isotope labeling by amino acids in cell culture, SILAC, as a simple and accurate approach to expression proteomics. *Mol Cell Proteomics* 1:376-86.
219. Schilling B, Rardin MJ, MacLean BX, Zawadzka AM, Frewen BE, Cusack MP, Sorensen DJ, Bereman MS, Jing E, Wu CC, Verdin E, Kahn CR, Maccoss MJ, Gibson BW. 2012. Platform-independent and label-free quantitation of proteomic data using MS1 extracted ion chromatograms in skyline: application to protein acetylation and phosphorylation. *Mol Cell Proteomics* 11:202-14.
220. Gillet LC, Navarro P, Tate S, Rost H, Selevsek N, Reiter L, Bonner R, Aebersold R. 2012. Targeted data extraction of the MS/MS spectra generated by data-independent acquisition: a new concept for consistent and accurate proteome analysis. *Mol Cell Proteomics* 11:O111 016717.
221. Zhang J, Sprung R, Pei J, Tan X, Kim S, Zhu H, Liu CF, Grishin NV, Zhao Y. 2009. Lysine acetylation is a highly abundant and evolutionarily conserved modification in *Escherichia coli*. *Molecular & cellular proteomics : MCP* 8:215-225.
222. Yu BJ, Kim JA, Moon JH, Ryu SE, Pan JG. 2008. The diversity of lysine-acetylated proteins in *Escherichia coli*. *Journal of microbiology and biotechnology* 18:1529-1536.
223. Baeza J, Dowell JA, Smallegan MJ, Fan J, Amador-Noguez D, Khan Z, Denu JM. 2014. Stoichiometry of site-specific lysine acetylation in an entire proteome. *J Biol Chem* 289:21326-38.
224. Kentache T, Jouenne T, De E, Hardouin J. 2016. Proteomic characterization of N-alpha- and N-epsilon-acetylation in *Acinetobacter baumannii*. *J Proteomics* 144:148-58.
225. Sun L, Yao Z, Guo Z, Zhang L, Wang Y, Mao R, Lin Y, Fu Y, Lin X. 2019. Comprehensive analysis of the lysine acetylome in *Aeromonas hydrophila* reveals cross-talk between lysine acetylation and succinylation in LuxS. *Emerg Microbes Infect* 8:1229-1239.
226. Lv Y. 2017. Proteome-wide profiling of protein lysine acetylation in *Aspergillus flavus*. *PLoS One* 12:e0178603.
227. Liu L, Wang G, Song L, Lv B, Liang W. 2016. Acetylome analysis reveals the involvement of lysine acetylation in biosynthesis of antibiotics in *Bacillus amyloliquefaciens*. *Sci Rep* 6:20108.

228. Sun XL, Yang YH, Zhu L, Liu FY, Xu JP, Huang XW, Mo MH, Liu T, Zhang KQ. 2018. The lysine acetylome of the nematocidal bacterium *Bacillus nematocida* and impact of nematode on the acetylome. *J Proteomics* 177:31-39.
229. Kim D, Yu BJ, Kim JA, Lee YJ, Choi SG, Kang S, Pan JG. 2013. The acetylproteome of Gram-positive model bacterium *Bacillus subtilis*. *Proteomics* 13:1726-36.
230. Ravikumar V, Nalpas NC, Anselm V, Krug K, Lenuzzi M, Sestak MS, Domazet-Loso T, Mijakovic I, Macek B. 2018. In-depth analysis of *Bacillus subtilis* proteome identifies new ORFs and traces the evolutionary history of modified proteins. *Sci Rep* 8:17246.
231. Reverdy A, Chen Y, Hunter E, Gozzi K, Chai Y. 2018. Protein lysine acetylation plays a regulatory role in *Bacillus subtilis* multicellularity. *PLoS One* 13:e0204687.
232. Carabetta VJ, Greco TM, Tanner AW, Cristea IM, Dubnau D. 2016. Temporal Regulation of the *Bacillus subtilis* acetylome and evidence for a Role of MreB acetylation in cell wall growth. *mSystems* 1.
233. Bontemps-Gallo S, Gaviard C, Richards CL, Kentache T, Raffel SJ, Lawrence KA, Schindler JC, Lovelace J, Dulebohn DP, Cluss RG, Hardouin J, Gherardini FC. 2018. Global profiling of lysine acetylation in *Borrelia burgdorferi* B31 reveals its role in central metabolism. *Front Microbiol* 9:2036.
234. Li Y, Xue H, Bian DR, Xu G, Piao C. 2020. Acetylome analysis of lysine acetylation in the plant pathogenic bacterium *Brenneria nigrifluens*. *Microbiologyopen* 9:e00952.
235. Xu JY, Xu Z, Liu X, Tan M, Ye BC. 2018. Protein acetylation and butyrylation regulate the phenotype and metabolic shifts of the endospore-forming *Clostridium acetobutylicum*. *Mol Cell Proteomics* 17:1156-1169.
236. Mizuno Y, Nagano-Shoji M, Kubo S, Kawamura Y, Yoshida A, Kawasaki H, Nishiyama M, Yoshida M, Kosono S. 2016. Altered acetylation and succinylation profiles in *Corynebacterium glutamicum* in response to conditions inducing glutamate overproduction. *Microbiologyopen* 5:152-73.
237. Chen Z, Zhang G, Yang M, Li T, Ge F, Zhao J. 2017. Lysine acetylome analysis reveals photosystem II manganese-stabilizing protein acetylation is involved in negative regulation of oxygen evolution in model *Cyanobacterium Synechococcus* sp. PCC 7002. *Mol Cell Proteomics* 16:1297-1311.

238. Fu Y, Zhang L, Song H, Liao J, Lin L, Jiang W, Wu X, Wang G. 2022. Acetylome and succinylome profiling of *Edwardsiella tarda* reveals key roles of both lysine acylations in bacterial antibiotic resistance. *Antibiotics (Basel)* 11.
239. Wu X, Vellaichamy A, Wang D, Zamdborg L, Kelleher NL, Huber SC, Zhao Y. 2013. Differential lysine acetylation profiles of *Erwinia amylovora* strains revealed by proteomics. *J Proteomics* 79:60-71.
240. Zhang K, Zheng S, Yang JS, Chen Y, Cheng Z. 2013. Comprehensive profiling of protein lysine acetylation in *Escherichia coli*. *J Proteome Res* 12:844-51.
241. Weinert BT, Satpathy S, Hansen BK, Lyon D, Jensen LJ, Choudhary C. 2017. Accurate quantification of site-specific acetylation stoichiometry reveals the impact of sirtuin deacetylase CobB on the *E. coli* acetylome. *Mol Cell Proteomics* 16:759-769.
242. Marakasova E, Ii A, Nelson KT, van Hoek ML. 2020. Proteome wide profiling of N-epsilon-lysine acetylation reveals a novel mechanism of regulation of the chitinase activity in *Francisella novicida*. *J Proteome Res* 19:1409-1422.
243. Zhou S, Wu C. 2019. Comparative acetylome analysis reveals the potential roles of lysine acetylation for DON biosynthesis in *Fusarium graminearum*. *BMC Genomics* 20:841.
244. Lee DW, Kim D, Lee YJ, Kim JA, Choi JY, Kang S, Pan JG. 2013. Proteomic analysis of acetylation in thermophilic *Geobacillus kaustophilus*. *Proteomics* 13:2278-82.
245. Guo J, Wang C, Han Y, Liu Z, Wu T, Liu Y, Liu Y, Tan Y, Cai X, Cao Y, Wang B, Zhang B, Liu C, Tan S, Zhang T. 2016. Identification of lysine acetylation in *Mycobacterium abscessus* using LC-MS/MS after immunoprecipitation. *J Proteome Res* 15:2567-78.
246. Xu JY, Zhao L, Liu X, Hu H, Liu P, Tan M, Ye BC. 2018. Characterization of the lysine acylomes and the substrates regulated by protein acyltransferase in *Mycobacterium smegmatis*. *ACS Chem Biol* 13:1588-1597.
247. Liu F, Yang M, Wang X, Yang S, Gu J, Zhou J, Zhang XE, Deng J, Ge F. 2014. Acetylome analysis reveals diverse functions of lysine acetylation in *Mycobacterium tuberculosis*. *Mol Cell Proteomics* 13:3352-66.

248. Bi J, Wang Y, Yu H, Qian X, Wang H, Liu J, Zhang X. 2017. Modulation of central carbon metabolism by acetylation of isocitrate lyase in *Mycobacterium tuberculosis*. *Sci Rep* 7:44826.
249. Xie L, Liu W, Li Q, Chen S, Xu M, Huang Q, Zeng J, Zhou M, Xie J. 2015. First succinyl-proteome profiling of extensively drug-resistant *Mycobacterium tuberculosis* revealed involvement of succinylation in cellular physiology. *J Proteome Res* 14:107-19.
250. Yang H, Sha W, Liu Z, Tang T, Liu H, Qin L, Cui Z, Chen J, Liu F, Zheng R, Huang X, Wang J, Feng Y, Ge B. 2018. Lysine acetylation of DosR regulates the hypoxia response of *Mycobacterium tuberculosis*. *Emerg Microbes Infect* 7:34.
251. Birhanu AG, Yimer SA, Holm-Hansen C, Norheim G, Aseffa A, Abebe M, Tonjum T. 2017. N(epsilon)- and O-acetylation in *Mycobacterium tuberculosis* lineage 7 and lineage 4 Strains: proteins involved in bioenergetics, virulence, and antimicrobial resistance are acetylated. *J Proteome Res* 16:4045-4059.
252. van Noort V, Seebacher J, Bader S, Mohammed S, Vonkova I, Betts MJ, Kuhner S, Kumar R, Maier T, O'Flaherty M, Rybin V, Schmeisky A, Yus E, Stulke J, Serrano L, Russell RB, Heck AJ, Bork P, Gavin AC. 2012. Cross-talk between phosphorylation and lysine acetylation in a genome-reduced bacterium. *Mol Syst Biol* 8:571.
253. Butler CA, Veith PD, Nieto MF, Dashper SG, Reynolds EC. 2015. Lysine acetylation is a common post-translational modification of key metabolic pathway enzymes of the anaerobe *Porphyromonas gingivalis*. *J Proteomics* 128:352-64.
254. Ouidir T, Jarnier F, Cosette P, Jouenne T, Hardouin J. 2015. Characterization of N-terminal protein modifications in *Pseudomonas aeruginosa* PA14. *J Proteomics* 114:214-25.
255. Gaviard C, Broutin I, Cosette P, De E, Jouenne T, Hardouin J. 2018. Lysine succinylation and acetylation in *Pseudomonas aeruginosa*. *J Proteome Res* 17:2449-2459.
256. Henriksen P, Wagner SA, Weinert BT, Sharma S, Bacinskaja G, Rehman M, Juffer AH, Walther TC, Lisby M, Choudhary C. 2012. Proteome-wide analysis of lysine acetylation suggests its broad regulatory scope in *Saccharomyces cerevisiae*. *Mol Cell Proteomics* 11:1510-22.

257. Huang D, Li ZH, You D, Zhou Y, Ye BC. 2015. Lysine acetylproteome analysis suggests its roles in primary and secondary metabolism in *Saccharopolyspora erythraea*. *Appl Microbiol Biotechnol* 99:1399-413.
258. Li L, Wang W, Zhang R, Xu J, Wang R, Wang L, Zhao X, Li J. 2018. First acetylproteome profiling of *Salmonella typhimurium* revealed involvement of lysine acetylation in drug resistance. *Vet Microbiol* 226:1-8.
259. Wang Q, Zhang Y, Yang C, Xiong H, Lin Y, Yao J, Li H, Xie L, Zhao W, Yao Y, Ning ZB, Zeng R, Xiong Y, Guan KL, Zhao S, Zhao GP. 2010. Acetylation of metabolic enzymes coordinates carbon source utilization and metabolic flux. *Science* 327:1004-7.
260. Wang Y, Wang F, Bao X, Fu L. 2019. Systematic analysis of lysine acetylome reveals potential functions of lysine acetylation in *Shewanella baltica*, the specific spoilage organism of aquatic products. *J Proteomics* 205:103419.
261. Meng Q, Liu P, Wang J, Wang Y, Hou L, Gu W, Wang W. 2016. Systematic analysis of the lysine acetylome of the pathogenic bacterium *Spiroplasma eriocheiris* reveals acetylated proteins related to metabolism and helical structure. *J Proteomics* 148:159-69.
262. Zhang Y, Wu Z, Wan X, Liu P, Zhang J, Ye Y, Zhao Y, Tan M. 2014. Comprehensive profiling of lysine acetylome in *Staphylococcus aureus*. *Science China Chemistry* 57:732-738.
263. Xia J, Liu J, Xu F, Zhou H. 2022. Proteomic profiling of lysine acetylation and succinylation in *Staphylococcus aureus*. *Clin Transl Med* 12:e1058.
264. Liu YT, Pan Y, Lai F, Yin XF, Ge R, He QY, Sun X. 2018. Comprehensive analysis of the lysine acetylome and its potential regulatory roles in the virulence of *Streptococcus pneumoniae*. *J Proteomics* 176:46-55.
265. Yang Y, Zhang H, Guo Z, Zou S, Long F, Wu J, Li P, Zhao GP, Zhao W. 2021. Global insights into lysine acylomes reveal crosstalk between lysine acetylation and succinylation in *Streptomyces coelicolor* metabolic pathways. *Mol Cell Proteomics* 20:100148.
266. Liao G, Xie L, Li X, Cheng Z, Xie J. 2014. Unexpected extensive lysine acetylation in the trump-card antibiotic producer *Streptomyces roseosporus* revealed by proteome-wide profiling. *J Proteomics* 106:260-9.

267. Cao J, Wang T, Wang Q, Zheng X, Huang L. 2019. Functional insights into protein acetylation in the hyperthermophilic archaeon *Sulfolobus islandicus*. *Mol Cell Proteomics* 18:1572-1587.
268. Turkowsky D, Esken J, Goris T, Schubert T, Diekert G, Jehmlich N, von Bergen M. 2018. A retentive memory of tetrachloroethene respiration in *Sulfurospirillum halorespirans* - involved proteins and a possible link to acetylation of a two-component regulatory system. *J Proteomics* 181:36-46.
269. Mo R, Yang M, Chen Z, Cheng Z, Yi X, Li C, He C, Xiong Q, Chen H, Wang Q, Ge F, 2015. Acetylome analysis reveals the involvement of lysine acetylation in photosynthesis and carbon metabolism in the model cyanobacterium *Synechocystis sp. PCC 6803*. *J Proteome Res* 14:1275-86.
270. Alpha-Bazin B, Gorlas A, Lagorce A, Joulie D, Boyer JB, Dutertre M, Gaillard JC, Lopes A, Zivanovic Y, Dedieu A, Confalonieri F, Armengaud J. 2021. Lysine-specific acetylated proteome from the archaeon *Thermococcus gammatolerans* reveals the presence of acetylated histones. *J Proteomics* 232:104044.
271. Jeffers V, Sullivan WJ, Jr. 2012. Lysine acetylation is widespread on proteins of diverse function and localization in the protozoan parasite *Toxoplasma gondii*. *Eukaryot Cell* 11:735-42.
272. Xue B, Jeffers V, Sullivan WJ, Uversky VN. 2013. Protein intrinsic disorder in the acetylome of intracellular and extracellular *Toxoplasma gondii*. *Mol Biosyst* 9:645-57.
273. Xu X, Liu T, Yang J, Chen L, Liu B, Wang L, Jin Q. 2018. The first whole-cell proteome- and lysine-acetylome-based comparison between *Trichophyton rubrum* conidial and mycelial Stages. *J Proteome Res* 17:1436-1451.
274. Pang H, Li W, Zhang W, Zhou S, Hoare R, Monaghan SJ, Jian J, Lin X. 2020. Acetylome profiling of *Vibrio alginolyticus* reveals its role in bacterial virulence. *J Proteomics* 211:103543.
275. Jers C, Ravikumar V, Lezyk M, Sultan A, Sjoling A, Wai SN, Mijakovic I. 2017. The global acetylome of the human pathogen *Vibrio cholerae* V52 reveals lysine acetylation of major transcriptional regulators. *Front Cell Infect Microbiol* 7:537.

276. Wang J, Pang H, Yin L, Zeng F, Wang N, Hoare R, Monaghan SJ, Li W, Jian J. 2022. A comprehensive analysis of the lysine acetylome in the aquatic animals pathogenic bacterium *Vibrio mimicus*. *Front Microbiol* 13:816968.
277. Pan J, Ye Z, Cheng Z, Peng X, Wen L, Zhao F. 2014. Systematic analysis of the lysine acetylome in *Vibrio parahemolyticus*. *J Proteome Res* 13:3294-302.
278. Pang R, Li Y, Liao K, Guo P, Li Y, Yang X, Zhang S, Lei T, Wang J, Chen M, Wu S, Xue L, Wu Q. 2020. Genome- and proteome-wide analysis of lysine acetylation in *Vibrio vulnificus* Vv180806 reveals its regulatory roles in virulence and antibiotic resistance. *Front Microbiol* 11:591287.
279. Zhang X, Cheng K, Ning Z, Mayne J, Walker K, Chi H, Farnsworth CL, Lee K, Figeys D. 2021. Exploring the microbiome-wide lysine acetylation, succinylation, and propionylation in human gut microbiota. *Anal Chem* 93:6594-6598.
280. Zhang X, Ning Z, Mayne J, Yang Y, Deeke SA, Walker K, Farnsworth CL, Stokes MP, Couture JF, Mack D, Stintzi A, Figeys D. 2020. Widespread protein lysine acetylation in gut microbiome and its alterations in patients with Crohn's disease. *Nat Commun* 11:4120.
281. Barak R, Welch M, Yanovsky A, Oosawa K, Eisenbach M. 1992. Acetyladenylate or its derivative acetylates the chemotaxis protein CheY in vitro and increases its activity at the flagellar switch. *Biochemistry* 31:10099-107.
282. Barak R, Prasad K, Shainskaya A, Wolfe AJ, Eisenbach M. 2004. Acetylation of the chemotaxis response regulator CheY by acetyl-CoA synthetase purified from *Escherichia coli*. *J Mol Biol* 342:383-401.
283. Barak R, Yan J, Shainskaya A, Eisenbach M. 2006. The chemotaxis response regulator CheY can catalyze its own acetylation. *J Mol Biol* 359:251-65.
284. Starai VJ, Celic I, Cole RN, Boeke JD, Escalante-Semerena JC. 2002. Sir2-dependent activation of acetyl-CoA synthetase by deacetylation of active lysine. *Science* 298:2390-2.
285. Gardner JG, Escalante-Semerena JC. 2008. Biochemical and mutational analyses of AcuA, the acetyltransferase enzyme that controls the activity of the acetyl coenzyme a synthetase (AcsA) in *Bacillus subtilis*. *J Bacteriol* 190:5132-6.

286. Gardner JG, Escalante-Semerena JC. 2009. In *Bacillus subtilis*, the sirtuin protein deacetylase, encoded by the *srtN* gene (formerly *yhdZ*), and functions encoded by the *acuABC* genes control the activity of acetyl coenzyme A synthetase. *J Bacteriol* 191:1749-55.
287. Lima BP, Thanh Huyen TT, Basell K, Becher D, Antelmann H, Wolfe AJ. 2012. Inhibition of acetyl phosphate-dependent transcription by an acetylatable lysine on RNA polymerase. *J Biol Chem* 287:32147-60.
288. Lima BP, Antelmann H, Gronau K, Chi BK, Becher D, Brinsmade SR, Wolfe AJ. 2011. Involvement of protein acetylation in glucose-induced transcription of a stress-responsive promoter. *Mol Microbiol* 81:1190-204.
289. Venkat S, Chen H, Stahman A, Hudson D, McGuire P, Gan Q, Fan C. 2018. Characterizing lysine acetylation of isocitrate dehydrogenase in *Escherichia coli*. *J Mol Biol* 430:1901-1911.
290. Venkat S, Chen H, McGuire P, Stahman A, Gan Q, Fan C. 2019. Characterizing lysine acetylation of *Escherichia coli* type II citrate synthase. *FEBS J* 286:2799-2808.
291. Schastnaya E, Doubleday PF, Maurer L, Sauer U. 2023. Non-enzymatic acetylation inhibits glycolytic enzymes in *Escherichia coli*. *Cell Rep* 42:111950.
292. Feid SC, Walukiewicz HE, Wang X, Nakayasu ES, Rao CV, Wolfe AJ. 2022. Regulation of translation by lysine acetylation in *Escherichia coli*. *mBio* 13:e0122422.
293. McCleary WR, Stock JB. 1994. Acetyl phosphate and the activation of two-component response regulators. *J Biol Chem* 269:31567-72.
294. Datsenko KA, Wanner BL. 2000. One-step inactivation of chromosomal genes in *Escherichia coli* K-12 using PCR products. *Proceedings of the National Academy of Sciences of the United States of America* 97:6640-6645.
295. Baba T, Ara T, Hasegawa M, Takai Y, Okumura Y, Baba M, Datsenko KA, Tomita M, Wanner BL, Mori H. 2006. Construction of *Escherichia coli* K-12 in-frame, single-gene knockout mutants: the Keio collection. *Molecular systems biology* 2:2006.0008.

296. Haldimann A, Wanner BL. 2001. Conditional-replication, integration, excision, and retrieval plasmid-host systems for gene structure-function studies of bacteria. *Journal of Bacteriology* 183:6384-6393.
297. Kitagawa M, Ara T, Arifuzzaman M, Ioka-Nakamichi T, Inamoto E, Toyonaga H, Mori H. 2005. Complete set of ORF clones of *Escherichia coli* ASKA library (a complete set of *E. coli* K-12 ORF archive): unique resources for biological research. *DNA Res* 12:291-9.
298. Garamella J, Marshall R, Rustad M, Noireaux V. 2016. The all *E. coli* TX-TL toolbox 2.0: a platform for cell-free synthetic biology. *ACS Synth Biol* 5:344-55.
299. Andersson DI, Bohman K, Isaksson LA, Kurland CG. 1982. Translation rates and misreading characteristics of *rpsD* mutants in *Escherichia coli*. *Molecular & general genetics* : MGG 187:467-472.
300. Shin J, Noireaux V. 2010. Efficient cell-free expression with the endogenous *E. Coli* RNA polymerase and sigma factor 70. *J Biol Eng* 4:8.
301. Knyphausen P, de Boor S, Kuhlmann N, Scislowski L, Extra A, Baldus L, Schacherl M, Baumann U, Neundorff I, Lammers M. 2016. Insights into lysine deacetylation of natively folded substrate proteins by sirtuins. *J Biol Chem* 291:14677-94.
302. Fredrick K, Dunny GM, Noller HF. 2000. Tagging ribosomal protein S7 allows rapid identification of mutants defective in assembly and function of 30 S subunits. *Journal of Molecular Biology* 298:379-394.
303. Robert F, Gagnon M, Sans D, Michnick S, Brakier-Gingras L. 2000. Mapping of the RNA recognition site of *Escherichia coli* ribosomal protein S7. *RNA (New York, NY)* 6:1649-1659.
304. Helgstrand M, Mandava CS, Mulder FA, Liljas A, Sanyal S, Akke M. 2007. The ribosomal stalk binds to translation factors IF2, EF-Tu, EF-G and RF3 via a conserved region of the L12 C-terminal domain. *Journal of Molecular Biology* 365:468-479.
305. Zhang BQ, Bu HL, You D, Ye BC. 2020. Acetylation of translation machinery affected protein translation in *E. coli*. *Applied Microbiology and Biotechnology* 104:10697-10709.

306. Zhang BQ, Chen ZQ, Dong YQ, You D, Zhou Y, Ye BC. 2022. Selective recruitment of stress-responsive mRNAs to ribosomes for translation by acetylated protein S1 during nutrient stress in *Escherichia coli*. *Commun Biol* 5:892.
307. Shimizu K. 2013. Regulation systems of bacteria such as *Escherichia coli* in response to nutrient limitation and environmental stresses. *Metabolites* 4:1-35.
308. Hua Q, Yang C, Baba T, Mori H, Shimizu K. 2003. Responses of the central metabolism in *Escherichia coli* to phosphoglucose isomerase and glucose-6-phosphate dehydrogenase knockouts. *J Bacteriol* 185:7053-67.
309. Burrington LR, Watts KR, Oza JP. 2021. Characterizing and improving reaction times for *E. coli*-based cell-free protein synthesis. *ACS Synth Biol* 10:1821-1829.
310. Christensen DG, Xie X, Basisty N, Byrnes J, McSweeney S, Schilling B, Wolfe AJ. 2019. Post-translational protein acetylation: an elegant mechanism for bacteria to dynamically regulate metabolic functions. *Front Microbiol* 10:1604.
311. Sun Y, Zhang Y, Zhao T, Luan Y, Wang Y, Yang C, Shen B, Huang X, Li G, Zhao S, Zhao GP, Wang Q. 2023. Acetylation coordinates the crosstalk between carbon metabolism and ammonium assimilation in *Salmonella enterica*. *EMBO J* doi:10.15252/emj.2022112333:e112333.

## VITA

The author, Sarah Caldwell Feid, was born in Pittsburgh, Pennsylvania on January 27<sup>th</sup>, 1993 to Richard and Kathleen Feid. She attended Indiana University in Bloomington, Indiana, where they earned a Bachelor of Science in Microbiology and a Bachelor of Arts in Germanic Studies in May 2015. During her time at Indiana University, Caldwell studied the regulation of swarming motility in the lab of Dr. Daniel Kearns.

After graduation, Caldwell matriculated into the Loyola University Chicago Stritch School of Medicine Integrated Program in Biomedical Sciences Graduate Program and began their graduate education in the Department of Microbiology and Immunology. She joined the lab of Dr. Alan J. Wolfe to study the role of lysine acetylation on the bacterial ribosome. Caldwell's dissertation work identified *in vitro* and *in vivo* changes in translation that are mediated by acetyl phosphate and nonenzymatic acetylation. In their final year of study, she was supported by the Arthur J. Schmitt Fellowship. Caldwell's work has been presented at several conferences, including an oral presentation at the Bacterial Locomotion and Signal Transduction meeting in Charleston, South Carolina in January 2023.

After receiving her Ph.D., Caldwell will pursue a postdoctoral fellowship in the lab of Dr. Babak Javid in the Department of Medicine at the University of California San Francisco.

